Aus dem Institut für Humanernährung und Lebensmittelkunde

der Christian-Albrechts-Universität zu Kiel

Profiles of the human intestinal microbiota during antibiotic perturbation and resilience

Dissertation

zur Erlangung des Doktorgrades

der Agrar- und Ernährungswissenschaftlichen Fakultät

der Christian-Albrechts-Universität zu Kiel

vorgelegt von

M.Sc. Femke-Anouska Heinsen

aus Buxtehude

Kiel, 2012

Dekanin: Prof. Dr. K. Schwarz
1. Berichterstatter: Prof. Dr. F. Döring
2. Berichterstatter: Prof. Dr. P. Rosenstiel
Tag der mündlichen Prüfung: 10. 05. 2012

Für meine Eltern

Table of Contents

List of Figures

List of Tables

Abbreviations

Abbreviation	Explanation
AMOVA	Analysis of molecular variance
AP-1	Activating protein-1
ATP	Adenosinetriphosphate
BLAST	Basic local alignment search tool
bp	basepair
CAU	Christian-Albrechts-University
CCD	Charge-coupled device
CD	Crohn´s Disease
C_t	Cycle threshold
ddNTP	Didesoxynucleosidetriphosphate
DES	DNAse/pyrogen-free water
DGGE	Denaturing gradient gel electrophoresis
DNA	Desoxyribonucleic acid
dNTP	Desoxynucleosidetriphosphate
Exo I	Exonuclease I
Fut2	Fucosyltransferase 2
GALT	Gut-associated lymphoid tissue
GIT	Gastrointestinal tract
IBD	Inflammatory bowel disease
IFN-γ	Interferon-gamma
IgA	Immunoglobulin A
IL-10	Interleukin 10
IL-12	Interleukin 12
LAB	Lactic acid bacteria
LB	Lysogeny broth
LPS	Lipopolysaccharide
LSU	Large subunit
MAPK	Mitogen-activated protein kinase
mRNA	Messenger RNA
NCBI	National Center for Biotechnology Information
NF-κB	Nuclear factor kappa-light-chain-enhancer of activated B cells
NLR	Nod-like receptor
Nod2	Nucleotide-binding oligomerization domain-containing protein 2
OTU	Operational taxonomic unit
PANGEA	Pipeline for analysis of next generation amplicons
PBMC	Peripheral blood mononuclear cell
PCo	Principal coordinate

Abbreviation	Explanation
PCoA	Principal coordinate analysis
PCR	Polymerase chain reaction
PP_i	Pyrophosphate
PPS	Protein precipitation solution
PRR	Pattern recognition receptor
qRT-PCR	Quantitative real time PCR
RDP	Ribosomal Database Project
RNA	Ribonucleic acid
rpm	Rounds per minute
rRNA	Ribosomal RNA
S	Svedberg unit
SAP	Shrimp alkaline phosphatase
SCFA	Short chain fatty acid
SIMPER	Similarity percentage
SOB	Super Optimal Broth
SOC	SOB + glucose
SSU	Short subunit
TNBS	Trinitrobenzenesulfonic acid
TNF-α	Tumor necrosis factor-alpha
TLR	Toll-like receptor
T-RFLP	Terminal restriction fragment length polymorphism
TTGE	Temporal temperature gradient gel electrophoresis
UC	Ulcerative Colitis
V	Variable region
X-Gal	5-bromo-4-chloro-indolyl-β-D-galactopyranoside

1 Introduction

The most abundant life form on earth are prokaryotes and humans are adapted to a life in symbiosis with this unseen majority of microorganisms (Whitman et al. 1998). Several skin locations like the forearm, palm, index finger, back of the knee and sole of the foot are inhabited by highly diverse communities (Costello et al. 2009, Hooper et al. 2001). Compared to all other body sites the human gastrointestinal tract (GIT) harbors the largest and most diverse community of microbes (Costello et al. 2009; Eckburg et al. 2005). The amount of microbes (10^{14}) inhabiting the intestinal tract of a human adult outnumbers the human cells by a factor of ten and the hundreds of species native to the colon, where microbial richness and abundance are maximal, contain 100-fold more genes than does the human genome. The amount of bacteria within the GIT increases from the stomach to the rectum, whereas each region harbors a specific composition of bacteria. The highest density of 10^{11} - 10^{12} bacteria per gram colonic content can be found within the large intestine (Hooper et al. 2001; Whitman et al. 1998; Franks et al. 1998). The healthy microbiota can usually be assigned to four main phyla: *Firmicutes*, *Bacteroidetes*, *Proteobacteria* and *Actinobacteria*. Only a minority of the intestinal bacteria are cultivable (10-30%), but culture-independent methods estimated between 800 and 1000 different bacterial species or phylotypes and more than 7000 different bacterial strains to be present in the human GIT (Bäckhed et al. 2005; Eckburg et al. 2005). The majority within the healthy GIT are anaerobic bacteria, but also fungi, archaeae and some protozoa can be found. Within the kingdom of archaeae *Methanobrevibacter smithii* is the predominant if not the only species of methanogens in the human intestine (Bäckhed et al. 2005; Eckburg et al. 2005). The lack of species diversity in the intestinal archaeae, in comparison to the diversity among bacteria, is striking but as yet unexplained.

1.1 The human microbiota: A stable fingerprint-like consortium

Several studies have shown that each individual retains a distinct microbiota profile over time. The microbial composition differs between individuals, but twins have a more similar bacterial community structure than unrelated individuals (Turnbaugh et al. 2009; Zoetendal et al. 2001). Furthermore some authors assume a core microbiome. Besides rare taxa that vary immensely there seems to be a common set of abundant microbial species that are shared among all / or most individuals with twins sharing significantly more phylotypes. However, this core may exist at the level of shared functional genes and metabolic pathways rather than

shared taxa (Qin et al 2010; Tap et al. 2009; Turnbaugh et al 2009). The temporal changes in the bacterial community structure within an individual are smaller in comparison to the differences between individuals. Maintaining habits result in a relatively stable microbiota over time (Claesson et al. 2011; Costello et al. 2009; Mai et al. 2004; Franks et al. 1998; Zoetendal et al. 1998). The diversity and the fingerprint-like individuality of the microbial composition as well as possible dynamics within can partly be explained by age, host genotype and microbial interactions, but also by life-style factors like diet and exercise. With regard to the host genotype it could be shown that obese leptin deficient mice had a lower abundance of *Bacteroidetes* and a proportional increase in *Firmicutes* as shown by Ley et al. (2005). Mutations in *Nod2* resulted in a significant increase in *Firmicutes* and *Bacteroidetes* in mice and human (Rehman et al. 2011, Petnicki-Ocwieja et al. 2009). Furthermore the *FUT2* genotype explains differences in the human microbial composition (Rausch et al. 2011). Variations based on diet and other environmental factors seem to influence the luminal microbiota in a greater amount than the mucosa-associated microbiota. The epithelial wall and the overlying mucus layer may possibly maintain a more stable environment than present in the lumen (Gillevet et al. 2010; Eckburg et al. 2005; Zoetendal et al. 2002).

1.2 Gut bacteria are workaholics

The microbiota of the human GIT is involved in maintaining human health and gastrointestinal tract homeostasis. It regulates the gut epithelial development and survival by stimulation of proliferation, angiogenesis and epithelial restitution (Mai et al. 2010; Neish et al. 2009). The gut bacteria are responsible for the digestion of otherwise indigestible dietary polysaccharides. Dietary fibers and host intestinal mucins are fermented into simple sugars, short chain fatty acids and other nutrients that can be absorbed and are used as energy source by the host. For example acetate is important for the muscle, heart and brain cells, propionate is used in host hepatic neoglycogenic processes, whereas butyrate is important for enterocytes. A number of amino acids are indispensable to humans and can be provided by bacteria as well as essential vitamins like vitamin K, vitamin B_{12} and folic acid. The gut bacteria are also involved in bile acid metabolism and bile acid recirculation (Mai et al. 2010; Qin et al. 2010). Furthermore, the gut bacteria play a role in the immunmodulation. They prevent the colonization as well as the crossing of the mucosal barrier by pathogens via modulation of innate defenses such as inducing the epithelial production of α-defensins and mucins (Hooper et al. 2001). If the integrity of the mucosal barrier is broken by cytoinvasive bacteria, the bacterial components, for instance lipopolysaccharides (LPS), peptidoglycans

and flagellin, are recognized by pattern recognition receptors (PRRs) like the membrane-bound toll-like receptors (TLRs) or intracellular Nod-like receptors (NLRs). This results in a protective signal cascade which aims to restore the integrity of the epithelial barrier. However, it has not been clarified completely how the intestinal epithelial cells are able to distinguish between pathogenic and nonpathogenic bacteria (Gomez-Llorente et al. 2010; Takeda and Akira 2005).

1.3 Perturbation of the microbiota

In a healthy host there is a balance between members of the microbiota, such that potential pathogenic and non-pathogenic organisms can be found in apparent harmony. During infection, this balance can become disturbed. Bacterial imbalance, so-called dysbiosis, occurs, leading to often dramatic changes in the composition of the microbiota resulting in pathologies such as inflammatory bowel disease (IBD) (Rehman et al. 2010; Ott et al. 2004). Several studies have implicated intestinal communities with diseases ranging from allergies to late-onset autism, IBD and cancer. For most bacterial infections, broad-spectrum antibiotics are used, eradicating the pathogens as well as the non-pathogenic members of the microbiota. Thereby they disrupt the natural microbiota with a simultaneous decrease in bacterial load and a transient reduction in taxonomic richness, diversity and evenness of the community for some time. This can lead to a substantial delay in the restoration of a healthy microbiota and result in intestinal problems, such as antibiotic-associated diarrhea (Jernberg et al. 2007; Jakobsson et al. 2010; Robinson et al. 2010). Disturbances of the metabolism and absorption of vitamins, alteration of susceptibility to infections and overgrowth of yeast and/or *Clostridium difficile* can follow so that there is a shift from potentially beneficial and health-promoting bacteria (like *Lactobacilli* and *Bifidobacteria*), towards harmful pathogenic microorganisms (such as *Clostridia*, sulphate-reducers and proteolytic *Bacteroides* species). This makes the host even more susceptible to infections by transient enteropathogens like *Salmonella*, *Campylobacter* and certain species of *Escherichia coli* and *Listeria* (Fooks and Gibson 2002). An additional harmful disadvantage of antibiotics is the increased prevalence in antibiotic resistance and the potential spreading of resistance genes to pathogenic bacteria, thereby reducing the possibility of successful future antibiotic treatments.

The antibiotic used in this study is paromomycin (brandname: Humatin®, Pfizer). Paromomycin is an aminoglycoside and active against most Gram-negative and many Gram-positive bacteria as well as some protozoa and cestodes. Like most aminoglycosides it binds

to the 30S-subunit of the bacterial ribosome and thereby impairs the protein synthesis. Orally administered paromomycin is only poorly absorbed. It is used as a treatment against visceral leishmaniasis and amebiasis, but also for the reduction of the microbiota before surgery. In this study it was used to completely clean the bowel to enable a better look onto the resilience of the gut microbiota (Davidson et al. 2009).

1.4 The resilience phenomenon

Usually the microbiota exerts a high self-regeneratory capacity, which describes the ability to restore the microbial equilibrium after an external perturbation, for example antibiotic treatment, also referred to as the resilience phenomenon. It is known that antibiotics cause short-term changes in the composition of the normal human microbiota, but long-term consequences have also been shown. Antibiotic perturbation is mainly characterized by a decreased colonization resistance of the commensal microbiota, which leads to varying states of disease as well as to the appearance of antibiotic-resistant strains. The extent of the antibiotic-induced alterations in the microbiota depends on several factors: the spectrum of the agent, dosage and duration of the treatment, route of administration and the pharmacokinetic and pharmacodynamic properties of the agent. It has been shown that the taxonomic composition of the community closely resembles its pretreatment state between one and three months after the end of the treatment, but that specific populations in the community were significantly affected and failed to recover within six months or up to two or even four years (Jakobsson et al. 2010; Antonopoulos et al. 2009; Dethlefsen et al. 2008). Jakobsson et al. (2010) further investigated the erm(B) gene, which encodes a ribosomal methylase that modifies the 23S rRNA, thereby preventing the antibiotic from binding and resulting in resistance to this antibiotic. The erm(B) gene levels increased dramatically by three to five orders of magnitude after starting an antibiotic treatment with clarithromycin, metronidazole and omeprazole. These high levels of the erm(B) gene were still distinct after four years post treatment, indicating that antibiotic resistance can persist for very long periods. Even studies in healthy humans, in which clindamycin was administered for a few days, could show that although there was a normalization of the overall intestinal flora and the number of species returned to pre-treatment levels within three months, specific populations within the community (especially *Bacteroides*) were significantly affected and disturbed in terms of richness and diversity. These severe disturbances even persisted for more than two years after treatment. Moreover, in these studies a dramatic and persistent increase in the levels of specific resistance genes towards the given antibiotic was detected (Jernberg et al.

2007, Löfmark et al. 2006). Another study showed that after five days of oral administration of amoxicillin, the fecal microbiota was already markedly altered within two to three days after beginning of antibiotic treatment. However, the dominant microbiota needed at least 60 days in most of the study participants to return to the initial composition (De La Cochetiere et al. 2005). Therefore it seems that the healthy human microbiota has a kind of regeneratory capacity, whereas the complete bacterial diversity is difficult to re-establish and may take time. The resilience in diseased individuals can be even more dramatic.

1.5 Probiotics: The possible miracle drug

Probiotics in general are defined as "live organisms which when administered in adequate amounts confer a health benefit on the host" (World Health Organization). There are several criteria an organism has to fulfill to be a probiotic: (1) The organism must be fully identified referring to genus, species and strain. (2) It must be safe for consumption, not pathogenic and is not allowed to carry antibiotic resistance genes. (3) The organism has to survive the intestinal tract (acid and bile tolerant), adhere and not degrade to the mucosal surface and colonize the intestine. (4) The probiotic organism has to possess documented health effects (at least one phase 2 study documenting benefit), produce antimicrobial substances and antagonize pathogenic bacteria. (5) Finally it must be stable during process and storage. Bacteria such as lactic-acid bacteria (LAB) and *Escherichia coli* strains (e. g. *E. coli* Nissle 1917), as well as yeast species including *Saccharomyces boulardii* are categories of probiotics that are in use today. Probiotics are available in a wide variety of formulations ranging from tablets and powders to yoghurts, milk and juices (Verna and Lucak 2010). The indication for using probiotics is the potential decrease of the pathogen density and thereby the restoration and maintenance of the gut microbial homeostasis and the patients tolerance to the own commensal flora. Probiotics are used as treatments for a variety of gastrointestinal disorders like antibiotic-associated diarrhea, *Clostridium difficile* colitis, infectious diarrhea and IBD (Avadhani and Miley 2011; McFarland 2009; D´Souza et al. 2002). Therapy of allergic diseases (e.g. atopic dermatitis), urinary tract infections and the prevention of dental caries or respiratory infections further show an increasing frequency of probiotic use (Tang et al. 2010; MacPhee et al. 2010; Bonifait et al. 2009).

The two major types of IBD are Ulcerative Colitis (UC) and Crohn´s Disease (CD). Medicating UC with probiotics resulted in enhancements in disease activity indices and cytokine profiles and in an (re)induction or maintenance in remission (Tursi et al. 2010;

Bibiloni et al. 2005). In CD the actual data are controversial and most of the studies failed to show a benefit of probiotic administration, which is not completely unexpected regarding that there is only little evidence of the microbial imbalance being the primary course of this disorder (Reid et al. 2011; Isaacs and Herfarth 2008). However a replicated evidence for the use of probiotics exists in the prevention and treatment of pouchitis (Verna and Lucak 2010; Kühbacher et al. 2006). The exact mechanism by which the probiotics function is not yet fully understood. An antagonistic activity against the pathogenic bacteria is discussed in terms of a competition for the adherence to binding sites and nutrients. Moreover, the fermentation of the nutrients results in an acidification of the colon which is also effective against pathogenic bacteria. Probiotics seem to inhibit the translocation of pathogenic bacteria and to stabilize the epithelial barrier function also by stimulating the production of mucin and bacteriocins as protective substances. Further, the gastrointestinal immunity can be modulated by altering the immune functions like the stimulated secretory IgA production and cytokine profiles like the induction of IL-10 as well as the downregulation of proinflammatory cascades (Verna and Lucak 2010; Borchers et al. 2009; Vanderpool et al. 2008; Cotter et al. 2005; Drakes et al. 2004). Yet the exact temporal sequence of colonization events of an administered probiotic that subsequently alters the microbiota and may result in an (beneficial) effect remains unclear. The behavior and possible effects of one probiotic strain cannot automatically be generalized for other strains. Some bacteria seem to result only in transient effects and are resistant to colonization. They persist only as long as they are ingested and rapidly disappear once the treatment is stopped.

The probiotic used in this study is VSL#3 (VSL Pharmaceutical, Inc. (Pfizer)). It is a combination of four different *Lactobacillus* species (*L. casei*, *L. plantarum*, *L. acidophilus*, *L. delbruekii*), three *Bifidobacterium* species (*B. longum*, *B. breve* and *B. infantis*) and one strain of *Streptococcus thermophilus*. VSL#3 is a dietary supplement, which is approved for the restoration of the gut after mucosal infection, for the relief of abdominal bloating and pain in diarrhea-predominant irritable bowel syndrome and for the sustainment of remission in pouchitis and ulcerative colitis in adults and children (Guandalini et al. 2010; Miele et al. 2009; Kühbacher et al. 2006; Bibiloni et al. 2005; Mimura et al. 2004; Kim et al. 2003; Gionchetti et al. 2000). On the molecular basis it is described that VSL#3 has an increasing effect on the epithelial barrier function and barrier integrity via an induction of proinflammatory pathways like NF-κB, AP-1 and MAPKs as well as on the mucin expression (Schlee et al. 2008; Otte et al. 2004). This occurs in combination with a reduction in mucosal

secretion of TNF-α and IFN-γ (Jijon et al. 2004; Madsen et al. 2001). Further VSL#3 is able to decrease the LPS induced production of IL-12 and thereby diminishing the proinflammatory effects of LPS, to enhance the IL-10 release by dendritic cells from blood and intestinal tissue and to induce the β-defensin production of enterocytes (Schlee et al. 2008; Drakes et al. 2004; Hart et al. 2004; Ulisse et al. 2001).

1.6 Analysis of microbial profiles

To identify microbial profiles in a culture-independent way it is common to analyse the 16S rRNA gene sequence. The 16S rRNA gene is a section of the prokaryotic DNA found in all bacteria and archaeae. The prokaryotic 70S ribosome of bacteria and archaeae consists of two subunits, the large 50S subunit (LSU) and the small 30S subunit (SSU). These two subunits enclose the mRNA during translation. The SSU is encoded by the 16S rRNA gene ("r" stands for ribosomal), the LSU is encoded by the 23S rRNA and the 5S rRNA gene. Therefore it is distinct from the 18S rRNA gene, which is the eukaryotic equivalent. The 16S rRNA gene is relatively short (1542 nucleotides) which makes it easier to sequence compared to many other genes. It can be subdivided into highly conserved primer binding sites and nine variable regions (V1-V9) (Baker et al. 2003). The variable regions depict species-specific signatures. The 16S rRNA gene can directly be isolated by PCR with universal primers targeting the conserved regions. Based on the amplification of the 16S rRNA gene the sequencing according to the method of Frederick Sanger as well as the 454 pyrosequencing approach was performed in this study. Additionally, quantitative real-time PCR was conducted.

Methods like TTGE (temporal temperature gradient gel electrophoresis) are rapid methods to investigate the dominant bacteria within a sample, but offer only a low taxonomic resolution of the less abundant community members. Sequencing in general has the advantage of a deeper insight into microbial profiles on a finer taxonomic scale. For the Sanger sequencing as well as for the pyrosequencing approach DNA and/or RNA can be used. The PCR primers bind to the conserved regions of the 16S rRNA or the 16S rRNA gene and amplify the variable regions in between.

The sequencing according to Frederick Sanger is performed due to the chain termination method (Sanger et al. 1977). The reaction closely resembles a PCR reaction, except for two key differences. Only one oligonucleotide primer is used, resulting in linear than exponential sequence amplification, and fluorescently labeled 2´,3´-didesoxynucleoside triphosphates (ddNTP) are included in the reaction in addition to dNTPs. The DNA polymerase requires a

free 3´ hydoxyl group for the enzymatic formation of a phosphodiester bond with new dNTPs, which is not present in ddNTPs. Therefore the elongation of a DNA fragment will be terminated when a ddNTP is incorporated. The incorporation of ddNTPs is a random procedure, which results in a mixture of fragments with differing length. The fragments are separated electrophoretically and are activated with a laser. Each of the four ddNTPs is labeled with another fluorescent dye, so that they fluoresce with different colors and can be identified with a detector. The chromatogram, which contains the trace of the color signals, directly shows the sequence of the bases of the sequenced DNA strand (Osborn and Smith 2005).

In contrast, the method of pyrosequencing observes the DNA polymerase in action. In this study a barcoded-tagged PCR approach was used. Each sample is tagged with an unique identifier, which enables the pooling of samples to a so-called library. Within the sequencing process individual nucleotides are flowed in a fixed order. Each incorporation of one (or more) nucleotide(s) complementary to the template strand results in a release of pyrophosphate (PP_i). Pyrophosphate is converted into adenosinetriphosphate (ATP) by the ATP-sulfurylase. ATP then activates the luciferase reaction, thereby converting luciferin into oxyluciferin resulting in a detectable light signal, which is recorded by the CCD camera within the instrument. The signal strength is proportional to the number of nucleotides incorporated in a single nucleotide flow. If the nucleotide does not fit there is no light signal.

Based on the sequences generated by the two different methods a first denoising step is performed to remove low quality sequences. The cleaned sequences are aligned and those that do not fit into the alignment properly are checked and potentially discarded. Furthermore, chimerical sequences are eliminated. The denoised dataset can then be analysed. For a first rough overview of the taxa that exist within the samples the sequences can be classified according to the reference sequences of the Ribosomal Database Project (RDP) (Wang et al. 2009; Cole et al. 2008). For a deeper and more accurate analysis the sequences are assigned into operational taxonomic units (OTUs) due to the fact that the sequence-based recognition of uncultivated microbial populations is not equivalent to the traditional taxonomic classification. The OTUs can be defined at different levels of resolution, which are based on the homology between the sequences. An OTU level of 0.03 therefore indicates that all sequences within one OTU have a least a homology of 97%. Based on the OTU assignment, samples and treatment groups can then be compared.

1.7 Aim of the study

The aim of this study is the investigation of the self-regeneratory capacity of the human colonic microbiota under placebo and probiotic therapy after an iatrogenic perturbation by an antibiotic agent. To characterise the microbial profiles under different treatment conditions at several timepoints, samples of the luminal as well as the mucosa-associated microbiota of twenty healthy individuals were taken at five and three different timepoints, respectively. The culture-independent analysis of the 16S rRNA and the 16S rRNA gene was used to generate clone as well as amplicon libraries, which result in the identification of treatment (antibiotic and placebo vs. probiotic) and/or timepoint-related microbial profiles.

In detail the following questions shall be answered:

- **How does the microbial profile of a healthy microbiota change due to an antibiotic treatment?**
- **Is the microbiota resilient?**
- **When does the resilient microbiota resemble its pre-treatment state?**
- **Is there a difference in the resilience with regard to the placebo and the probiotic therapy?**
- **Is there a difference in the resilience between the luminal and the mucosa-associated microbiota?**
- **Is there a difference between the active and the present bacteria of the mucosa-associated microbiota?**

The didesoxy chain termination method according to the method of Sanger was used for the sequencing of the 16S rRNA gene of the luminal microbiota. The mucosa-associated microbiota was sequenced according to the FLX pyrosequencing method. In addition, a real time PCR was performed for the relative quantification of the total bacteria as well as the two most abundant phyla.

2 Material and Methods

2.1 Material

2.1.1 Companies of purchased kits, chemicals, consumables and equipment

The used kits, chemicals, consumables and equipment were purchased from the following companies: Ambion, (Austin, USA), Applied Biosystems (Foster City, USA), BD (Becton, Dickinson and Company, Heidelberg), Bio 101 (Heidelberg), Biorad (München), Biostep (Jahnsdorf), Eppendorf (Hamburg), Fermentas (St Leon-Rot), GE Healthcare (München), HJ Bioanalytik GmbH (Mönchengladbach), Invitrogen (Karlsruhe), Kendro (Hanau), Metabion (Martinsried), MP Biomedicals (Heidelberg), PeqLab (Erlangen), Pfizer (New York, USA), Qiagen (Hilden), Ratiolab (Dreieich), Roche (Basel, Switzerland), Roth (Karlsruhe), Sarstedt (Nürnbrecht), Sigma-Aldrich (St. Louis, USA), ThermoFisher Scientific (Waltham, USA), VSL Pharmaceuticals, Inc. (Gaithersburg, Maryland, USA), WTB binder (Tuttlingen).

2.1.2 Kits and chemicals

Table 2-1: Used kits and chemicals.

Kit / chemical	Producing company
ABI PRISM® BigDye® Terminator v1.1 Cycle Sequencing Kit	Applied Biosystems
AllPrep DNA/RNA Mini Kit	Qiagen
FastDNA® SPIN for Soil Kit	MP Biomedicals
High Capacity cDNA Reverse Transcription Kit	Applied Biosystems
Min Elute® Gel Extraction Kit	Qiagen
Phusion Hot Start DNA Polymerase	ThermoFisherScientific
Qubit® ds DNA BR Assay Kit	Invitrogen
TOPO® TA Cloning Kit	Invitrogen
100 bp Gene Ruler	Fermentas
Ampicillin	Sigma-Aldrich
β-Mercaptoethanol	Sigma-Aldrich
Difco™ Agar Noble	BD
dNTPs	Peqlab
Ethanol (99.9%)	Sigma-Aldrich
ExonucleaseI (E.coli)	Fermentas
Isopropanol (2-Propanol)	Sigma-Aldrich
LB-Medium (Luria/Miller)	Roth
N,N-Dimethylformamide	Sigma-Aldrich
Nuclease-Free Water	Ambion
Paromomycin (Humatin®)	Pfizer

Kit / chemical	Producing company
Power SYBR® Green PCR Master Mix	Applied Biosystems
Proteinase K	Fermentas
RNase-Free DNase Set	Qiagen
RT-PCR Grade Water	Ambion
Sephadex™ G-50 Superfine	GE Healthcare
Shrimp Alkaline Phosphatase	Fermentas
SOC Medium	Invitrogen
SYBR® Safe DNA gel stain	Invitrogen
TL Buffer	Peqlab
VSL#3®	VSL Pharmaceuticals
X-gal	Fermentas

2.1.3 Consumables and equipment

Table 2-2: Used consumables and equipment.

Consumable / equipment	Producing company
96-Deep-Well Plates	HJ-Bioanalytik GmbH
96 Well Multiply®-PCR Plate	Sarstedt
Biosphere® FilterTips	Sarstedt
Costar Thermowell® 96 Well PCR Plate	ThermoFisher Scientific
Coverfilms	Ratiolab
Disposable Gel Excision Tips	Biostep
Reaction tube (1.5 and 2 ml)	Eppendorf
Lysing Matrix E tubes	MP Biomedicals
Petri dishes	Sarstedt
QIAshredder™	Qiagen
Qubit® assay tubes	Invitrogen
3730*xl* DNA Analyzer	Applied Biosystems
7900HT Fast Real-Time PCR System	Applied Biosystems
Centrifuge 5415 R	Eppendorf
FastPrep FP 120	Bio 101
Gel Doc XR	Biorad
GeneAmp® PCR System 9700	Applied Biosystems
GS FLX Instrument	Roche
Heraeus Labofuge 400	Kendro
Incubator	WTB binder
Qubit® Fluorometer	Invitrogen
Thermomixer comfort	Eppendorf

2.1.4 Primers

Table 2-3: Used primers.

Target Gene	Name	DNA-Sequence (5´-3´)		
Bacteria universal				
16S rRNA gene	TPU1	AGA GTT TGA TCM TGG CTC AG		
V1-V4	805R	GAC TAC CAG GGT ATC TAA TCC		
16S rRNA gene	Pyro_27F	CTA TGC GCC TTG CCA GCC CGC TCA GTC AGA		
V1-V2		TGA TCC TGG CTC AG		
for Pyrosequencing	MIDX _338R	CGT ATC GCC TCC CTC GCG CCA TCAG (MID) CAT		
		GCT GCC TCC CGT AGG AGT		
MID / barcode	MID1_338R	ACGAGTGCGT	MID28_338R	ACTACTATG
	MID2_338R	ACGCTCGACA	MID29_338R	ACTGTACAG
	MID3_338R	AGACGCACTC	MID30_338R	AGACTATAC
	MID4_338R	AGCACTGTAG	MID31_338R	AGCGTCGTC
	MID5_338R	ATCAGACACG	MID32_338R	AGTACGCTA
	MID6_338R	ATATCGCGAG	MID33_338R	ATAGAGTAC
	MID7_338R	CGTGTCTCTA	MID34_338R	CACGCTACG
	MID8_338R	CTCGCGTGTC	MID35_338R	CAGTAGACG
	MID10_338R	TCTCTATGCG	MID36_338R	CGACGTGAC
	MID11_338R	TGATACGTCT	MID37_338R	TACACACAC
	MID13_338R	CATAGTAGTG	MID38_338R	TACACGTGA
	MID14_338R	CGAGAGATAC	MID39_338R	TACAGATCG
	MID15_338R	ATACGACGTA	MID40_338R	TACGCTGTC
	MID16_338R	TCACGTACTA	MID41_338R	TAGTGTAGA
	MID17_338R	CGTCTAGTAC	MID42_338R	TCGATCACG
	MID18_338R	TCTACGTAGC	MID43_338R	TCGCACTAG
	MID19_338R	TGTACTACTC	MID44_338R	TCTAGCGAC
	MID20_338R	ACGACTACAG	MID45_338R	TCTATACTA
	MID21_338R	CGTAGACTAG	MID46_338R	TGACGTATG
Target Gene	**Name**	**DNA-Sequence (5´-3´)**		
MID / barcode	MID22_338R	TACGAGTATG	MID47_338R	TGTGAGTAG
	MID23_338R	TACTCTCGTG	MID48_338R	ACAGTATAT
	MID24_338R	TAGAGACGAG	MID49_338R	ACGCGATCG
	MID25_338R	TCGTCGCTCG	MID50_338R	ACTAGCAGT
	MID26_338R	ACATACGCGT	MID51_338R	AGCTCACGT
	MID27_338R	ACGCGAGTAT	MID52_338R	AGTATACAT
Insert of the vector pCR® 2.1 of the TOPO TA Cloning				
Vector pCR® 2.1	M13(16)F	GTA AAA CGA CGG CCA G		
	M13(17)R	CAG GAA ACA GCT ATG AC		

Target Gene	Name	DNA-Sequence (5´-3´)
Real-Time PCR		
All Bacteria	Eub338F	ACT CCT ACG GGA GGC AGC AG
	Eub518R	ATT ACC GCG GCT GCT GG
Bacteroidetes	Bact934F	GGA RCA TGT GGT TTA ATT CGA TGA T
	Bact1060R	AGC TGA CGA CAA CCA TGC AG
Firmicutes	Firm934F	GGA GYA TGT GGT TTA ATT CGA AGC A
	Firm1060R	AGC TGA CGA CAA CCA TGC AC
β-Actin	bActin_F	GAT GGT GGG CAT GGG TCA G
	bActin_R	CTT AAT GTC ACG CAC GAT TTC

The used primers were purchased from the company Metabion.

2.1.5 Software and database

Table 2-4: Used computer programs.

Program	Webpage
ActivePerl	http://www.activestate.com/activeperl/
FastTree	http://www.microbesonline.org/fasttree/
MOTHUR version v.1.21.0	http://www.mothur.org/
MS Office 2007	Microsoft, Redmont, USA
NCBI	http://www.ncbi.nlm.nih.gov/
PANGEA	http://www.microgator.org/pangea/
PAST	http://folk.uio.no/ohammer/past/
R	http://www.r-project.org/
SDS 2.3	Applied Biosystems
Tinn-R	http://sciviews.org/Tinn-R/
Ribosomal database project (RDP)	http://rdp.cme.msu.edu/

2.1.6 Study participants and study design

Twenty healthy individuals were included in this study. The criteria for participation were between 18 and 50 years of age, no antibiotic or antimycotic treatment in the previous 6 months, no probiotic therapy, no hospitalization, no diarrhea in the previous 6 months, no current infection, normal inflammatory markers, no relative or absolute contraindications against paromomycin (Humatin®) or VSL#3®. All individuals gave their written consent as approved by the local ethical committee of the Christian-Albrechts-University (CAU) of Kiel, Germany.

Paromomycin (brandname: Humatin®, Pfizer) was administered at a dose of 4g per day over a period of three days to all twenty healthy individuals. After antibiotic therapy for three days, the group was split: half of the patients (n=10) were allocated to a probiotic therapy with VSL#3® (VSL Pharmaceuticals, Inc.) at a dose of 900 billion bacteria per day, the other group (n=10) received a placebo. Biopsies were sampled from the sigmoid colon before (day 0) and after the antibiotic treatment (day 4). After six weeks of probiotic or placebo treatment (day 46) the study was completed by a last sigmoidoscopy. Stool samples were collected in parallel and at additional timepoints at day 14 and 28. Biopsies as well as fecal samples were stored at -80°C until further use.

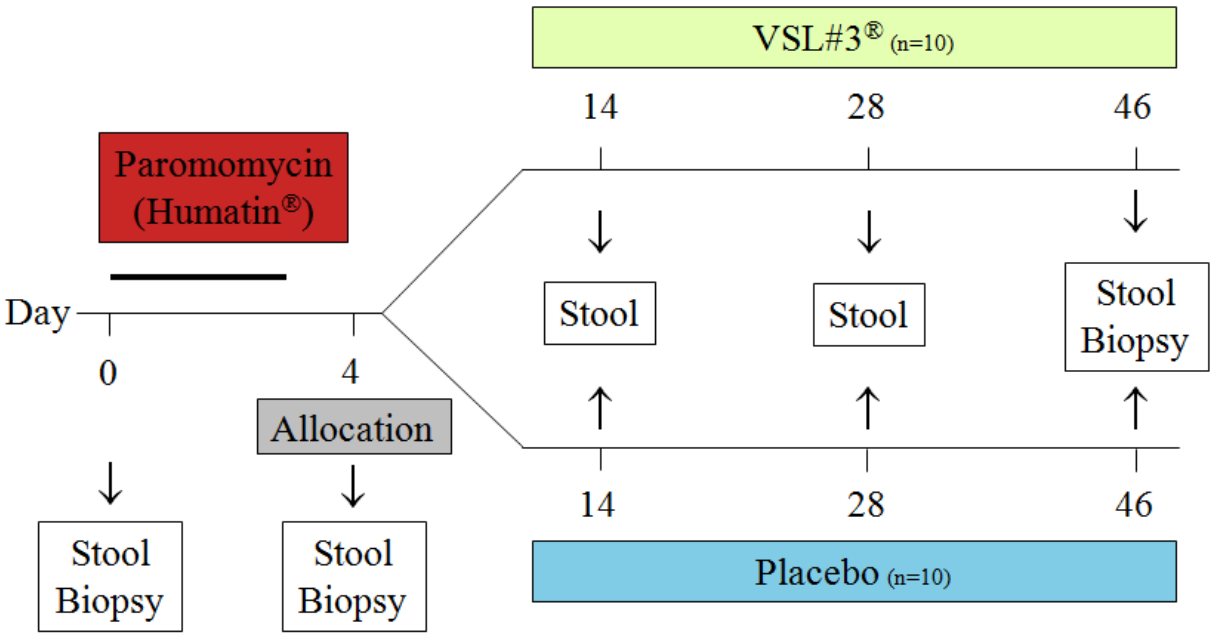

Figure 2-1: Study design.

2.2 Methods

As previously described, the microbial profiles of the different timepoints were analysed by using the culture-independent approach of amplification and sequencing of the 16S rRNA gene which is found in all bacteria and archaeae. It can be subdivided into highly conserved primer binding sites and nine variable regions (V1-V9), which depict species-specific signatures. The 16S rRNA gene can directly be isolated by PCR with universal primers targeting the conserved regions.

2.2.1 16S rRNA gene clone libraries from stool samples

Five stool samples have been collected from each individual: At the beginning of the study (Day 0), after the three day antibiotic treatment (Day 4) and three more samples during the allocation to placebo or the probiotic VSL#3 (Days 14, 28 and 46). For the generation of the clone libraries the bacterial 16S rRNA gene encompassing the variable regions one to four (V1-V4) was amplified, ligated into the pCR® 2.1 vector, transformed into competent *E. coli* cells and finally Sanger sequenced.

2.2.1.1 Extraction and purification of DNA from stool samples

The extraction as well as the purification of the DNA from stool samples were performed with the FastDNA® SPIN for Soil Kit (MP Biomedicals). For the extraction of the stool-DNA a small amount of the thawed stool sample (around 50 mg) was filled into a 1,5 ml reaction tube (Eppendorf). To disrupt the cell walls 200 µl of TL buffer (PeqLab) and 25 µl of proteinase K (Fermentas) were added and the tube was stirred at 55°C for 2 h. The dissolved stool sample was transferred to a Lysing Matrix E tube and 978 µl sodium phosphate buffer and 122 µl MT buffer were added. After a homogenization step for 45 seconds at speed 4 in a FastPrep FP 120 (Bio 101), a centrifugation step (13.000 rpm (rounds per minute), 30 seconds) for pelletizing the debris followed. The supernatant was transferred into a clean 2 ml reaction tube and 250 µl Protein Precipitation Solution (PPS) were added and mixed by inverting the tube several times. To pellet the precipitate the tube was centrifuged at 13.000 rpm for five minutes. 1 ml of the resuspended Binding Matrix was filled into a new 2 ml tube. After settling of the silica matrix 300 µl were discarded. The supernatant of the centrifuged sample was added and the reaction tube (containing the Binding Matrix and the sample) was inverted by hand for two minutes to allow the binding of the DNA to the matrix. The tubes were placed in a rack for seven minutes until the silica matrix had settled. 1.5 ml of the supernatant

were discarded. The matrix was resuspended in the remaining liquid, transferred to a SPIN™ Filter and centrifuged at 13.000 rpm for one minute. The Filter was placed onto a new tube (the catch tube was discarded) and 500 µl SEWS-M were added to resuspend and wash the pellet followed by a centrifugation step of 13.000 rpm for one minute. After emptying the catch tube the SEWS-M and the centrifugation step were repeated. To dry the matrix another centrifugation step at 13.000 rpm for two minutes was performed. The SPIN™ Filter was put into a new 1.5 ml reaction tube and air dried at room temperature for seven minutes. For the first elution 80 µl DES (DNAse/Pyrogen-Free Water) were pipetted onto the matrix, incubated for 15 minutes and centrifuged at 13.000 rpm for one minute. For the second elution 20 µl DES were pipetted onto the Filter and (without incubation) centrifuged at 13.000 rpm for one minute. The SPIN™ Filter was discarded and the DNA within the tube was stored at -20°C.

For the DNA purification the same kit was used. 50 µl of the DNA were mixed with 489 µl sodium phosphate buffer, 61 µl MT buffer and 125 µl PPS in a 2 ml reaction tube by inverting ten times by hand. 500 µl of the resuspended Binding Matrix were added and mixed for two minutes. After settling of the matrix (approx. seven minutes) 650 µl of the supernatant were discarded and the matrix was resuspended in the remaining liquid and transferred onto a SPIN™ Filter. The SPIN™ Filter was centrifuged for one minute at 13.000 rpm. After emptying the catch tube 250 µl SEWS-M are pipetted onto the filter and the filter containing tube was centrifuged at 13.000 rpm for one minute and afterwards dried at 13.000 rpm for two minutes. The SPIN™ Filter was placed onto a new 1.5 ml tube and air dried for seven minutes. The following two elution steps were performed as described above.

2.2.1.2 Amplification of the V1-V4 region of the 16S rRNA gene from stool samples

To target the variable regions V1 to V4 of the 16S rRNA gene a fragment of around 800 base pairs (bp) was amplified from each stool sample with the universal primers TPU1 and 805R (Table 2-3). Table 2-5 shows the composition of a standard PCR reaction with an end volume of 50 µl.

Table 2-5: Composition of a standard PCR reaction for the amplification of the V1-V4 region of the 16S rRNA gene from stool samples.

Components	Volume/Reaction	Final Concentration
Nuclease-Free Water	39.8 µl	
10x PCR Buffer (15 mM)	5 µl	1 x (1.5 mM $MgCl_2$)
$MgCl_2$ (25 mM)	2 µl	1 mM
Forward Primer TPU1 (10 µM)	0.5 µl	0.1 µM
Reverse Primer 805R (10 µM)	0.5 µl	0.1 µM
dNTPs	1 µl	200 µM of each
Taq DNA Polymerase (5 U/µl)	0.2 µl	1 U (0.02 U/ µl)
Template DNA	1 µl	
Final volume	50 µl	

The reagents were purchased from Qiagen, Peqlab (dNTPs) and Metabion (primers). The PCR program is described in Table 2-6.

Table 2-6: PCR program for the amplification of the V1-V4 region of the 16S rRNA gene from stool samples.

95°C	5 min	
95°C	30 sec	30 cycles
55°C	30 sec	
72°C	1 min	
72°C	10 min	

The PCR products were analyzed on a 1.5 % agarose gel to ascertain the correct amplicon size (about 800 bp, verified with the 100 bp Gene Ruler (Fermentas)). The amplicons were then ligated and transformed into competent *E. coli* cells.

2.2.1.3 Ligation of the amplified V1-V4 region into the pCR® 2.1 vector

The pCR® 2.1 TOPO TA Cloning® Kit (Invitrogen) was used for the ligation of the amplified 800 bp fragments and the subsequent transformation into competent *E. coli* cells. The employed taq polymerase has a nontemplate-dependent activity that adds a single deoxyadenosin (A) to the 3´ends of the PCR products. The linearized vector supplied in the kit has single 3´deoxythymidine (T) residues thereby allowing the PCR inserts to ligate efficiently with the vector.

Table 2-7: Ligation reaction mix.

Component	Volume/Reaction	Final Concentration
Sterile Water	4 µl	
10 x Ligation Buffer	1 µl	1 x
pCR® 2.1 vector (25 ng/µl)	2 µl	5 ng/µl
T4 DNA Ligase (4 U/µl)	1 µl	4 U (0.4 U/µl)
Fresh PCR product	2 µl	
Final volume	10 µl	

All components were pipetted into a pre-cooled Eppendorf tube, mixed gently and incubated at 14°C overnight.

2.2.1.4 Transformation into competent *E. coli* cells and subsequent growing of clones

One 50 µl vial of frozen competent *E.coli* cells was thawed on ice. Two µl of the ligation reaction were pipetted directly into the vial, mixed and incubated on ice for 30 minutes. A heat shock was performed for 30 seconds at 42°C and the vial was immediately placed back on ice for two minutes. 200 µl pre-warmed (37°C) SOC-Medium (Invitrogen) were added and the vial was stirred in a shaking incubator at 37°C at 350 rpm for one hour. 60 µl of the bacteria-SOC-mixture were spread on ampicillin-containing (50 µl/ml LB media) X-gal-coated (40 µl/plate) LB agar plates and incubated at 37°C overnight. Three plates were prepared for each sample. To allow a proper blue-white staining the plates were stored at 4°C for one additional day.

The technique of blue-white screening is based on a gap within the *lacZ* gene with the *lacZ* gene coding for the n-terminal α fragment of the β-galactosidase. The multiple cloning site of the pCR® 2.1 vector is located within the *lacZα* gene. Therefore successful ligation disrupts the *lacZα* gene and no functional β-galactosidase can be formed resulting in white colonies after incubation with X-gal. Colonies without insert express the α fragment and color blue.

200 µl of the liquid LB media containing ampicillin (50 µl/ml LB) were pipetted into each well of a deep-well-plate. For each sample 192 white colonies were picked from the agar plates with an autoclaved toothpick and put into the LB containing wells. The plates were sealed and the colonies were allowed to grow at 37°C in a shaking incubator overnight.

LB-medium was produced by dissolving 12.5 g LB-Medium (Luria/Miller (Roth) and 7.5 g Difco™ Agar Noble (BD) in 500 ml aqua dest. The medium was autoclaved and stored at 4°C. For plate pouring the medium was liquefied, ampicillin (50 µl/ml LB media) was added

to the hand-warm medium and the plates were poured into petri dishes. After hardening, they were coated with X-gal (40 µl/plate). X-gal consists of 40 mg X-gal (Fermentas) per one ml dimethylformamide. For the preparation of liquid LB medium 12.5 g LB-Medium (Luria/Miller (Roth)) were dissolved in 500 ml aqua dest.. After autoclaving it was stored at 4°C. Before use the medium was mixed with ampicillin at a concentration of 50 µl/ml LB. In general ampicillin was prepared by solubilizing 0.2 g ampicillin (Sigma-Aldrich) in one ml nuclease-free water.

2.2.1.5 Colony PCR

To check for the correct insert size a colony PCR was performed. Inserts were amplified using the vector specific primers M13(16)F and M13(17)R in a final volume of 50 µl. After the denaturation of 2.5 µl of the overnight grown bacteria (per well) at 95°C for ten minutes the PCR mix described in table 2-6 was simply added to the 96 well-format plates.

Table 2-8: Composition of the M13-colony-PCR reaction.

Component	Volume/Reaction	Final Concentration
Nuclease-Free Water	40.35 µl	
10 x Dream Taq™ Buffer (20 mM $MgCl_2$)	5 µl	1 x (2 mM $MgCl_2$)
Forward Primer M13(16)F (10 µM)	0.5 µl	0.1 µM
Reverse Primer M13(17)R (10 µM)	0.5 µl	0.1 µM
dNTPs	1 µl	200 µM of each
Dream Taq™ DNA Polymerase (5 U/ µl)	0.15 µl	0.75 U (0.015 U/ µl)
Denaturated Bacteria	2.5 µl	
Final volume	50 µl	

The reagents were purchased from Fermentas, Peqlab (dNTPs) and Metabion (primers).

Table 2-9: PCR program for the M13-colony-PCR reaction.

95°C	10 min	
95°C	1 min	32 cycles
52°C	30 sec	
72°C	1 min	
72°C	10 min	

The PCR products were analyzed on a 1.5 % agarose gel to ascertain the correct amplicon size (about 970 bp, verified with the 100 bp Gene Ruler (Fermentas)).

2.2.1.6 PCR product purification for the sequencing according to the method of Sanger

For Sanger sequencing the PCR products underwent a purification step with an ExoI-SAP mixture. The exonuclease I (Exo I) (Fermentas) removes single stranded DNA and primer, the shrimp alkaline phosphatase (SAP) (Fermentas) hydrolyses remaining dNTPs. For one reaction 5.625 µl water were mixed with 0.3 µl SAP and 0.075 µl Exo I. Four µl of the M13-colony-PCR product were added for the final volume of 10 µl and placed into a 37 °C thermo cycler for 15 minutes. With the subsequent incubation at 72 °C for 15 minutes the enzymes ExoI and SAP were inactivated.

2.2.1.7 Sequencing according to the method of Sanger

The sequencing was performed with the chain termination method according to Frederick Sanger as described in 1.6. (Sanger et al. 1977).

The composition of the sequencing reaction is described in Table 2-10, the PCR program in Table 2-11.

Table 2-10: Composition of the sequencing PCR reaction according to the method of Sanger.

Component	Volume/Reaction	Endconcentration
Sterile water	4.8 µl	
5x BigDye® Terminator v1.1 Sequencing Buffer	1.85 µl	0.93x
BigDye® Terminator v1.1 Ready Reaction mix	0.35 µl	
Primer TPU1 (3.2 µM)	1 µl	0.32 µM
Purified PCR product	2 µl	
Final volume	10 µl	

Table 2-11: PCR program for the sequencing reaction according to the method of Sanger.

96°C	1 min	
96°C	10 sec	25 cycles
50°C	5 sec	
60°C	4 min	

For the sequencing reaction the ABI PRISM® BigDye® Terminator v1.1 Cycle Sequencing Kit (Applied Biosystems) was used, with the BigDye® Terminator v1.1 Ready Reaction mix containing the dNTPs, the different labeled ddNTPs and the polymerase. The sequencing reaction product had to be purified of not-incorporated ddNTPs before the electrophoretic separation. Therefore Sephadex™ G-50 Superfine (GE Healthcare) containing columns were

used. The ddNTPs were absorbed by the Sephadex™ matrix, whereas the DNA passed the columns and was purified concomitantly. The eluate was then sequenced on a 3730*xl* DNA Analyzer (Applied Biosystems).

2.2.1.8 Analysis of the 16S rRNA gene sequences generated by the method of Sanger

The sequences were analyzed with the program MOTHUR version v.1.21.0 if not stated otherwise (Schloss et al. 2009). The sequences were aligned and screened for a minimum length of 700 bp and a maximum of seven homopolymers. The start and end points of the sequences were trimmed to range from position 43 to 754 (*E.coli* reference) and therefore encompass the variable regions V1 to V4. The sequences were further checked for possible chimeras with the chimera uchime command implemented in MOTHUR. Sequences that did not fulfill the given criteria or were detected to be chimerical, were excluded.

For a first overview of the present phyla the sequences were classified according to the reference sequences of the Ribosomal Database Project (RDP) (Wang et al. 2009; Cole et al. 2008). The identification of the microbial profiles on a finer taxonomic level was performed with an OTU-based analysis (operational taxonomic unit). For the OTU-based analysis a distance matrix was created by calculating uncorrected pair-wise distances between the aligned sequences. The cluster command using the average neighbor method (MOTHUR) was then performed to assign the sequences into OTUs (Schloss and Westcott 2011). The cutoff was set to 0.03, therefore clustering sequences showing at least 97% similarity into the same OTU, which indicates species level. A cutoff of 0.05 indicates genus level, whereas family level is indicated by a cutoff of 0.10. The OTU assignment was the basis for the subsequent analysis of the diversity and the identification of microbial profiles. The diversity, which is the variation, can be subdivided into α-diversity and β-diversity (Whittaker 1972).

The α-diversity refers to diversity within a particular sample. Therefore the Good´s coverage estimation (Good 1953) was calculated. The coverage is defined as [1 - (n/N)] x 100, where n is the number of singleton sequences (OTUs with only one sequence) and N is the total number of sequences within the analyzed clone library. In addition the rarefaction curves were plotted showing the function of the number of species found to the clones that have been picked and sequenced. A steep increase and therefore also a low coverage indicates that a large amount of species are undetected and could be discovered by further sampling, whereas a smoother curve and therefore also a higher coverage indicates for appropriate sampling. With regard to richness, which is expressed as the number of species and is therefore just the simple count of the species found, the number of observed OTUs as well as the Chao1 species

richness were calculated (Chao 1984). The Chao1 species richness is an estimate of how many different sequences would be identified, if no more species would be found by further sampling. The equation therefore takes into account the observed number of species (which is the observed number of OTUs), the number of singletons (OTUs with only one sequence) and the number of doubletons (OTUs with only two sequences). Apart from richness, evenness quantifies how consistent the abundance of the species is. Richness combined with evenness results in diversity. The Shannon diversity H´ is calculated taking into account the number of species/sequences in OTUi and the total number of species/sequences within the community/all OTUs (Magurran 1988; Shannon 1948).

The β-diversity refers to the diversity between the samples. Based on the OTU assignment the unweighted and weighted sample-wise Bray-Curtis index was calculated with the R package vegan. The unweighted index is a qualitative measurement and compares the community composition regarding presence and absence of the data, whereas the weighted index is a quantitative measure and takes into account the relative abundance of each species. The Bray-Curtis index (BC) is a common metric that describes the dissimilarity between two communities and compares them in terms of the minimum abundance of each species/OTU. The exact formula is defined by one minus twice the sum of the minimum number of individuals in the ith OTU of community A and B divided by the sum of the number of individuals in the ith OTU of community A and community B [$D_{Bray\text{-}Curtis} = 1 - 2*(\Sigma \min (S_{A,i}, S_{B,i})) / \Sigma S_{A,i} + \Sigma S_{B,i})$]. The Bray-Curtis index is directly linked to the Sørensen similarity index (QS) and is one minus the Sørensen index (BC = 1-QS) between the same two communities. The Bray-Curtis index ranges between 0 and 1, where 0 indicates the two communities having the same composition and 1 that they do not share any species (Legendre & Legendre 1998; Bray & Curtis, 1957). Based on the unweighted as well as the weighted Bray-Curtis indices the MOTHUR-implemented PCoA command (Principal Coordinate Analysis) turned the indices into points in a space with a number of dimensions one less than the number of samples. The data points were visualized in a biplot using R. Possible significant differences between the clusters representing the different timepoints/treatments were tested with an AMOVA (2.2.1.9). To reduce the dataset and to take into account only the most abundant OTUs a SIMPER (similarity percentage) analysis implemented in the program PAST was conducted (Hammer et al. 2001). The SIMPER analysis is a simple method to assess which OTUs are primarily responsible for an observed difference between groups of samples (Clarke 1993). OTUs that contributed at least 0.5% to the overall similarity were included in the subsequent analyses. Based on the reduced dataset a Spearman correlation was

performed using R to identify OTUs that are responsible for the clustering of the timepoints and treatment groups. Further the Spearman correlation was performed on the taxon level, in which all OTUs representing the same genus were treated as one group. All correlated OTUs and taxa were plotted into the proper biplots. Another approach to check for responsible OTUs explaining differences between treatment groups and timepoints is the metastats approach and the search for indicator species. The same SIMPER-reduced datasets were used for the metastats approach as well as for the search for indicator species. The metastats approach compares the mean proportion and the variance of the OTUs between two environments (here: timepoint/treatment) (White et al. 2009). The indicator species defines a trait which is characteristic for the difference of two investigated environments (here: timepoints or treatments). In contrast to the metastats approach it not only compares the mean and the variance of the OTUs, but also the patterns of distribution of the OTUs found in the environment. Since the indicator species approach is a permutation model, 10^4 permutations were conducted (Dufrêne and Legendre 1997).

The final classification of the OTUs and taxa was performed with a BLAST against the reference sequences of the Ribosomal Database Project (RDP), which is implemented in MOTHUR (Cole et al. 2009). The classification on species level was conducted with a BLAST against the 16S ribosomal RNA sequences database of the NCBI (National Center for Biotechnology Information).

2.2.1.9 Statistical analysis

To test for significant differences in the richness and diversity indices the R package exactRankTests was used. The significance of differences between the timepoints "Day 0" and "Day 4" was calculated with the paired Wilcoxon signed rank test (Wilcoxon 1945). To check for an influence of the probiotic in comparison to the placebo the timepoint "Day 46" was set as the most important timepoint and displays the central question of the study. Due to the fact that for the analysis of the mucosa-associated microbiota this "Day 46" was the only timepoint at which samples had been taken during the probiotic and placebo therapy, the differences between the therapies at the "Day 14" and "Day 28" within the analysis of the luminal microbiota were seen as less important intermediate timepoints. For the analysis of the influence of the probiotic the difference between the timepoints "Day 0" and "Day 46" was calculated and the subsequent unpaired Wilcoxon rank sum test (also called Mann-Whitney U) was used to test the placebo against the probiotic group (Mann and Whitney 1947). The same procedure was used for the timepoints "Day 14" and "Day 28", but those

values had not to be corrected for multiple testing due to the fact that this was a secondary approach. The appropriate randomization into the later placebo and probiotic group was checked by calculating the difference between the timepoints "Day 0" and "Day 4" and to test the later placebo group against the later probiotic group with the Wilcoxon rank sum test. To check for resilience the timepoints "Day 14", "Day 28" an "Day 46" were compared to the "Day 0" by the Wilcoxon signed rank test. All results of the statistical tests were corrected for multiple testing by the Bonferroni-Holm correction (Holm 1979). P values less than 0.05 after Bonferroni-Holm correction indicated a significant difference between the two tested groups.
To test if the samples cluster together according to the timepoint or treatment and if clusters are significantly separated from each other as supposed by the PCoA an analysis of molecular variance (AMOVA) was performed by using the Bray-Curtis indices. The AMOVA in general is the non-parametric analog of the analysis of variance and tests whether the centers of the clusters representing the different treatment groups or timepoints are more separated than the variance among the samples within a cluster. For each AMOVA 10^4 permutations were performed. The resulting p-values were corrected for multiple testing due to the Bonferroni-Holm correction. A corrected p-value below 0.05 was considered significant.

2.2.2 16S rRNA and 16S rRNA gene libraries from biopsy samples

For each individual three biopsies from the sigmoid colon had been collected via sigmoidoscopy. The first at the beginning of the study (day 0), the second after the three days of antibiotic treatment (day 4) and the last at the end of the study (day 46). The bacterial 16S rRNA gene encompassing the variable regions one and two (V1-V2) was amplified and sequenced with the pyrosequencing 454 technology.

2.2.2.1 Extraction of DNA and RNA from biopsy samples

The extraction of DNA and RNA from the biopsy samples was performed with the AllPrep DNA/RNA Mini Kit (Qiagen). The biopsies had been stored at -80°C and the first steps of the extraction were performed in liquid nitrogen. The biopsy was transferred into a pre-cooled reaction tube (Eppendorf) and squashed with a pestle. 600 µl of the RLT-buffer/β-Mercaptoethanol mixture (1 µl β-Mercaptoethanol per 100 µl RLT-buffer) were added. After the biopsy was thawed it was filled into a Lysing Matrix E tube (MP Biomedicals) and homogenized in a FastPrep FP 120 (Bio 101) at speed 4 for 45 seconds twice. After the incubation for two hours at room temperature, the tube was centrifuged at 13.000 rpm for 30 seconds. The supernatant was transferred into a QIAshredder™ column and centrifuged at

13.000 rpm for two minutes. The supernatant was pipetted into the AllPrep DNA Mini Spin Column and the column was centrifuged at 10.000 rpm for 30 seconds. The collection tube contained the RNA, while the filter contained the DNA and was placed onto a new 2 ml collection tube and temporarily stored at 4°C.

600 µl of 70% ethanol (Sigma-Aldrich) were pipetted into the collection tube containing the RNA and gently mixed with the pipette tip. The RNA/ethanol solution was transferred into a RNeasy Mini Spin Column and centrifuged at 10.000 rpm for 15 seconds. The flow-through was discarded and the step repeated with the remaining RNA-ethanol solution. 350 µl of RW1 buffer were pipetted onto the column and centrifuged at 10.000 rpm for 15 seconds. The flow-through was discarded. 80 µl of the DNAse-Incubation-Mix (70 µl RDD buffer + 10 µl DNAse Solution) were pipetted onto the column membrane and incubated for 15 minutes at room temperature. 350 µl RW1 buffer were added and the column was centrifuged at 10.000 rpm for 15 seconds. The flow-through was discarded. 500 µl RPE were added and centrifuged at 10.000 rpm for 15 seconds, the flow-through was discarded. 500 µl RPE were pipetted a second time and centrifuged at 10.000 rpm for two minutes. The flow-through was discarded and the column centrifuged an additional time at 13.000 rpm for one minute. The collection tube was discarded and the column placed into a RNAse-free 1.5 ml reaction tube. 50 µl RNAse-free water were added and incubated at room temperature for five minutes. The tube was centrifuged at 10.000 rpm for one minute. The reaction tube now contained the RNA and was stored at -80°C.

500 µl of buffer AW1 were added to the temporarily stored collection tube containing the DNA and centrifuged at 10.000 rpm for 15 seconds. The flow-through was discarded. 500 µl buffer AW2 were pipetted onto the column and centrifuged at 13.000 rpm for two minutes. The flow-through was again discarded. The column was placed onto an new 1.5 ml reaction tube, 100 µl EB-buffer were directly pipetted onto the membrane and incubated at room temperature for one minute. The tube was centrifuged at 10.000 rpm for one minute and the solution within the tube was once again eluted via the column. The reaction tube was centrifuged at 10.000 rpm for one minute, contained the DNA then and was stored at -20°C.

2.2.2.2 Reverse Transcription of RNA

The extracted RNA had to be reverse transcribed into cDNA. This was done with the High Capacity cDNA Reverse Transcription Kit (Applied Biosystems). The composition of the PCR reaction can be looked up in Table 2-12.

Table 2-12: Composition of the reverse transcription PCR reaction.

Component	Volume/Reaction	Endconcentration
RT-PCR Grade Water	3.2 µl	
10x RT Buffer	2.0 µl	1x
10x RT Random Primers	2.0 µl	1x
25x dNTP Mix (100 mM)	0.8 µl	1x (4 mM)
MultiScribe™ Reverse Transcriptase (50 U/µl)	1.0 µl	50 U (2.5 U/µl)
RNAse Inhibitor (20 U/µl)	1.0 µl	20 U (1 U/µl)
RNA template	10 µl	
Final volume	20 µl	

The program for the reverse transcription PCR was ten minutes at 25°C followed by 120 minutes at 37°C and five seconds at 85°C.

2.2.2.3 Amplification of the V1-V2 region of the 16S rRNA and the 16S rRNA gene from biopsy samples

The pyrosequencing approach targeted the V1 and V2 region. Therefore specific primers were used (see Table 2-1). The Pyro_27F primer (5´- CTA TGC GCC TTG CCA GCC CGC TCA GTC *AGA GTT TGA TCC TGG CTC AG* -3´) consists of the B-Adaptor (underlined) and the universal primer 8F (italic). The MIDX_338R primers (5´- CGT ATC GCC TCC CTC GCG CCA TCAG NNNNNNNNNN CA *TGC TGC CTC CCG TAG GAG T* -3´) comprises the A-Adaptor (underlined), a unique 10-base barcode (N) and the broad range bacterial 338R primer (italic). Due to 50 different barcodes (and therefore 50 different reverse primers (see Table 2-3)) it was possible to pool up to 50 different samples into the same library (see 2.2.2.4). Each sample was amplified in a final volume of 25 µl in duplicate. To be sure of having uncontaminated PCR products a negative control was moved along with each sample/MID.

Table 2-13: Composition of a standard PCR reaction for the amplification of the V1-V2 region of the 16S rRNA gene and the 16S rRNA from biopsy samples.

Component	Volume/Reaction	Endconcentration
RT-PCR Grade Water	ad 25 µl	
5x Phusion® HF Reaction Buffer (7.5 mM $MgCl_2$)	5.0 µl	1x (1.5 mM $MgCl_2$)
Pyro_27F (10 µM)	0.5 µl	0.2 µM
dNTPs	0.5 µl	200 µM of each
Phusion® Hot Start II DNA Polymerase (2 U/µl)	0.25 µl	0.5 U (0.02 U/µl)
MIDX-338R (10 µM)	0.5 µl	0.2 µM
DNA/cDNA template	2-4 µl	
Final volume	25 µl	

Buffer and polymerase were contained in the Phusion® Hot Start DNA Polymerase Kit from ThermoFisher Scientific. The other reagents were purchased from Peqlab (dNTPs) and Metabion (primers).

Table 2-14: PCR-program for the amplification of the V1-V2 region of the 16S rRNA gene and the 16S rRNA from biopsy samples.

98°C	3 min	
98°C	10 sec	30 cycles
57°C	30 sec	
72°C	30 sec	
72°C	10 min	

The replicate PCR products were pooled and loaded on a 2% agarose gel. After an electrophoresis at 100V for 75 min, the band with the size of about 420 bp (verified with the 100 bp Gene Ruler (Fermentas)) was cut with a gel excision tip (Biostep) under UV light and transferred into a 1.5 ml reaction tube for further gel extraction.

2.2.2.4 Gel extraction and pooling of amplicons

For the gel extraction the Min Elute® Gel Extraction Kit (Qiagen) was used. 200 µl of buffer QG were added to the cut band and incubated at 50°C for ten minutes. For a better dissolution of the band the tube was vortexed every 2-3 minutes during the incubation. 68 µl 2-Propanol (Sigma-Aldrich) were added to the sample and mixed by inverting several times. The liquid was transferred into a MinElute column and centrifuged at 13.000 rpm for one minute. The flow-through was discarded, 500 µl buffer QG were added and the tube centrifuged again at 13.000 rpm for one minute. A washing step was performed with 750 µl buffer PE followed by a subsequent centrifugation at 13.000 rpm for one minute. The flow-through was discarded

and the tube centrifuged for an additional minute. The MinElute column was placed into a new 1.5 ml reaction tube. For the elution 10 µl buffer EB were directly pipetted on to the filter membrane. After an incubation for one minute, the tube was centrifuged for one minute. Again 10 µl of buffer EB were added, incubated for one minute and centrifuged at 13.000 rpm for one minute. The extracted DNA/cDNA was contained within the tube. The concentration of DNA and cDNA was measured with the Qubit® ds DNA BR Assay Kit (Invitrogen) with a Qubit® 2.0 Fluorometer. Equal concentrations of the samples/amplicons containing different MIDs were pooled into one library. Each library was sequenced on a quarter slide with the 454 GS FLX (Roche) according to the recommended procedures of Roche.

2.2.2.5 Pyrosequencing with the GS FLX according to Roche

In comparison to the Sanger sequencing the pyrosequencing observes the DNA polymerase in action where one after the other nucleotide is incorporated into the newly synthesized DNA strand. The successful integration of a nucleotide is recognized via an enzyme system and a luciferase converted into light which is recognized by a detector. If the nucleotide does not fit there is no light.

For the generation of amplicon libraries PCR products were created by amplifying the template with specific fusion primers containing the 454 sequencing adaptor sequences as described in chapter 2.2.2.3. The adaptors were used for the subsequent purification, quantitation, amplification and sequencing steps. The single-stranded libraries were immobilized onto specifically designed DNA Capture Beads with each bead carrying a unique single-stranded library fragment. The beads were than emulsified with amplification reagents in a water-in-oil mixture mimicking microreactors containing just one bead with one unique sample-library fragment. The entire emulsions were than amplified in their microreactors in parallel to create millions of clonally copies of each library fragment on each bead. Subsequently the emulsions were broken while the amplified fragments remained bound to their specific beads. The fragments were enriched and the beads were loaded onto a PicoTiterPlate device, whereas the surface design allowed for only one bead per well. The PTP Device was then sequenced in the GS FLX (Roche). Individual nucleotides were flowed in a fixed order across the thousands of wells, each containing one bead. Each incorporation of one (or more) nucleotide(s) complementary to the template strand resulted in a detectable light signal which was recorded by the CCD camera within the instrument, with the signal strength being proportional to the number of nucleotides incorporated in a single nucleotide

flow. The 454 Sequencing Data Analysis software used the signal intensity of each incorporation event at each well position to determine the sequence of all reads in parallel.

2.2.2.6 Analysis of the 16S rRNA and the 16S rRNA gene sequences generated by pyrosequencing

The resulting sequence- and quality file containing all reads and Phred quality scores of a quarter slide were checked and sequences with a length of less than 200 bp and a minimum mean Phred quality score of 25 were discarded by utilizing the Perl-based software PANGEA (pipeline for analysis of next generation amplicons (Giongo et al. 2010)). The remaining sequences were split according to their sample-barcode using PANGEA as well. Samples with less than 2000 sequences were eliminated and repeated. The remaining sequences were denoised by eliminating sequences with ambiguous bases, with more than one difference to the primer sequence, more than seven homopolymers, a length less than 200 bp and sequences being chimerical using the software MOTHUR version v.1.21.0 (Schloss et al. 2009). Further the sequences were adjusted concerning the start and end point of the sequences ranging from position 43 to 337 (*E.coli* reference) and therefore covering the V1 and V2 region. To get rid of the uneven distribution of the sequence amount all samples were normalized to the lowest number of sequences.

The subsequent analyses were performed as described for the sanger-sequenced data. Again a first superficial classification and subsequent OTU-based analysis were performed (see 2.2.1.8).

2.2.2.7 Statistical analysis

Statistical significant differences within the different α-diversity indices were identified with the Wilcoxon signed rank test (paired samples) and the Wilcoxon rank sum test (unpaired samples) by using the exactRankTest package implemented in R. For the statistical analysis of the β-diversity an AMOVA (MOTHUR) was conducted. The Bonferroni-Holm correction was assessed to adjust for multiple testing (see 2.2.1.9) (Holm 1979).

2.2.3 Quantitative real-time PCR for quantitative results of bacteria

To receive additional information on the quantitative abundances of the total bacteria, the *Firmicutes* and the *Bacteroidetes* within the luminal as well as in the mucosa-associated microbiota a quantitative real-time PCR was performed with beta actin functioning as housekeeping gene. For the real-time PCR approach the Power SYBR® Green PCR Master Mix (Applied Biosystems) was used. 4.5 µl of the master mix were prepared with 0.0625 µl template (luminal DNA or mucosa-associated DNA or reverse transcribed RNA (see 2.2.1.1, 2.2.2.1 and 2.2.2.2), 0.125 µl of the forward and the reverse primer (10 µM each) and RT-PCR Grade Water to a final volume of 10 µl. Each sample was analysed in triplicate. The PCR program was as described in Table 2-15.

Table 2-15: PCR program of the quantitative real-time PCR.

50°C	2 min	
95°C	10 min	
95°C	15 sec	45 cycles (luminal samples)
60°C	1 min	50 cycles (fecal samples)
95°C	15 sec	establishes the melting curve
60°C	15 sec	
95°C	15 sec	

The results were obtained with the 7900HT Fast Real-Time PCR System (Applied Biosystems) and visualized with the software SDS 2.3 (Applied Biosystems).

2.2.3.1 Analysis of quantitative real-time results

The resulting cycle thresholds (C_t) were converted into a linear signal by calculating 2^{-Ct}. The median of the triplicates was used for the further analysis. Each sample was normalised to the beta actin value by calculating the ratio of the median 2^{-Ct} of the target to the median 2^{-Ct} of the respective beta-actin. The values of *Firmicutes* and *Bacteroidetes* could then be further set into relation to the values of the total bacteria. Differences between timepoints and treatments were calculated by using the Wilcoxon signed rank test (paired samples) and the Wilcoxon rank sum test (unpaired samples) with the exact RankTest package implemented in R as already described in 2.2.1.9 and 2.2.2.7). The correction for multiple testing was performed by the Bonferroni-Holm method (Holm 1979).

3 Results

3.1 16S rRNA gene clone libraries from luminal samples

For the generation of the clone libraries, the V1-V4 region of the 16S rRNA gene from stool (luminal) samples were amplified, ligated into the pCR® 2.1 vector and transformed into competent *E. coli* cells. 192 clones from each sample were picked, checked for the correct insert size and finally sequenced according to the method of Sanger.

The resulting 19.200 sequences (100 samples (20 individuals at five different timepoints) with 192 picked clones each) were cleaned by eliminating bad quality sequences (length less than 700 bp, more than seven homopolymers) as well as chimerical sequences with the program MOTHUR v.1.21.0 (Schloss et al. 2009). 3.292 sequences (17%) had to be discarded, resulting in a denoised final data set of 15.908 sequences for further analysis.

For the analysis, a first classification was performed to receive an overview of the involved phyla and the overall influence of the antibiotic and the subsequent probiotic or placebo therapy. In addition, an OTU-based analysis was performed. This approach assigns the sequences into "groups", the so-called Operational Taxonomic Units (OTUs), based on a threshold of 0.03. Therefore OTUs with a least 97% identity are assigned into the same OTU.

3.1.1 First classification of the denoised dataset of the luminal microbiota

A classification with the Ribosomal Database Project (RDP) (Cole et al. 2009) gave a first impression of the involved phyla. Figure 3-1 shows the percentages of the five phyla found within the fecal samples at timepoint "Day 0". These are in descending occurrence: *Firmicutes*, *Bacteroidetes*, *Actinobacteria*, *Proteobacteria* and others which encompass *Verrucomicrobia* and unclassified bacteria. This is a common picture of the phyla distribution of healthy individuals.

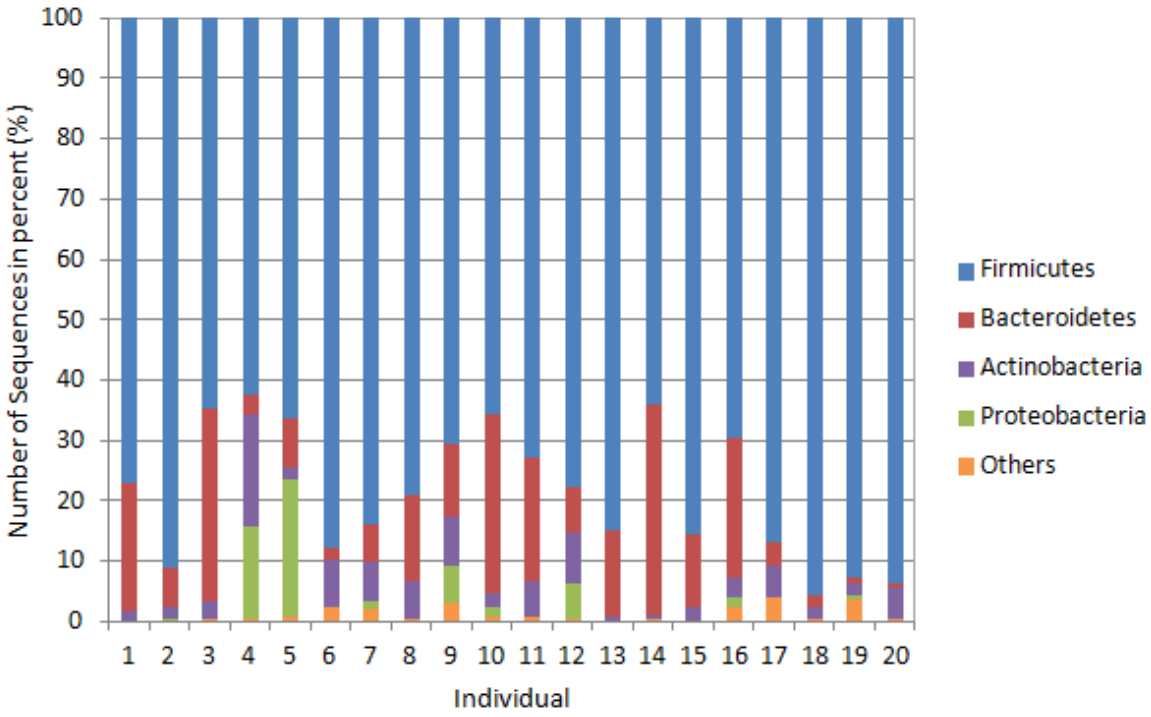

Figure 3-1: Phylum distribution of the luminal microbiota of the twenty healthy individuals at timepoint "Day 0". Described in percent. Sequences were generated by sequencing according to the method of Sanger.

To obtain an overview of the influence of the antibiotic and the subsequent placebo as well as probiotic treatment onto the phylum distribution, the sequences of the other timepoints were also classified via RDP. The median and the quartiles of the two main phyla, *Firmicutes* and *Bacteroidetes*, of each treatment group/timepoint were calculated and plotted into boxplots.

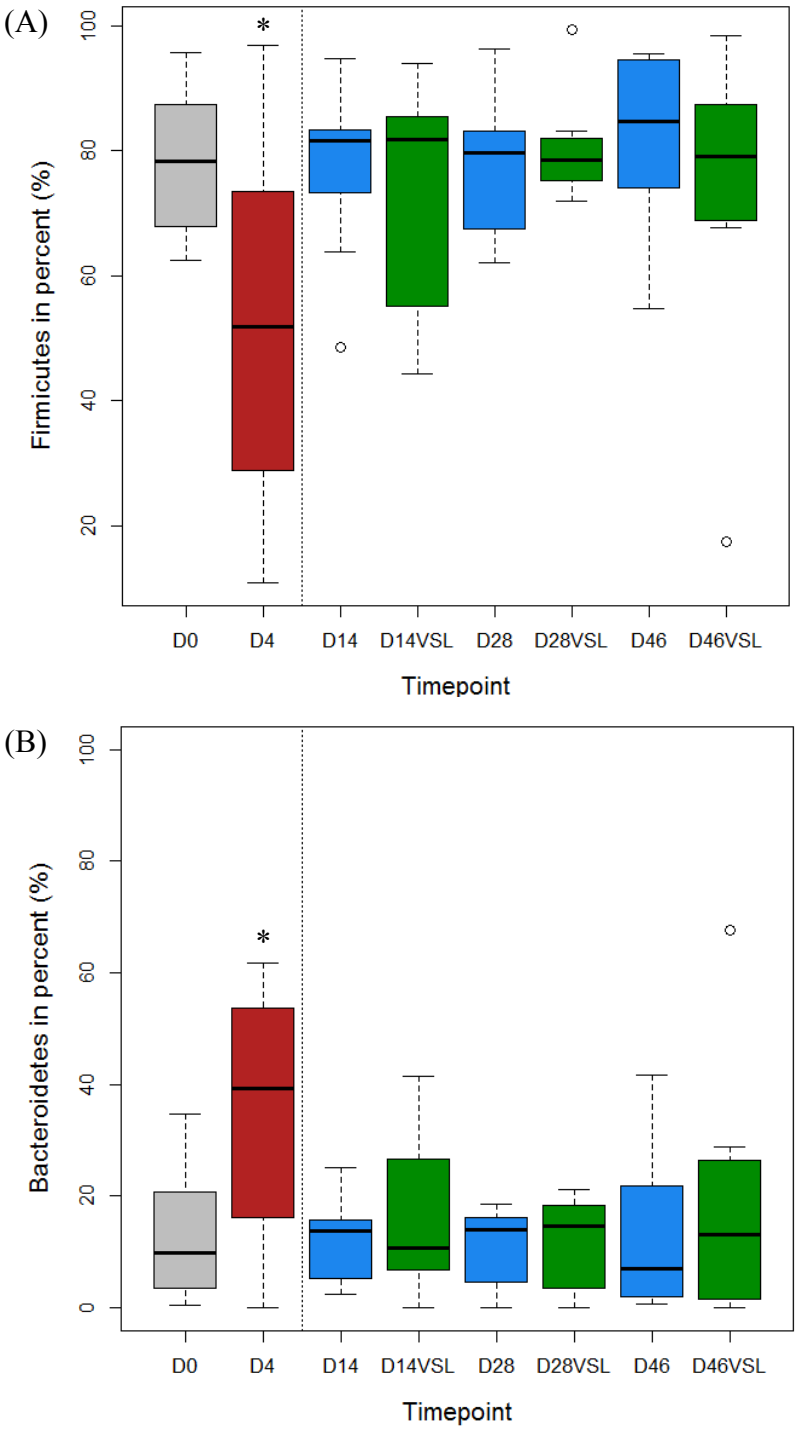

For the *Firmicutes* (Figure 3-2 (A)), which is the most abundant phylum in the luminal microbiota (nearly 80%), there was a significant decrease (p_{corr} = 0.0031) down to 52% due to the antibiotic treatment. After allocation to placebo or probiotic *Firmicutes* recovered reaching nearly the initial amount at Day 46 (comparison of "Day 0" and "Day 46", p_{corr} > 1). However, there is no significant difference between the placebo and the probiotic therapy at either of the three timepoints ("Day 14" and "Day 28" p_{corr} > 1 and "Day 46" p_{corr} = 0.8704). For *Bacteroidetes* (Figure 3-2 (B)) the opposite trend could be seen. Due to the antibiotic treatment there was a significant increase

Figure 3-2: Changes in the two main luminal phyla due to antibiotic treatment and subsequent placebo or probiotic therapy. (A) Firmicutes. (B) Bacteroidetes. Median, upper and lower quartile as well as upper and lower whisker are plotted. Grey (D0): Timepoint "Day 0" (n = 20), Red (D4): Timepoint "Day 4" after antibiotic treatment (n = 20), blue (D46): Timepoint "Day 46" after placebo therapy (n = 10), green (D46VSL): Timepoint "Day 46" after probiotic therapy (n = 10). * indicates significant difference compared to timepoint "D0" after Bonferroni-Holm correction.

(p_{corr} = 0.0019) of *Bacteroidetes* from 10% to nearly 40%. The allocation to the placebo or the probiotic treatment resulted in a decrease. Again there were no significant differences between the placebo and the probiotically treated group at all the three timepoints (p_{corr} > 1). Furthermore there was no significant difference between the timepoints "Day 0"and "Day 46" (p_{corr} > 1), indicating a good recovery.

Since the simple classification of the sequences will not give any more information regarding diversity and compositional changes of the microbiota an OTU-based analysis was performed.

3.1.2 OTU-based analysis

As a first step the cleaned 15.908 sequences within the final dataset were aligned by the Needleman-Wunsh algorithm. A distance matrix was then generated by calculating the uncorrected pair-wise distances between the aligned sequences. Based on the distances the sequences were assigned into OTUs with sequences having at least 97% similarity belonging to the same OTU, which corresponds to species level. Further the clustering was performed on the genus level, describing 95% identity. The clustering itself was based on the average neighbor method (for further details see chapter 2.2.1.8). The final dataset of 15.908 sequences were grouped into 6.862 OTUs, which are the basis for the subsequent analysis.

3.1.2.1 Alpha-Diversity

Measures of alpha diversity were applied to evaluate the aspects of bacterial diversity that may be influenced by treatment or timepoint. The alpha diversity in general describes the species composition within a specific sample.

The Good´s coverage estimation (Good 1953) is defined as [1 - (n/N)] x 100, where n is the number of singleton sequences and N is the total number of sequences within the analyzed clone library. It was very unequal in the investigated samples ranging between 4.19% to 94.59 % (for individual data see Table 7.2 in the appendix). A low coverage indicates many singletons and a therefore incomplete sampling. The rarefaction curves (Figure 3-3) show this figuratively. The sample with the lowest coverage represents a very steep rarefaction curve (10_D0), whereas the sample with the best coverage represents a quite smooth rarefaction curve (19_D4). The rarefaction curve of the sample 14_D14 is characterized by a median coverage.

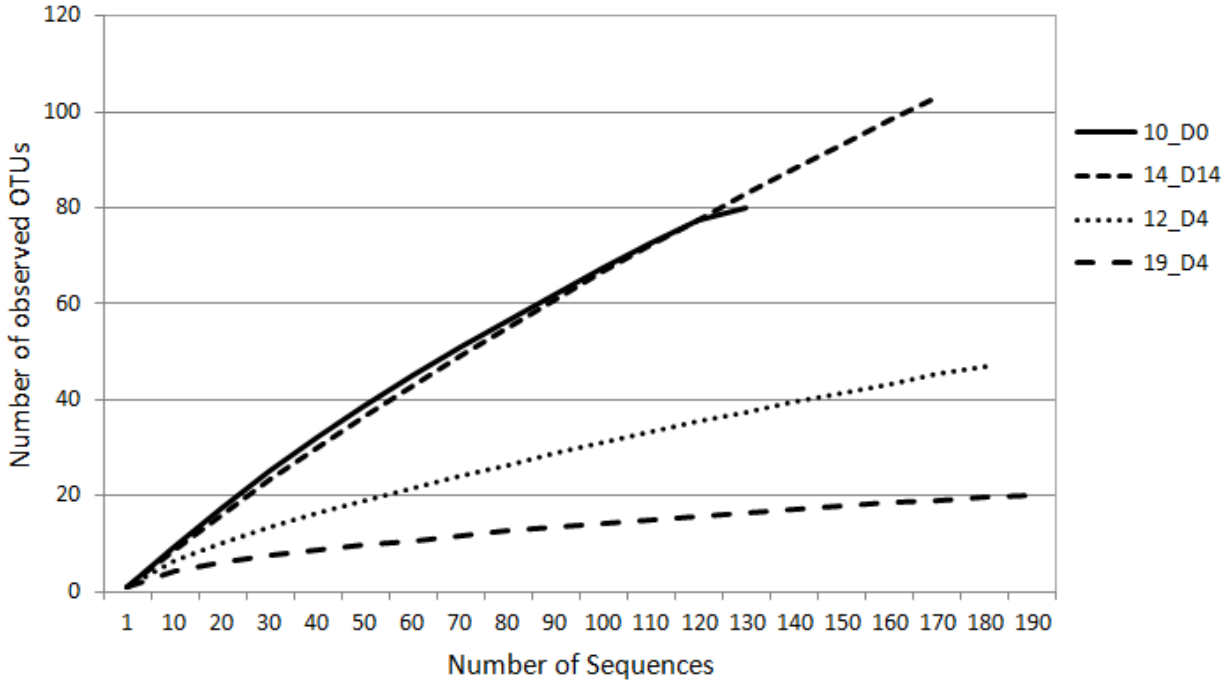

Figure 3-3: Rarefaction curves of the luminal samples of four individuals. Steep curves represent samples with a low coverage, whereas smoother curves represent a higher coverage.

The low coverage as well as the steep rarefaction curve of several samples show that the number of 192 clones that had been picked for each sample is not sufficient to catch all the different bacteria inhabited in this sort of sample to present a complete microbial profile. Nevertheless, the data enable a first estimation of the microbial variety. Therefore different measures that focus on species richness and diversity have been calculated.

Species richness in general is the number of different species in a given sample. Therefore the number of observed species as well as the Chao1 estimated richness was calculated. Based on the individual values (see Table 7.2 in the appendix) the means and the quartiles of the treatments and the timepoints were calculated and depicted as boxplots. The timepoints "Day 0" and "Day 4" comprise 20 individuals. Due to the subsequent allocation to different treatment groups the timepoints "Day 14", "Day 28" and "Day 46" are comprised of ten individuals within the placebo as well as in the probiotic group.

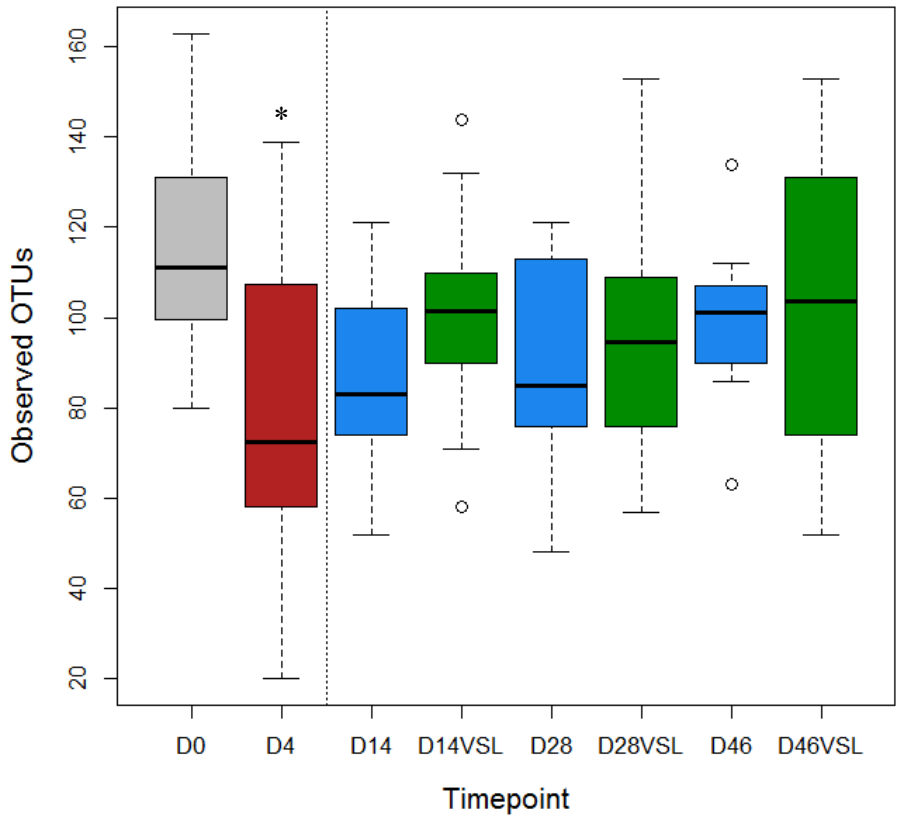

Figure 3-4: Boxplots of the number of observed OTUs of the luminal microbiota. Median, upper and lower quartile as well as upper and lower whisker are plotted. Grey (D0): Timepoint "Day 0" (n = 20), Red (D4): Timepoint "Day 4" after antibiotic treatment (n = 20), blue (D46): Timepoint "Day 46" after placebo therapy (n = 10), green (D46VSL): Timepoint "Day 46" after probiotic therapy (n = 10). * indicates significant differences after Bonferroni-Holm correction compared to timepoint "D0".

As depicted in Figure 3-4 the antibiotic treatment led to a significant decrease within the number of observed OTUs (Wilcoxon signed rank test: p_{corr} = 0.000504). The subsequent placebo as well as the probiotic therapy resulted in a regeneration. The central question was whether a significant difference between the placebo and the probiotic treatment at "Day 46" could be observed. That was not the case (Wilcoxon rank sum test: $p_{corr} > 1$). Also the differences between the placebo and the probiotic group at the timepoints "Day 14" (p_{corr} = 0.5508) and "Day 28" ($p_{corr} > 1$) were not significantly different. Since there was no significant difference between the placebo and the probiotic group at either of the timepoints, the placebo and the probiotic group of each timepoint were combined for the comparison to the initial timepoint "Day 0". For the comparison between Day 0 the particular timepoints "Day 14", "Day 28" and "Day 46" a Wilcoxon signed rank test was performed. All three comparisons were significant ("Day 14" p_{corr} = 0.0004082; "Day 28" p_{corr} = 0.00132 and "Day 46" p_{corr} = 0.02972), indicating that even after 43 days post antibiotic treatment the microbiota was not able to fully recover to the initial state of observed OTUs. To test for an appropriate randomization the differences of “Day 4” and “Day 0” were calculated and the later placebo and the later probiotic group were then compared with the Wilcoxon rank sum test. The result was not significant. Further no gender-dependent effects could be detected.

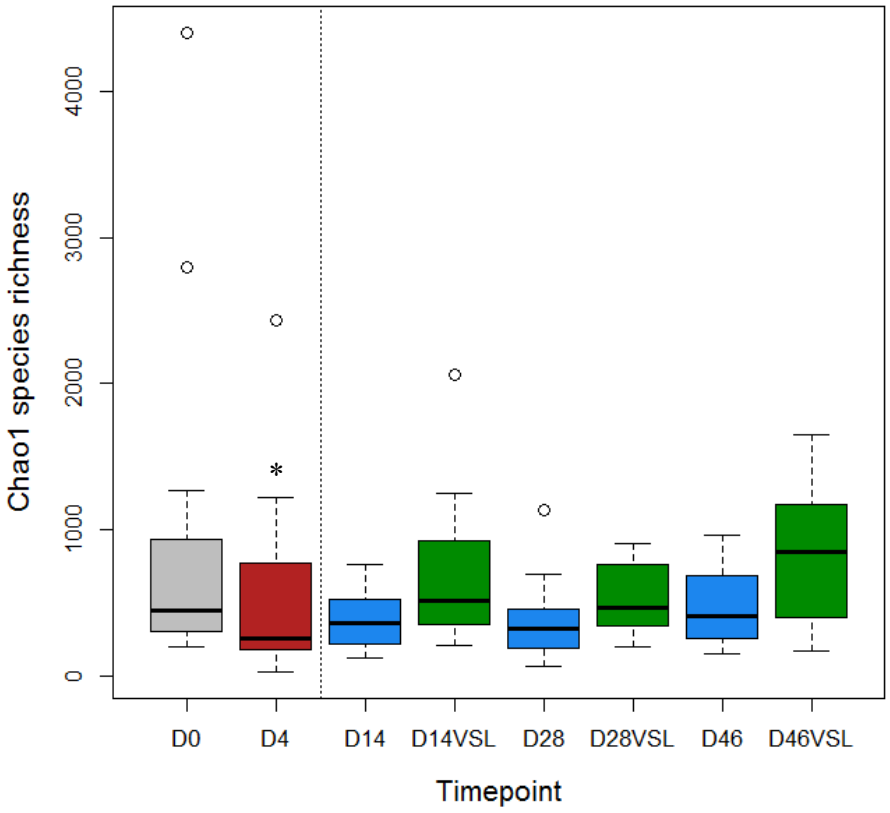

Figure 3-5: Boxplots of the Chao1 species richness of the luminal microbiota. Median, upper and lower quartile as well as upper and lower whisker are plotted. Grey (D0): Timepoint "Day 0" (n = 20), Red (D4): Timepoint "Day 4" after antibiotic treatment (n = 20), blue (D46): Timepoint "Day 46" after placebo therapy (n = 10), green (D46VSL): Timepoint "Day 46" after probiotic therapy (n = 10). * indicates significant differences after Bonferroni-Holm correction compared to timepoint "D0".

In addition to the observed OTUs the Chao1 estimator of species richness (Chao 1984) takes into account the number of OTUs with only one sequence ("singletons") and the number of OTUs with only two sequences ("doubletons"). A significant decrease (p_{corr} = 0.0441) in the Chao1 richness could be observed due to the antibiotic therapy (Figure 3-5). The subsequent randomisation was appropriate (p_{corr} = 0.6842). The regeneration resulted in a steady increase of richness, with values being higher within the probiotic group at each of the timepoints. However, the differences between the placebo and the probiotic do not reach statistical significance at either of the timepoints (“Day 14” p_{corr} = 0.786; “Day 28” p_{corr} > 1 and “Day 46” p_{corr} = 0.369). The comparisons of the timepoints "Day 14", "Day 28" and "Day 46" to timepoint "Day 0" revealed no significant differences. Further there was no gender-dependent effect.

Species diversity of a given sample is the number of different species in a particular sample weighted by the number of individuals belonging to a species (= species evenness). As shown before for the richness, diversity shows a decrease due to the antibiotic treatment (p_{corr} = 0.00014) (Figure 3-6). The randomization afterwards was appropriate (p_{corr} = 0.22578). However, there was no difference between the placebo and the probiotic group in the subsequent resilience at the timepoints "Day 14" (p_{corr} = 0.786) , "Day 28" (p_{corr} > 1) and "Day 46" (p_{corr} > 1). Further there were significant differences in the comparison of those

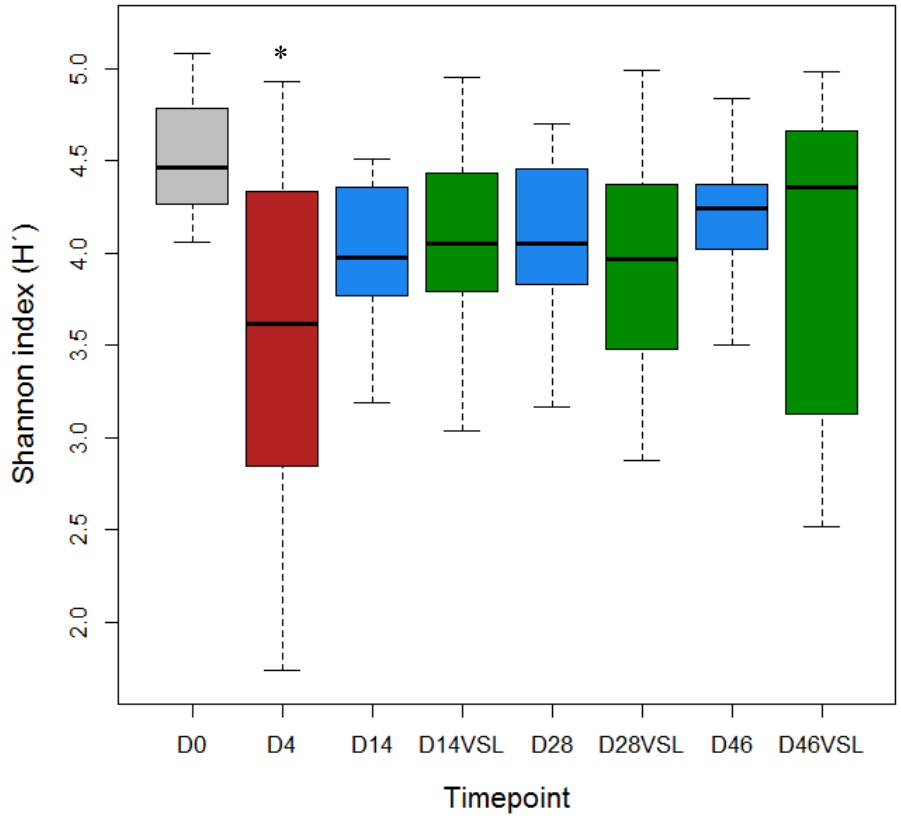

Figure 3-6: Boxplots of the Shannon H´ of the luminal microbiota. Median, upper and lower quartile as well as upper and lower whisker are plotted. Grey (D0): Timepoint "Day 0" (n = 19), Red (D4): Timepoint "Day 4" after antibiotic treatment (n = 19), blue (D46): Timepoint "Day 46" after placebo therapy (n = 10), green (D46VSL): Timepoint "Day 46" after probiotic therapy (n = 9). * statistically significant at a level of 0.05 after Bonferroni-Holm correction.

timepoints and the initial diversity of timepoint "Day 0" ("Day 14" p_{corr} = 5.7e-06; "Day 28" p_{corr} = 3.3e-04; "Day 46" p_{corr} = 0.0091). This indicates that the microbiota with regard to diversity is recovering and approximates to the initial composition during the time, but is finally not able to recover completely within the timeframe of the study.

Concerning alpha diversity it can be summed up that due to the antibiotic treatment there is a significant decrease in microbial richness as well as in diversity. A regeneration of the microbiota after allocation to placebo or probiotics is obvious (richness as well as diversity index increase again), but the recovery does not reach the initial composition as indicated by significant differences between the timepoints "Day 0" and "Day 46". Therefore it can be concluded that resilience is incomplete. Furthermore, the resilience process is independent of the probiotic therapy as there are no significant differences between the placebo and the probiotic group at any timepoint.

3.1.2.2 Beta-diversity

In general, beta diversity calculates the membership (presence/absence) and the structure (diversity) between the samples. Based on the OTU grouping the unweighted as well as the weighted Bray-Curtis indices were calculated for each sample-wise comparison with the R package vegan. The indices were transformed into data points by using a Principal Coordinate Analysis (PCoA) with three principal coordinates. This allows to look for the most important axes along which the samples vary and to find clusters. The results were plotted into a three-dimensional biplot using R.

Unweighted Bray-Curtis indices

Unweighted beta-diversity is a qualitative measurement and takes into account the absence and the presence of an OTU.

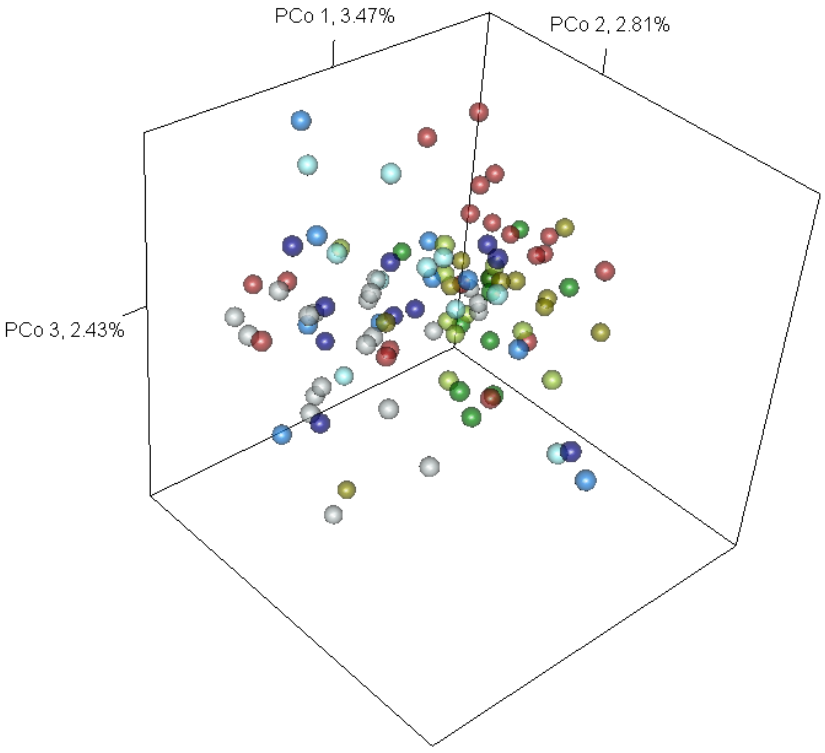

Figure 3-7: Biplot of unweighted Bray-Curtis indices of the luminal microbiota. "Day 0" (n = 20); "Day 4" (after antibiotic treatment; n = 20); probiotic treated group at "Day 14","Day 28" and "Day 46"; placebo treated group at "Day 14", "Day 28" and "Day 46" (n = 10 for all the remaining groups).

Figure 3-7 shows the biplot of unweighted Bray-Curtis indices of the fecal samples. Each dot represents one individual (n = 100). The grey circles represent all individuals at timepoint "Day 0" (n = 20), the red circles all individuals at "Day 4", after the antibiotic treatment (n = 20). The greenish circles represent those individuals that were administered probiotic treatment at the three timepoints "Day 14", "Day 28" and "Day 46", whereas the bluish circles represent all placebo treated individuals (n = 10 per treatment group at one timepoint). The first principal coordinate (PCo 1), which separates out the data as much as possible, explains 3.47% of the variation of the samples.

To test if there are significant differences between the treatment groups and timepoints an AMOVA was performed. Table 3-1 shows the results of the AMOVA for the unweighted Bray-Curtis indices after correction for multiple testing.

Table 3-1: Results of the AMOVA for unweighted Bray-Curtis indices of the luminal microbiota. 10^4 permutations were performed. Values after Bonferroni-Holm correction for multiple testing (n = 28). Cells highlighted in grey show statistical significant results.

		Unweighted							
Time point			Day 4	Day 14		Day 28		Day 46	
	Treatment	Day 0	Antibiotic	Placebo	VSL#3	Placebo	VSL#3	Placebo	VSL#3
	Day 0		5.6e-04	0.0504	0.0145	1	0.0504	1	0.0315
Day 4	Antibiotic			0.1748	1	0.5280	0.5280	0.5941	0.5280
Day 14	Placebo				0.0008	1	0.3249	1	0.0081
	VSL#3					0.0300	1	0.0638	1
Day 28	Placebo						1	1	0.5280
	VSL#3							1	1
Day 46	Placebo								0.3454
	VSL#3								

The result of the AMOVA shows a significant difference between "Day 0" (grey circles) and the antibiotically treated group at "Day 4" (red circles), indicating a significant influence of the antibiotic onto the gut microbiota. Further there is a significant difference between the placebo and the probiotic group at timepoint "Day 14" (light blue circles compared to light green circles), but not at "Day 28" and “Day 48”.

Since there are some significant differences shown within the AMOVA, it is interesting to see which OTUs were responsible for the clustering and the separation of the different treatment groups. For this purpose a SIMPER analysis was performed. Therefore only OTUs with a minimum contribution of 0.5% to the overall similarity have been taken into account for the subsequent Spearman correlation, correlating the OTUs to the axes of the biplot. Table 3-2 shows the results of the Spearman correlation with OTUs fulfilling the false discovery rate (fdr) of 0.05. To give a hint in which direction the OTUs show, only those OTUs that survived the fdr of 0.0001 (as highlighted in grey within the Table 3-2), were plotted into the biplot in Figure 3-8.

Table 3-2: Statistical significant results of the Spearman correlation of OTUs and unweighted Bray-Curtis indices of the luminal microbiota. OTUs with a minimum contribution of 0.5% to the overall similarity. Fdr of 0.05. Cells highlighted in grey: OTUs that are plotted into the biplot in Figure 3-8 fulfilling the fdr of 0.0001.

OTU number/BLAST hit	PCo 1	PCo 2	PCo 3	length	p.min	q.val
4 uncl. Lachnospiraceae	-0.3277	-0.0363	-0.0880	0.3413	2.62e-03	5.70e-03
7 Blautia	-0.3300	-0.5369	0.0545	0.6326	2.55e-08	4.25e-07
8 Blautia	-0.4453	-0.0227	0.0423	0.4478	1.04e-05	6.47e-05
13 Blautia	-0.4913	-0.3903	0.0233	0.6279	6.32e-07	6.31e-06
17 uncl. Lachnospiraceae	-0.4996	0.2933	-0.4696	0.7458	3.64e-07	4.55e-06
18 uncl. Lachnospiraceae	-0.2930	0.4146	-0.3222	0.6013	5.39e-05	2.44e-04
24 uncl. Lachnospiraceae	-0.3614	0.1893	-0.3390	0.5305	6.61e-04	1.65e-03
33 Faecalibacterium	-0.3210	-0.0395	-0.1887	0.3745	3.38e-03	6.76e-03
46 Blautia	-0.4590	-0.2245	-0.1407	0.5300	4.68e-06	3.90e-05
47 Akkermansia	-0.1984	0.1400	-0.3297	0.4094	2.43e-03	5.58e-03
69 Sporacetigenium	-0.4480	0.0419	0.1597	0.4775	8.86e-06	6.33e-05
80 Dialister	-0.2106	-0.3157	-0.2262	0.4418	4.13e-03	7.94e-03
81 Bacteroides	-0.3294	0.0861	0.2495	0.4221	2.46e-03	5.58e-03
91 Bacteroides	-0.1172	0.3264	0.1165	0.3658	2.76e-03	5.75e-03
173 Bacteroides	-0.1768	0.1282	0.3942	0.4507	1.48e-04	5.75e-03
182 Bacteroides	0.0288	0.0357	0.5485	0.5504	1.04e-08	2.60e-07
247 Pseudomonas	-0.2716	-0.1732	-0.1052	0.3389	1.88e-02	2.99e-02
287 Bacteroides	-0-0437	0-0532	-0-2710	0-2796	1-91e-02	2.99e-02
330 Turicibacter	-0.2543	0.4130	-0.1181	0.4992	5.86e-05	2.44e-04
352 uncl. Peptostreptococcaceae	-0.3751	0.1433	0.0905	0.4116	3.62e-04	1.00e-03
369 Dorea	-0.2684	0.1900	-0.2036	0.3868	2.08e-02	3.08e-02
387 uncl. Lachnospiraceae	-0.2665	0.2314	0.0667	0.3592	2.21e-02	3.16e-02
389 Dorea	-0.3116	0.1725	-0.1198	0.3757	4.81e-03	8.90e-03
403 Subdoligranulum	-0.5921	0.2461	0.0805	0.6462	2.60e-10	1.30e-08
436 Ruminococcus	-0.3858	0.1759	0.0309	0.4251	2.21e-04	6.91e-04
447 Clostridium	-0.2774	0.1168	0.1460	0.3345	1.56e-02	2.69e-02
448 Blautia	-0.3069	-0.2049	0.0318	0.3704	5.69e-03	1.02e-02
453 Roseburia	-0.3340	0.3760	0.1454	0.5235	3.47e-04	1.00e-03
455 Subdoligranulum	-0.3862	0.3017	0.2717	0.5603	2.17e-04	6.91e-04
507 Blautia	-0.3870	-0.1137	0.2480	0.4735	2.09e-04	6.91e-04
513 Bacteroides	-0.1302	-0.1417	0.2682	0.3301	2.10e-02	3.08e-02
622 Escherichia/Shigella	-0.1947	0.1002	0.4181	0.4720	4.50e-05	2.42e-04
1008 Lactobacillus	0.1159	-0.4167	0.1033	0.4447	4.84e-05	2.42e-04
1403 uncl. Lachnospiraceae	-0.1942	0.0149	-0.3734	0.4211	3.90e-04	1.03e-03
1811 Subdoligranulum	-0.2723	-0.0947	-0.0730	0.2974	1.84e-02	2.99e-02

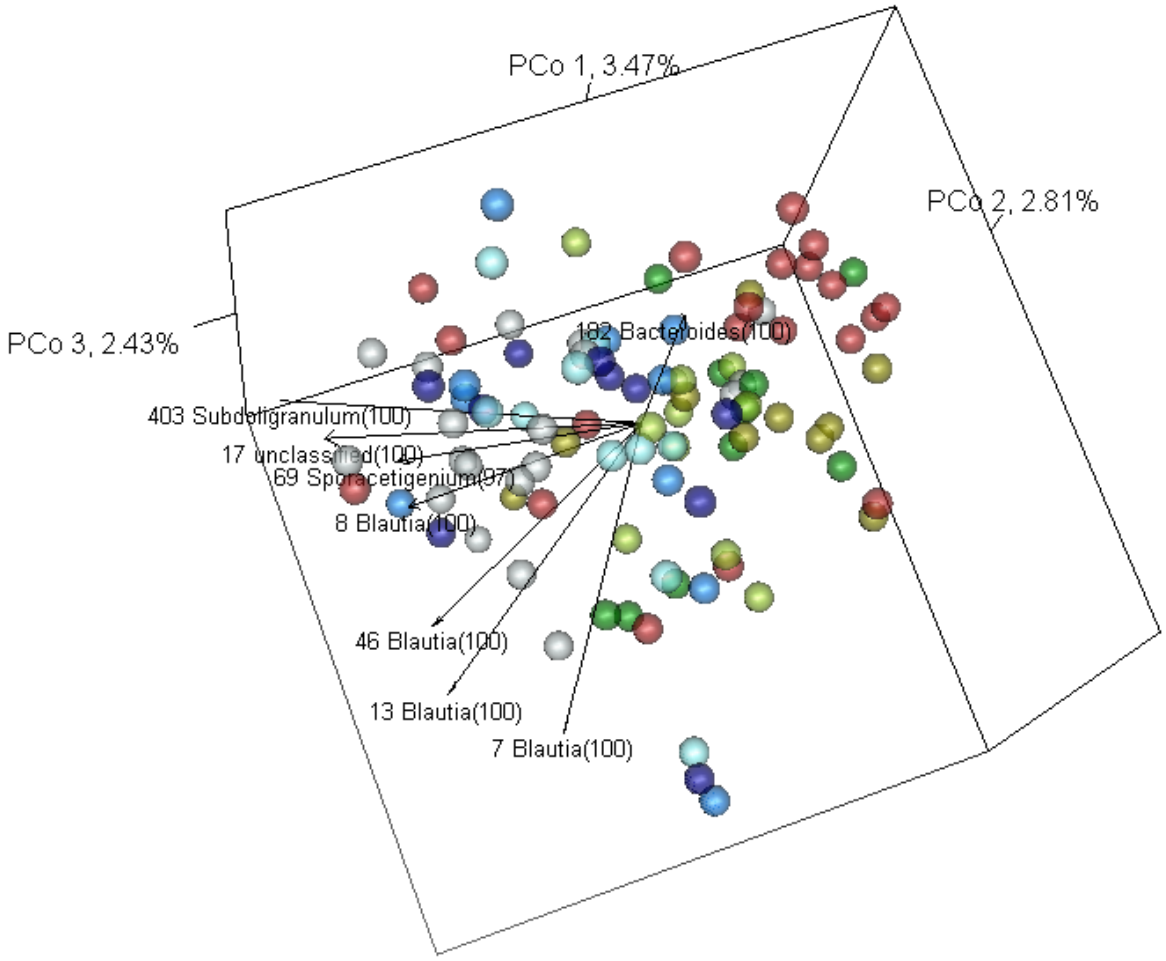

Figure 3-8: Biplot of unweighted Bray-Curtis indices of the luminal microbiota and correlated OTUs. Correlated OTUs contribute at least 0.5% to the overall similarity and fulfill the fdr of 0.0001. "Day 0"(n = 20) ; "Day 4" (after antibiotic treatment; n = 20) ; probiotic treated group at "Day 14", "Day 28" and "Day 46"; placebo treated group at "Day 14", "Day 28" and "Day 46" (n = 10 for all the remaining groups).

The arrow of an OTU points into the direction of the presence of an OTU, whereas the opposite direction indicates the absence of the respective OTU. This means that many OTUs were present within the normal microbiota and absent within the antibiotically treated microbiota, as most of the arrows point into the direction of the grey circles. This is also indicated by negative prefixes of the principal coordinate 1 (Table 3-2). When classifying these OTUs it becomes obvious that many OTUs having a 97% homology to the genus *Blautia* and the family *Lachnospiraceae* seemed to be absent within the antibiotically treated microbiota.

Weighted Bray-Curtis indices

Whereas unweighted beta-diversity takes into account the absence and the presence of an OTU, weighted beta diversity "weighs" the presence of an OTU by its abundance and is therefore a quantitative measurement.

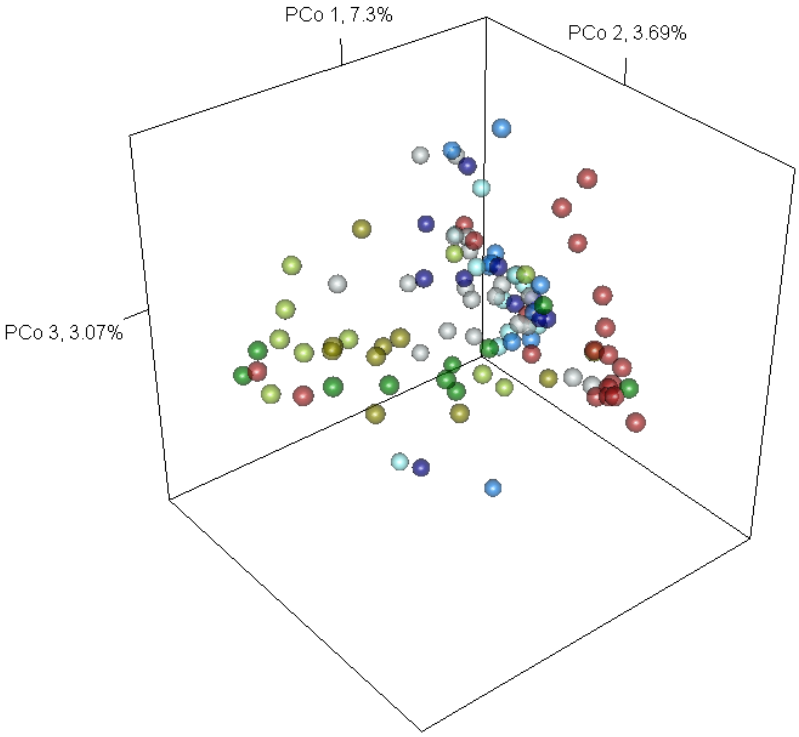

Figure 3-9: Biplot of weighted Bray-Curtis indices of the luminal microbiota. "Day 0" (n = 20); "Day 4" (after antibiotic treatment; n = 20); probiotic treated group at "Day 14","Day 28" and "Day 46"; placebo treated group at "Day 14", "Day 28" and "Day 46" (n = 10 for all the remaining groups).

Based on weighted Bray-Curtis indices a biplot was generated as shown in Figure 3-9. The color code is the same as in the figures shown before. The principal coordinate 1 explains 7.3% of the variation between the samples. 3.69% variation is explained along the principal coordinate 2, followed by 3.07% explained variation by the third principal coordinate. At a first glance the different colored circles look much more separated than within the biplot of the unweighted Bray-Curtis indices (Figure 3-7). To check for possible significant differences between the timepoints and the treatment groups an AMOVA was conducted. The results are show in Table 3-3.

As depicted within the biplot by the grey and the red circles, a significant difference between the timepoints "Day 0" and "Day 4" could be confirmed, indicating a significant influence onto the gut microbiota due to the antibiotic treatment. Furthermore, there was a significant difference between the placebo and the probiotically treated group at "Day 14" and "Day 28" as well as "Day 46". In comparison to the initial timepoint "Day 0" there was a significant difference to the probiotically treated group at all three timepoints, but not to the placebo treated group except for timepoint "Day 14". The placebo treated microbiota seemed to be

similar to the initial microbiota from "Day 28" on, which could be a hint for the resilience of the gut microbiota. A gender-dependent difference between the treatment was not detected.

Table 3-3: Results of the AMOVA for weighted Bray-Curtis indices of the luminal microbiota. 10^4 permutations were performed. Values after Bonferroni-Holm correction for multiple testing (n = 28). Cells highlighted in grey show statistical significant results.

	Time point	Treatment	Day 0	Day 4 Antibiotic	Day 14 Placebo	Day 14 VSL#3	Day 28 Placebo	Day 28 VSL#3	Day 46 Placebo	Day 46 VSL#3
Weighted		Day 0								
	Day 4	Antibiotic	2.8e-04							
	Day 14	Placebo	0.0179	0.0005						
		VSL#3	2.8e-04	0.0122	0.0021					
	Day 28	Placebo	1	0.0480	1	0.0026				
		VSL#3	0.0005	0.0146	0.0095	1	0.0146			
	Day 46	Placebo	1	0.0541	1	0.0058	1	0.0368		
		VSL#3	2.8e-04	0.0541	0.0089	1	0.0057	1	0.0179	

A Spearman correlation was performed to have a look at OTUs that might be responsible for the differences of the timepoints and treatments, respectively. OTUs that showed a minimum contribution of 0.5% within the SIMPER analysis and fulfilled the fdr of 0.05 within the Spearman correlation are listed in Table 3-4.

Table 3-4: Statistical significant results of the Spearman correlation of OTUs and weighted Bray-Curtis indices of the luminal microbiota. OTUs with a minimum contribution of 0.5% to the overall similarity. Fdr of 0.05. Cells highlighted in grey: OTUs that are plotted into the biplot in Figure 3-8 fulfilling the fdr of 0.0001.

OTU number/BLAST hit	PCo 1	PCo 2	PCo 3	length	p.min	q.val
4 uncl. Lachnospiraceae	0.0422	0.2939	-0.1474	0.3315	8.99e-03	1.66e-02
7 Blautia	-0.0169	0.3322	-0.3558	0.4870	8.42e-04	2.63e-03
8 Blautia	0.2695	0.3423	-0.1220	0.4524	1.47e-03	4.08e-03
13 Blautia	0.0336	0.4502	-0.1352	0.4713	7.81e-06	4.88e-05
17 uncl. Lachnospiraceae	0.3468	0.2798	0.0465	0.4481	1.22e-03	3.60e-03
18 uncl. Lachnospiraceae	0.2674	0.1895	0.1113	0.3461	2.14e02	3.64e-02
24 uncl. Lachnospiraceae	0.2669	0.4464	-0.0428	0.5218	9.74e-06	5.41e-05
33 Faecalibacterium	0.1774	0.3132	-0.1488	0.3895	4.54e-03	9.86e-03
37 Streptococcus	-0.6841	0.1130	0.1652	0.7128	1.29e-14	6.45e-13
46 Blautia	0.0633	0.4944	-0.2682	0.5660	5.14e-07	6.42e-06
69 Sporacetigenium	0.3808	0.4855	0.2527	0.6668	9.17e-07	9.17e-06
81 Bacteroides	0.3062	0.0539	0.2264	0.3847	5.83e-03	1.17e-02
91 Bacteroides	0.2605	-0.0800	0.3200	0.4203	3.52e-03	8.80e-03
173 Bacteroides	0.1318	0.1200	0.3943	0.4327	1.48e-04	5.68e-04
182 Bacteroides	0.1281	0.0421	0.5166	0.5339	1.13e-07	1.88e-06
247 Pseudomonas	0.3032	0.0098	-0.3228	0.4429	3.17e-03	8.34e-03
254 Pseudomonas	0.1168	-0.1575	-0.2668	0.3311	2.19e-02	3.64e-02

OTU number/BLAST hit	PCo 1	PCo 2	PCo 3	length	p.min	q.val
330 Turicibacter	0.3647	0.0689	0.1069	0.3863	5.73e-04	2.05e-03
352 uncl. Peptostreptococcaceae	0.3185	0.2728	0.0938	0.4297	3.73e-03	8.87e-03
387 uncl. Lachnospiraceae	0.2687	0.0991	0.1445	0.3208	2.06e-02	3.64e-02
403 Subdoligranulum	0.6208	0.4374	0.0450	0.7607	1.68e-11	4.19e-10
436 Ruminococcus	0.2038	0.3066	0.1711	0.4060	5.75e-03	1.17e-02
447 Clostridium	0.3581	0.3329	0.1137	0.5020	7.61e-04	2.54e-03
453 Roseburia	0.3462	0.3992	0.3160	0.6157	1.17e-04	4.86e-04
455 Subdoligranulum	0.4154	0.2977	0.2275	0.5594	5.19e-05	2.36e-04
507 Blautia	0.0952	0.3171	-0.0383	0.3333	3.91e-03	8.89e-03
622 Escherichia/Shigella	0.1429	0.1463	0.4621	0.5053	3.91e-06	2.79e-05
768 Streptococcus	-0.4790	-0.0497	0.0301	0.4825	1.38e-06	1.15e-05
1008 Lactobacillus	-0.4372	0.0905	-0.0051	0.4465	1.62e-05	8.12e-05
2490 Streptococcus	-0.2987	0.1201	0.0208	0.3226	7.62e-03	1.46e-02

For a better overview only OTUs that survived the fdr of 0.001 were plotted into the biplot within Figure 3-10. The OTUs 7, 37, 768 and 1008 point into the negative direction of the first principal coordinate (PCo 1 in Table 3-4) and were therefore more abundant within the probiotically treated group (green circles in Figure 3-10). The classification of these OTUs revealed three of them having a high homology to the genera *Streptococcus* and *Lactobacillus*. The other listed OTUs point into the direction of timepoint "Day 0" and the placebo treated individuals (positive PCo 1 and PCo 2), meaning that those OTUs were much more abundant in the placebo and at "Day 0" and tend to decrease due to antibiotic treatment. As within the unweighted approach OTUs with a 97% homology to *Blautia* and *Lachnospiraceae* seem to fall in this group (OTUs 7, 8, 13, 24 and 46). It also becomes obvious that OTUs that are similar to the same genus can point into opposite directed clusters. OTU 91 and OTU 254 point into the direction of the antibiotically treated microbiota, whereas the OTUs 81 and 247 point into the direction of the timepoint "Day 0" and the placebo treated microbiota. OTU 81 as well as OTU 91 are similar to *Bacteroides*, OTU 247 and OTU 254 to *Pseudomonas*.

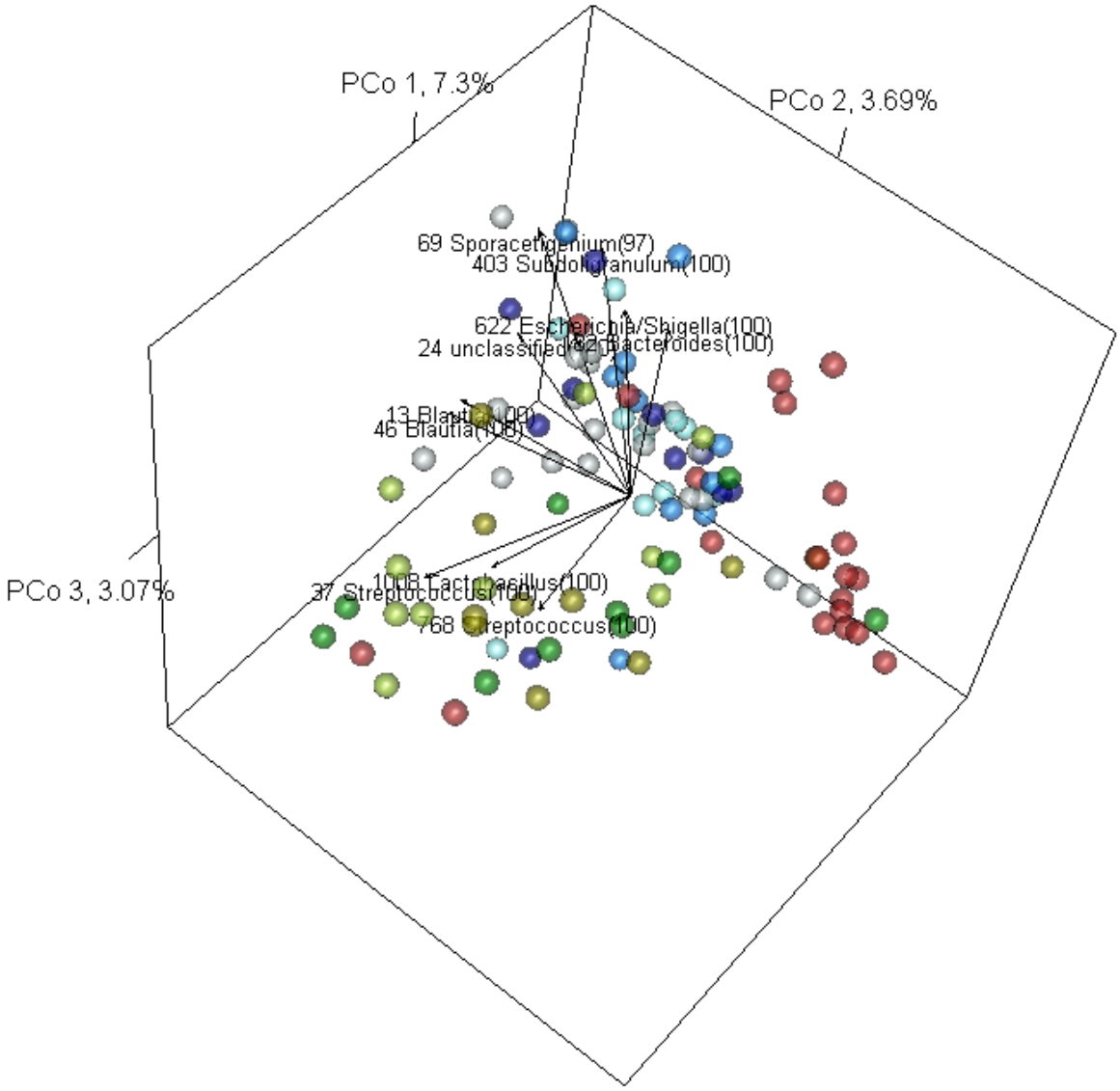

Figure 3-10: Biplot of weighted Bray-Curtis indices of the luminal microbiota and correlated OTUs. Correlated OTUs contribute at least 0.5% to the overall similarity and fulfilled the fdr of 0.0001. "Day 0" (n = 20) ; "Day 4" (after antibiotic treatment; n = 20) ; probiotic treated group at "Day 14" , "Day 28" and "Day 46" ; placebo treated group at "Day 14" , "Day 28" and "Day 46" (n = 10 for all the remaining groups).

In addition to the correlation analysis the metastats command was used to determine if any OTUs are differentially represented between the different timepoints/treatment groups. Again only those OTUs were analyzed that contributed at least 0.5% to the overall contribution (SIMPER analysis). Table 3-5 shows the results of the metastats analysis between the placebo and the probiotically treated group at the three different timepoints. OTUs which were absent in one timepoint, but present at the other timepoint are listed as "appears" or "disappears". At timepoint "Day 14" there could be found more OTUs that differ in their abundance between the placebo and the probiotic treatment than at the timepoints "Day 28" and "Day 46". Interestingly, OTUs having homology to *Blautia* (OTUs 7, 8, 13) and *Subdoligranulum*

(OTUs 403 and 455) seemed to be significantly decreased within the probiotic group at "Day 14". These differences could not be found within the other timepoints. A difference between the placebo and the probiotic group within all three timepoints was OTU 37, which was found to have a 97% homology to *Streptococcus* and highly abundant within the probiotic groups. On the other hand there was not a single OTU significantly decreased within all timepoints due to the probiotic therapy.

Table 3-5: Statistical significant results of the metastats analysis comparing the placebo and probiotic group at the respective timepoints. Ratio is relative to the placebo. 1000 permutations were performed. p values after Bonferroni-Holm correction for multiple testing. Appears= present in probiotic, but absent in placebo group, Disappears= absent in probiotic group, but present in placebo. n = 10 for each groups. Cells highlighted in grey: Indicator species at 97% level.

	Day 14	**Day 28**	**Day 46**
OTU number/BLAST hit	**ratio (log_{10})**	**ratio (log_{10}))**	**ratio (log_{10})**
4 uncl. Lachnospiraceae			0.108 (-0.966)
7 Blautia	0.325 (-0.488)		
8 Blautia	disappears		
13 Blautia	0.252 (-0.598)		
37 Streptococcus	5.762 (0.761)	5.132 (0.710)	3.62 (0.559)
69 Sporacetigenium	0.076 (-1.121)		0.081 (-1.089)
80 Dialister	0.353 (-0.453)		
254 Pseudomonas	disappears		
352 uncl. Peptostrepococcaceae	0.227 (-0.644)		
403 Subdoligranulum	0.123 (-0.910)		0.171 (-0.768)
447 Clostridium		0.054 (-1.266)	disappears
453 Roseburia	disappears		
455 Subdoligranulum	disappears		
768 Streptococcus	appears	appears	
1008 Lactobacillus			appears
1378 uncl. Lachnospiraceae		appears	
2490 Streptococcus	disappears		
4732 Prevotella			disappears
6245 Lactobacillus		disappears	
6611 Streptococcus	appears		

Since the AMOVA showed a significant difference between the initial and the antibiotically treated microbiota, it was expected for some OTUs to be over- or underrepresented within one of the groups within the metastats analysis. Further the difference of the placebo and the probiotic group at the end of the study ("Day 46") was compared to the initial composition of "Day 0".

Table 3-6: Statistical significant results of the metastats analysis comparing timepoint "Day 0" and different groups. Ratio is relative to "Day 0". 1000 permutations were performed. p values after Bonferroni-Holm correction for multiple testing. Disappears= absent at "Day 4"/"Day 46", but present at "Day 0". n = 20 for "Day 0" and "Day 4"; n = 10 for each of the other groups. Cells highlighted in grey: Indicator species at 97% level.

	Day 4	Day 46 Placebo	Day 46 Probiotic
OTU number/BLAST hit	**ratio (log_{10})**	**ratio (log_{10})**	**ratio (log_{10})**
13 Blautia	0.275 (-0.561)		
17 uncl. Lachnospiraceae	0.371 (-0.431)		0.219 (-0.660)
18 uncl. Lachnospiraceae	0.593 (-0.227)	0.165 (-0.782)	
24 uncl. Lachnospiraceae	0.189 (-0.724)		0.485 (-0.313)
33 Faecalibacterium	0.022 (-1.664)		
37 Streptococcus			5.01 (0.699)
46 Blautia	0.099 (-1.006)		
69 Sporacetigenium			0.147 (-0.8209)
81 Bacteroides	13.18 (1.120)		
91 Bacteroides	5.56 (0.745)		
182 Bacteroides			0.258 (-0.585)
447 Clostridium	0.014 (-1.851)		disappears
1839 Bacteroides	disappears		

Table 3-6 shows the results of the metastats analysis. Due to the antibiotic treatment (column "Day 4") all OTUs listed in the table, except for the OTUs 81 and 91, showed a significant decrease. The classification of these OTUs revealed a 97% homology to the family *Lachnospiraceae* and the genera *Blautia*, *Faecalibacterium* and *Clostridium*. OTU 81 and OTU 91, which showed a higher abundance due to the antibiotic, were all classified as *Bacteroides*.

Regeneration of the microbiota shown by the comparison of "Day 46" compared to "Day 0" revealed that there was still a decrease within the OTU 18 (having homology to *Lachnospiraceae*) in the placebo treated group. The probiotic group indicated differences in two other OTUs also having homology to *Lachnospiraceae*. Further a significant decrease in three OTUs with homology to *Sporacetigenium*, *Bacteroides*, and *Clostridium* was identified. Many of the OTUs that were significantly decreased by the antibiotic treatment could recover during time, not very much influenced by the probiotic.

The comparison between the placebo or probiotic group of the timepoints "Day 14" or "Day 28" to timepoint "Day 0" can draw a clearer picture when certain OTUs recover (Table 3-7). All OTUs that were characterized as *Blautia* and were significantly decreased due to the antibiotic treatment seem to recover very fast as there was no significant difference within the comparison of "Day 0" and "Day 14", independent of the probiotic therapy. OTU 33

(*Faecalibacterium*) needed a longer time period for recovery as this OTU was still significantly decreased at "Day 14" and "Day 28", but not at "Day 46" (Table 3-6), again independent of the probiotic therapy. Very high abundant within the probiotic group compared to "Day 0" was OTU 37 (*Streptococcus*) at "Day 14" and at "Day 28" as well as the OTU 768 (*Streptococcus*) at "Day 14".

Table 3-7: Statistical significant results of the metastats analysis comparing timepoint "Day 0" and different groups. Ratio is relative to "Day 0". 1000 permutations were performed. p values after Bonferroni-Holm correction for multiple testing. Disappears= absent at "Day 14"/"Day 28", but present at "Day 0". Appears = present at "Day 14"/"Day 28", but absent at "Day 0". n = 20 for "Day 0"; n = 10 for each of the other groups. Cells highlighted in grey: Indicator species at 97% level.

OTU number/ BLAST hit	Day 14 Placebo ratio (log_{10})	Day 14 Probiotic ratio (log_{10})	Day 28 Placebo ratio (log_{10})	Day 28 Probiotic ratio (log_{10}
17 uncl. Lachnosp.	0.095 (-1.020)	0.342 (-0.466)		
18 uncl. Lachnosp.	disappears	0.646 (-0.190)		0.170 (-0.769)
24 uncl. Lachnosp.		0.203 (-0.692)		0.273 (-0.564)
33 Faecalibacterium	0.075 (-1.1268)	0.117 (-0.932)	0.565 (-0.248)	0.141 (-0.850)
37 Streptococcus		5.795 (0.763)		5.58 (0.747)
69 Sporacetigenium		0.103 (-0.988)		
447 Clostridium				0.06 (-1.189)
768 Streptococcus		42.95 (1.633)		
2490 Streptococcus		disappears		
4286 Lactobacillus			appears	
6245 Lactobacillus			appears	
6611 Streptococcus		appears		

Apart from the metastats command the indicator species command implemented in MOTHUR can be used. This will output OTUs that define and characterize a timepoint or treatment. As for the metastats approach only OTUs with a minimum contribution of 0.5 % and 1% were included within the analysis (as revealed by SIMPER analysis), respectively. The indicator species command was performed on species (97% identity) and on genus level (95% identity).

On species level with a contribution of at least 0.5% the OTUs 24 and 33 were identified as indicator species between the groups "Day 0" and "Day 4", which is after the antibiotic treatment. As shown in Table 3-6 these OTUs have a homology to the family *Lachnospiraceae* and the genus *Faecalibacterium* and are decreased due to the antibiotic treatment. Comparing the placebo and the probiotic group at the respective timepoints there were no indicator species found for the timepoints "Day 14" and "Day 46". For the timepoint "Day 28" the OTU 37 (*Streptococcus*) tended (p_{corr} = 0.0837) to be an indicator species when

1% contribution was set as minimum. Comparing the probiotic group of "Day 28" to the initial timepoint "Day 0" OTU 37 (*Streptococcus*) again was designed as indicator species highly abundant within the probiotically treated group (with 1% contribution). Comparing the other timepoints to the initial timepoint "Day 0" no indicator species could be found.

On genus level (95% identity) the OTUs 20 (*Faecalibacterium*), 9 and 12 (both *Lachnospiraceae*), which had a contribution of at least 0.5% were identified as indicator species between the timepoints "Day 0" and "Day 4" and therefore characterized the antibiotically treated microbiota compared to the normal one. Further the OTUs 2 and 7 (contribution of at least 1%) tended to be an indicator species (OTU 2 p_{corr} = 0.0561 and OTU 7 p_{corr} = 0.08622). Both OTUs have at least 95% similarity to the genus *Blautia*. Comparing the placebo to the probiotic group there were no indicator species found at each of the respective timepoints. Comparing the two treatment groups at the respective timepoints to the initial timepoint "Day 0", the OTU 12 (*Lachnospiraceae*) characterized the difference between the placebo group at "Day 14" and the "Day 0" as an indicator species. Also for the probiotic group at this timepoint "Day 14" OTU 12 was found. In addition OTU 9 (*Lachnospiraceae*) tended to be characteristic (p_{corr} = 0.0792) when taking into account only OTUs with a contribution of 1%. Since these two OTUs were decreased due to the antibiotic and still showed a lower abundance within the placebo and probiotic group than within the initial composition, this result shows that the two OTU were not able to recover until "Day 14". The OTU 24 (*Streptococcus*) tended to be an indicator species between the probiotic group of "Day 28" and "Day 0" at 1% contribution level (p_{corr} = 0.08712).

Since the analysis shown before was OTU-based, the correlation showed OTUs that are responsible for the clustering of the treatment groups and timepoints. Another correlation was performed taking into account the whole taxa on genus level. Only taxa contributing at least 0.5% to the overall similarity were included.

Table 3-8: Statistical significant results of the Spearman correlation of the taxa on genus level and weighted Bray-Curtis coefficients of the luminal microbiota. Taxa with a minimum contribution of 0.5% to the overall similarity. Fdr of 0.05. Cells highlighted in grey: Taxa that are plotted into the biplot in Figure 3-11 fulfilling the fdr of 0.001.

Taxon	PCo 1	PCo 2	PCo 3	length	p.min	q.val
Alistipes	0.1023	-0.2255	0.2970	0.3866	8.09e-03	1.70e-02
Bacteroides	0.2386	-0.2206	0.4316	0.5402	2.20e-05	1.32e-04
uncl. Bacteroidales	-0.0125	-0.4845	-0.0064	0.4847	9.81e-07	8.24e-06
Blautia	-0.0941	0.5951	-0.3446	0.6941	1.98e-10	2.78e-09
Clostridium	0.4123	0.3024	0.1911	0.5458	6.08e-05	2.93e-04
Coprococcus	0.3998	0.1594	0.1361	0.4514	1.13e-04	3.96e-04
Dorea	0.1155	0.2755	-0.1573	0.3376	1.66e-02	3.32e-02
Escherichia/Shigella	0.1225	0.0825	0.4076	0.4335	7.69e-05	3.06e-04
Holdemania	0.0199	-0.3166	0.08371	0.3281	3.99e-03	9.31e-03
uncl. Lachnospiraceae	0.2516	0.3089	-0.0681	0.4042	5.29e-03	1.17e-02
Lactobacillus	-0.4068	0.0702	-0.1018	0.4252	8.01e-05	3.06e-04
uncl. Lactobacillales	-0.6440	-0.1618	-0.0492	0.6659	1.47e-12	3.08e-11
uncl. Peptostreptococcaceae	0.3331	0.2185	0.1318	0.4196	2.12e-03	5.94e-03
Pseudomonas	0.3150	0.0043	-0.3312	0.4571	2.29e-03	6.02e-03
uncl. Pseudomonadaceae	0.2025	-0.1490	-0.2615	0.3628	2.58e-02	4.92e-02
Roseburia	0.4382	0.3878	0.1422	0.6022	1.54e-05	1.08e-04
Ruminococcus	0.1765	0.3268	0.0930	0.3829	2.71e-03	6.70e-03
uncl. Ruminococcaceae	0.3636	-0.0972	0.0872	0.3863	6.02e-04	1.95e-03
Sporacetigenium	0.3773	0.4116	0.2016	0.5936	6.28e-05	2.93e-04
Streptococcus	-0.7057	0.1402	0.1004	0.7265	7.29e-16	3.06e-14
Subdoligranulum	0.5039	0.3189	0.0408	0.5977	2.73e-07	2.86e-06
Turicibacter	0.3496	0.0365	0.0901	0.3628	1.09e-03	3.27e-03

Table 3-8 shows the results of the correlation of the taxa on genus level. Eleven of the taxa are plotted into the biplot in Figure 3-11.

Table 3-8 and Figure 3-11 show that the genus *Bacteroides* and the associated order *Bacteroidales,* both having a negative principal coordinate 2, were highly abundant within the antibiotically treated microbiota. The genera having a positive principal coordinate 1 and 2 were therefore highly abundant within the normal microbiota and tended to decrease due to antibiotic treatment. Families like *Lachnospiraceae* and *Peptostreptococcaceae*, but also genera like *Clostridium*, *Coprococcus*, *Escherichia*, *Roseburia*, *Ruminococcus*, *Sporacetigenium* and *Turicibacter* seem to belong to this group. The probiotically treated

microbiota is characterized by *Lactobacillales* and by *Lactobacillus* as well as *Streptococcus* with a high negative value for the principal coordinate 1. The genus *Blautia* represents a state between the initial and the probiotically treated microbiota and was highly diminished in the antibiotically treated microbiota.

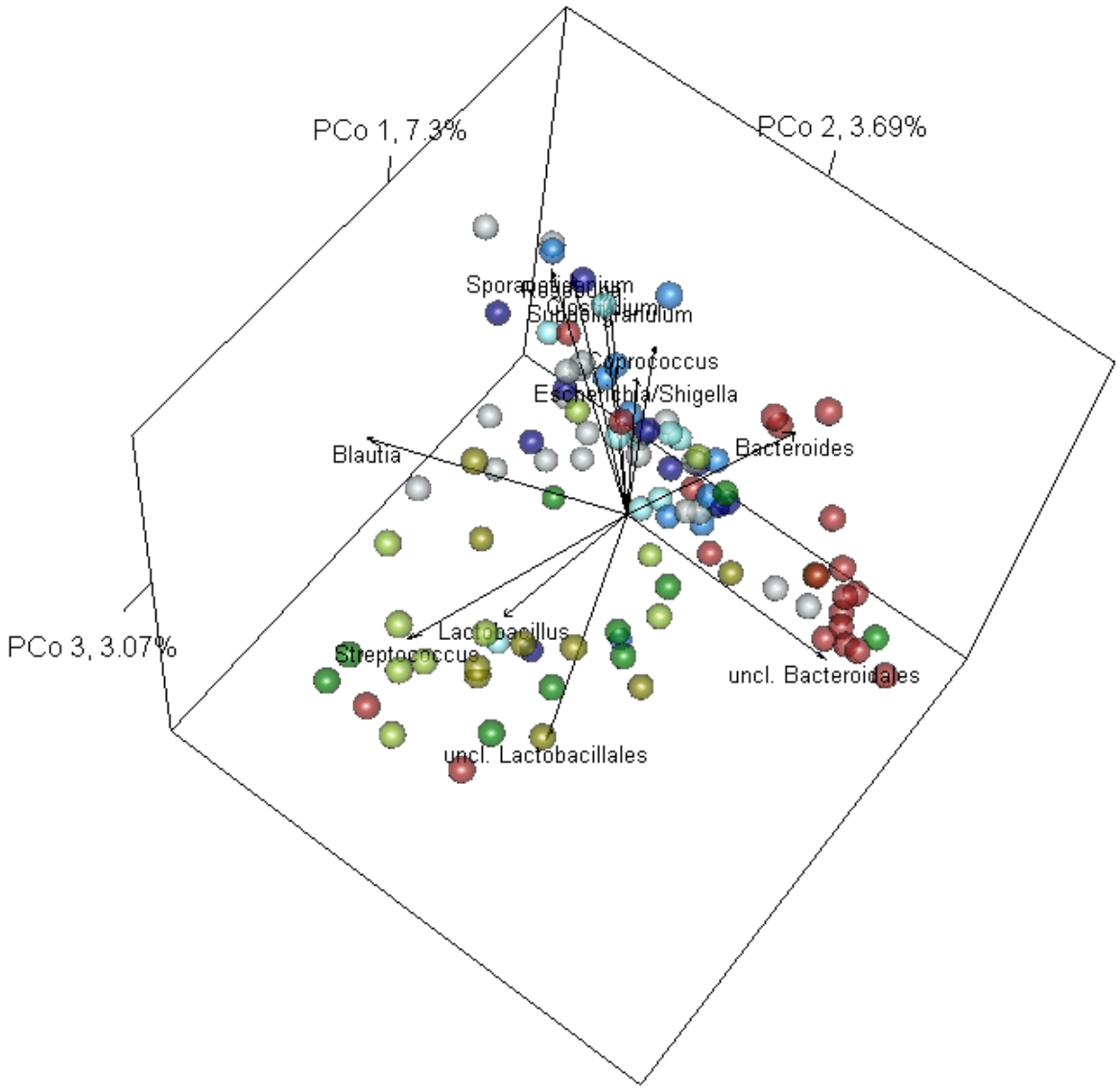

Figure 3-11: Biplot of weighted Bray-Curtis distances of the luminal microbiota and correlated taxa. Correlated taxa contribute at least 0.5% to the overall similarity and fulfill a fdr of 0.001. "Day 0" (n = 20) ; "Day 4" (after antibiotic treatment; n = 20) ; probiotic treated group at "Day 14" , "Day 28" and "Day 46" ; placebo treated group at "Day 14" , "Day 28" and "Day 46" (n = 10 for all the remaining groups).

3.2 16S rRNA and 16S rRNA gene amplicon libraries from mucosa-associated samples

In addition to the fecal samples, sigmoid biopsy samples had been collected via sigmoidoscopy on three different timepoints. The first at timepoint "Day 0", the second after the antibiotic treatment at "Day 4" and the third at timepoint "Day 46" from both the placebo as well as the probiotically treated group. From these biopsy samples DNA and RNA were extracted and RNA was reverse transcribed into cDNA. Amplicon libraries from DNA as well as from cDNA were generated by amplifying the V1-V2 region within a barcode-tagged PCR approach and sequenced via 454 pyrosequencing.

This resulted in 920.064 reads. The reads were split according to their barcode and checked for their mean Phred quality score with the software PANGEA (Giongo et al. 2010). Further MOTHUR was used (Schloss et al. 2009) to eliminate reads with no perfect match to the primer, ambiguous bases, homopolymers and a length less than 200 bp. Also chimerical sequences were eliminated. The denoising step resulted in 808.430 cleaned sequences. The uneven distribution of sequences per sample (1.506 until 34.742 sequences per sample, median 4.184) was ameliorated by normalizing the number of sequences of each sample to 1.506. This resulted in the final data set of 180.720 sequences.

A classification against the reference sequences of RDP was performed for a first overview. In addition an OTU-based analysis was performed.

3.2.1 First classification of the denoised data set of the mucosa-associated microbiota

To obtain a first impression of the phylum distribution within the mucosa-associated microbiota, the sequences of all twenty individuals at timepoint "Day 0" were classified using the classifier of the Ribosomal Database Project (RDP). As shown in Figure 3-12 (A) the four main abundant phyla within the present mucosa-associated microbiota are *Firmicutes*, *Bacteroidetes*, *Proteobacteria* and *Actinobacteria*. This is an expected picture of the phyla distribution of healthy individuals. The small amount specified as "Others" represents phyla like *Acidobacteria*, *Cyanobacteria*, *Deinococcus-Thermus*, *Fusobacteria*, *Verrucomicrobia* and some unclassified bacteria.

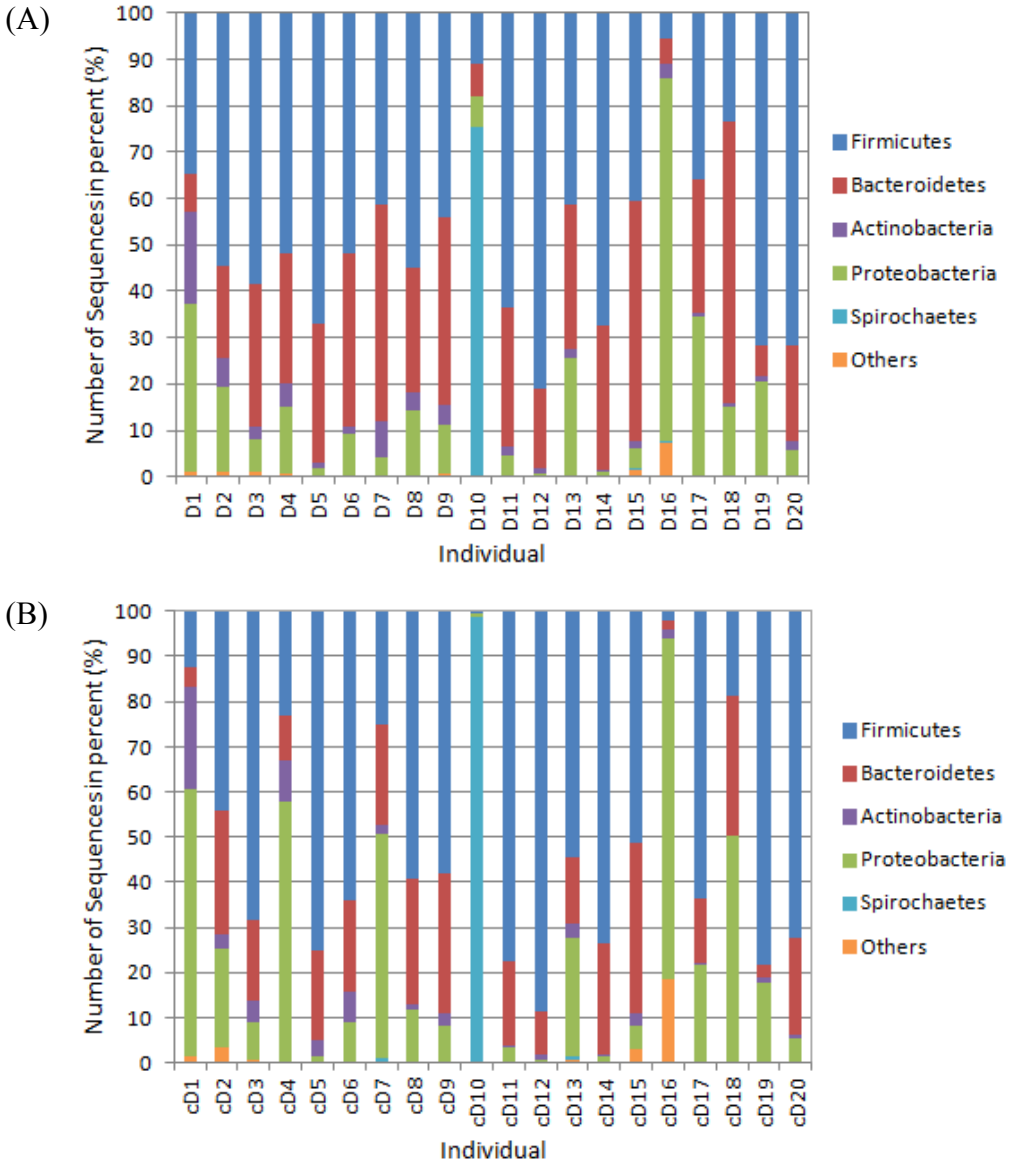

Figure 3-12: Phylum distribution of the (A) present mucosa-associated microbiota and (B) active mucosa-associated microbiota at timepoint "Day 0". Description in percent. n = 20.

However, the phylum distribution of individual 10 (D10) is characterized by a huge amount of *Spirochaetes*, which is very abnormal for healthy individuals. Since this phylum was not found in the other individuals and the effect onto the bacterial community is unclear, individual 10 was discarded from further analysis.

The phylum distribution of the active mucosa-associated microbiota, as depicted in Figure 3-12 (B), looks quite similar. Again the four main phyla are *Firmicutes*, *Bacteroidetes*, *Proteobacteria* and *Actinobacteria*. And again "Others" represents phyla like *Acidobacteria*, *Cyanobacteria*, *Deinococcus-Thermus*, *Fusobacteria* and some unclassified bacteria. In contrast to the present microbiota the phylum *Verrucomicrobia* was not found in the active one. Individual 10 also shows a very high amount of active *Spirochaetes*. As decided previously individual 10 was discarded from further analysis.

Based on the 180.720 cleaned sequences 171.684 were used for further analysis due to the elimination of individual 10.

The classification of the remaining timepoints gave a simple overview onto the effect of the antibiotic and the subsequent probiotic or placebo therapy. The two main phyla, *Firmicutes* and *Bacteroidetes*, were classified according to RDP.

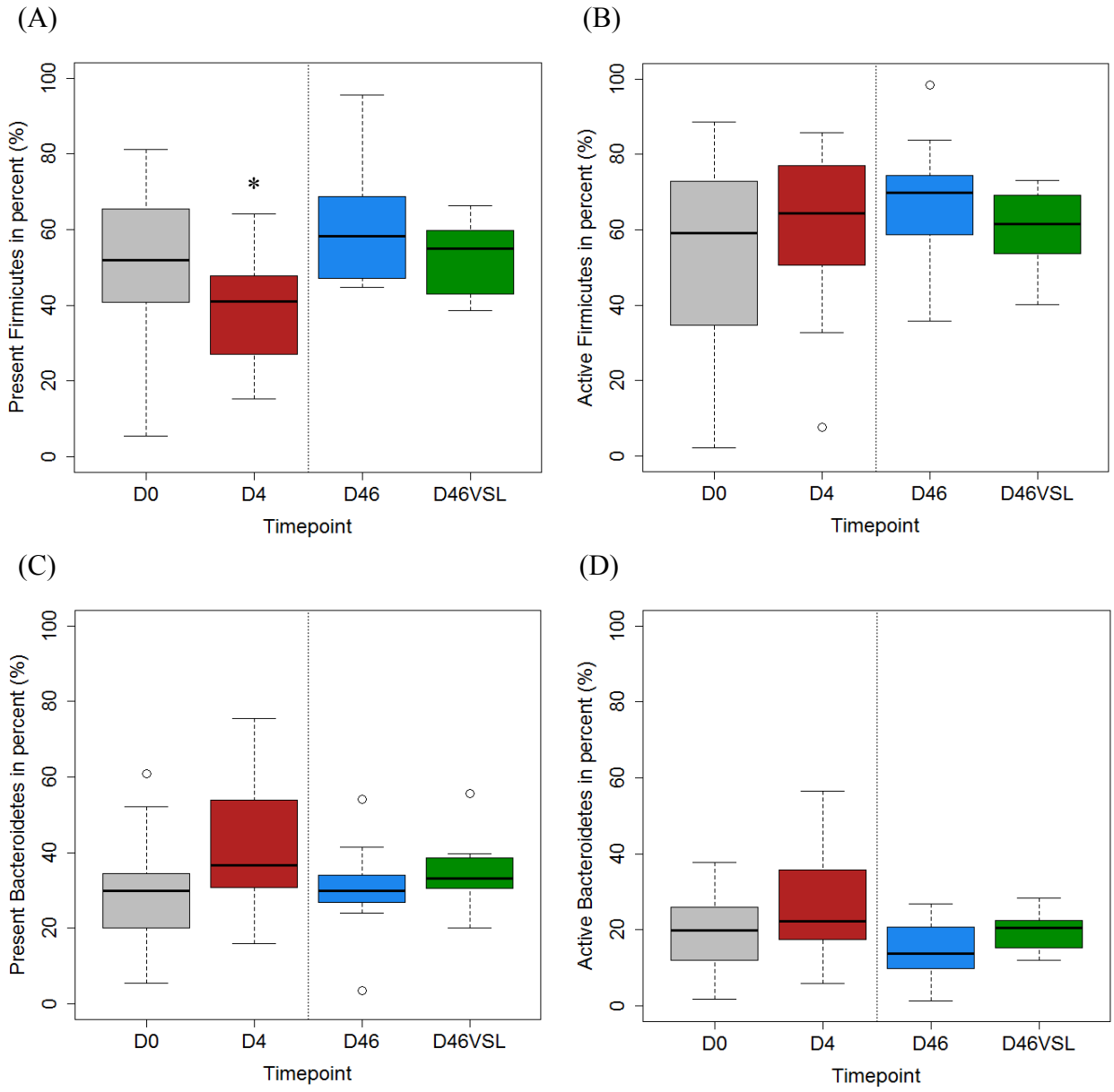

Figure 3-13: Changes in the two main mucosa-associated phyla due to antibiotic treatment and subsequent placebo or probiotic therapy. (A) Present Firmicutes. (B) Active Firmicutes. (C) Present Bacteroidetes. (D) Active Bacteroidetes. Median, upper and lower quartile as well as upper and lower wisker are plotted**.** Grey (D0): Timepoint "Day 0" (n = 19), Red (D4): Timepoint "Day 4" after antibiotic treatment (n = 19), blue (D46): Timepoint "Day 46" after placebo therapy (n = 10), green (D46VSL): Timepoint "Day 46" after probiotic therapy (n = 9). * statistically significant at a level of 0.05 after Bonferroni-Holm correction.

Based on the classification the median and the quartiles were calculated for each treatment and plotted into boxplots (Figure 3-13). Due to the antibiotic treatment a significant decrease within present *Firmicutes* (p_{corr} = 0.0247) could be observed. In active *Firmicutes* (p_{corr} = 0.3736) as well as within present and active *Bacteroidetes* (present: p_{corr} = 0.0987; active: p_{corr}

= 0.2268) antibiotic therapy resulted in an increase of the respective phyla, but this increase was not significant. The subsequent allocation to placebo or the probiotic therapy (the randomization was appropriate) revealed no difference at timepoint "Day 46" in neither active or present *Bacteroidetes* (active: p_{corr} = 0.633 and present: p_{corr} = 0.3999) nor in active or present *Firmicutes* (active: p_{corr} = 0.9934, present: p_{corr} = 1), respectively. The comparison between the timepoints "Day 0" and "Day 46" did not show any significant difference in any of the groups, indicating a good recovery of active and present *Firmicutes* as well as *Bacteroidetes*. With regard to the phylum *Proteobacteria*, which was highly abundant in some of the study participants in its active and in the present form (figure 3-12 and 3-13), the median for present *Proteobacteria* was around 10% and did not respond to any of the treatments. The same applies for active *Proteobacteria*, which had a mean abundance of about 12%.

For deeper analysis an OTU-based analysis was performed for the active and the present mucosa-associated microbiota.

3.2.2 OTU-based analysis

The 171.684 sequences were aligned according to the Needleman-Wunsh algorithm. A distance matrix was then generated by calculating the uncorrected pair wise distances between the aligned sequences. Based on the distances the sequences were assigned into OTUs at the levels of 97% (species level) and 95% (genus level) according to the average neighbor method. The final dataset of 171.684 sequences was grouped into 5.986 OTUs on species level, which are the basis for the subsequent analysis.

3.2.2.1 Alpha-Diversity

As far as the Good´s coverage of the remaining samples is concerned, it was in the range of 91.43% to 98.67% (median = 95.62%) for the present and between 86.39% and 98.07% (median = 93.23%) for the active microbiota. In addition to the Good´s coverage rarefaction curves of the sample with the best and the worst coverage were plotted for the DNA and the cDNA samples, respectively (Figure 3-14).

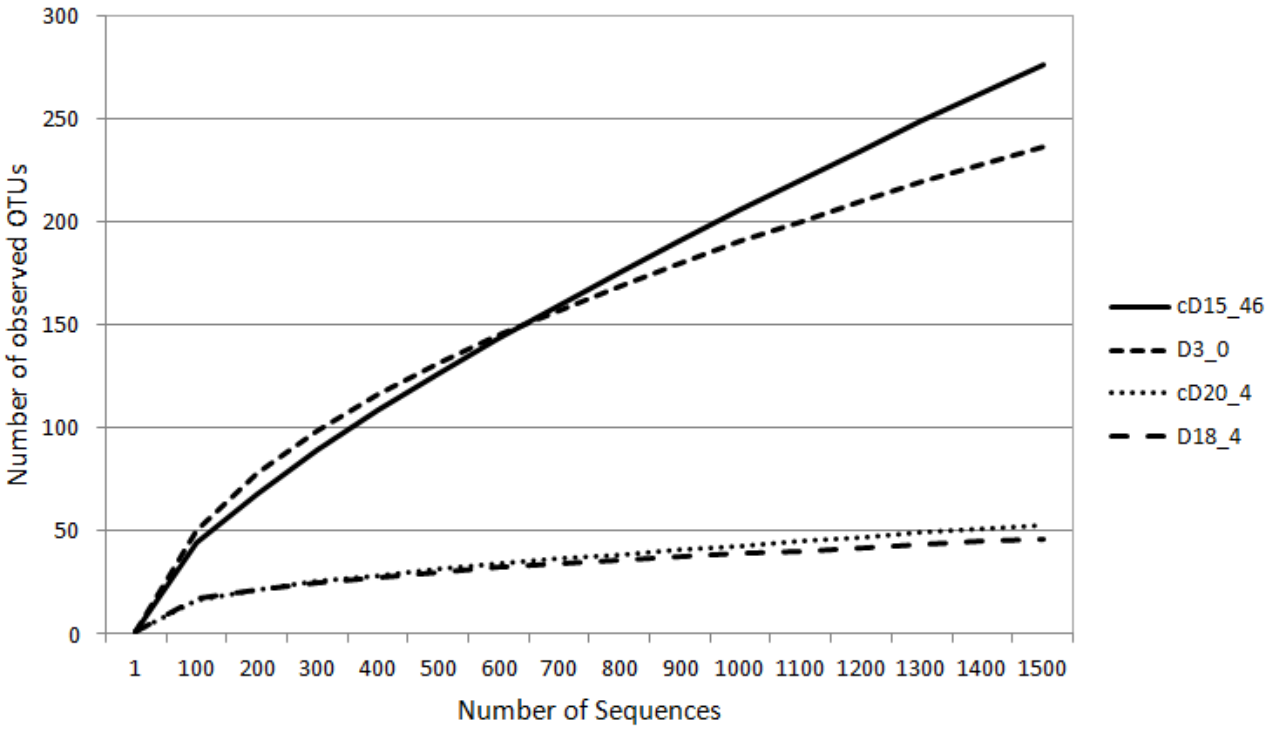

Figure 3-14: Rarefaction curves of the active and the present mucosa-associated microbiota with maximal, minimal and medial coverage.

The rarefaction curves and especially the Good´s coverages show that most of the bacteria present in the samples could be found. This indicates an adequate sampling. Therefore the analysis was continued with the different measurements of alpha diversity, which analyses the composition within a certain sample.

For this purpose the measurement of the observed OTUs, the Chao 1 richness estimator as well as the Shannon index were calculated. The individual values can be found within the appendix in Table 7-3, whereas the median and the quartiles of each parameter are plotted into the following boxplots.

For all three of the calculated parameters (observed OTUs, Chao1 richness estimator and Shannon index) there were no gender-specific effects in either of the comparisons. Furthermore the differences between the timepoints "Day 0" and "Day 4" were calculated and tested with the Wilcoxon rank sum test comparing the later placebo to the later probiotic group. The results were not significant indicating an appropriate randomization. All unpaired tests were performed with the exact Wilcoxon rank sum test, whereas the exact Wilcoxon signed rank test was used for paired samples.

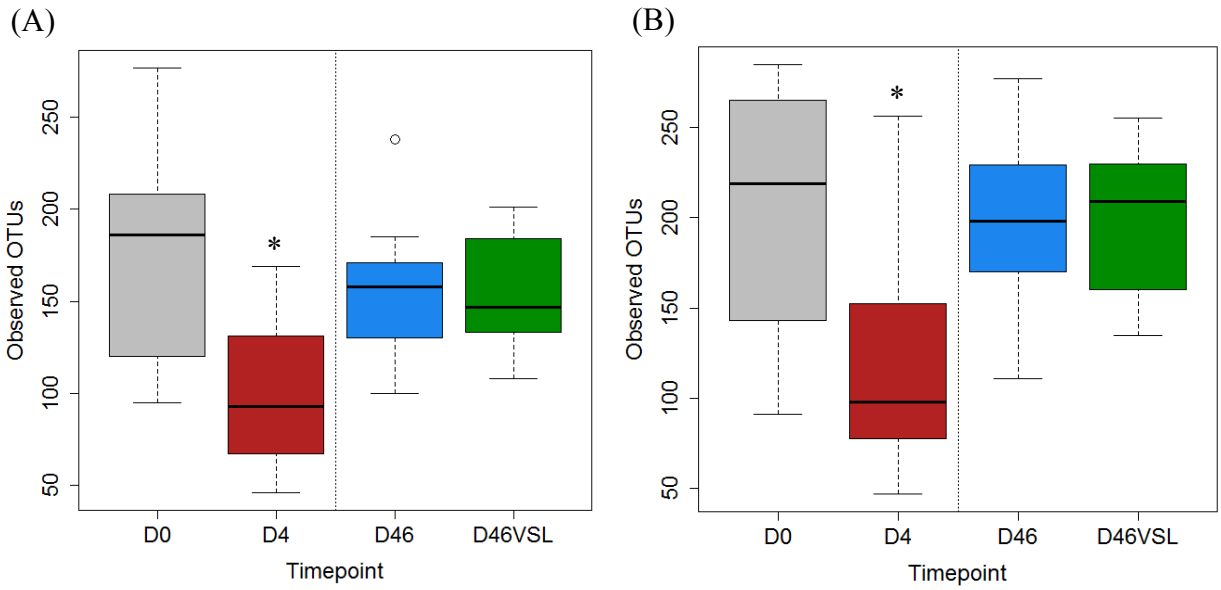

Figure 3-15: Boxplots of the observed OTUs for the present (A) and the active (B) mucosa-associated microbiota. Median, upper and lower quartile as well as upper and lower whisker are plotted. Grey (D0): Timepoint "Day 0" (n = 19), Red (D4): Timepoint "Day 4" after antibiotic treatment (n = 19), blue (D46): Timepoint "Day 46" after placebo therapy (n = 10), green (D46VSL): Timepoint "Day 46" after probiotic therapy (n = 9). * statistically significant compared to timepoint "Day 0" at a level of 0.05 after Bonferroni-Holm correction (n = 3).

For the observed OTUs one could see a significant decrease due to the antibiotic treatment from timepoint "Day 0" to "Day 4" in the present (Figure 3-15: (A); p_{corr} = 2.8e-04) as well in the active mucosa-associated bacteria (Figure 3-15: (B); p_{corr} = 0.0048). However, in both cases there was no difference between the placebo and the probiotic treatment (p_{corr} = 0.9744 for present and active microbiota), which means that both therapies resulted in nearly the same amount of observed OTUs at the end of the study. Further there was no significant difference between the timepoints "Day 0" and "Day 46" (p_{corr} = 0.2927 (present); p_{corr} > 1 (active)) within the present and the active microbiota, respectively.

The same picture can be seen if the richness is estimated by the Chao1 richness estimator. The antibiotic treatment led to a significant decrease within the present (Figure 3-16: (A); p_{corr} = 0.0053) microbiota as well as for the active bacteria (Figure 3-16: (B); p_{corr} = 0.0029), but again there was no difference between the probiotic and the placebo therapy in the present (p_{corr} = 0.6607) as well as in the active microbiota (p_{corr} = 0.9744) and there was no difference between the timepoints "Day 0" and "Day 46" (p_{corr} = 0.5153 (present); p_{corr} > 1 (active)).

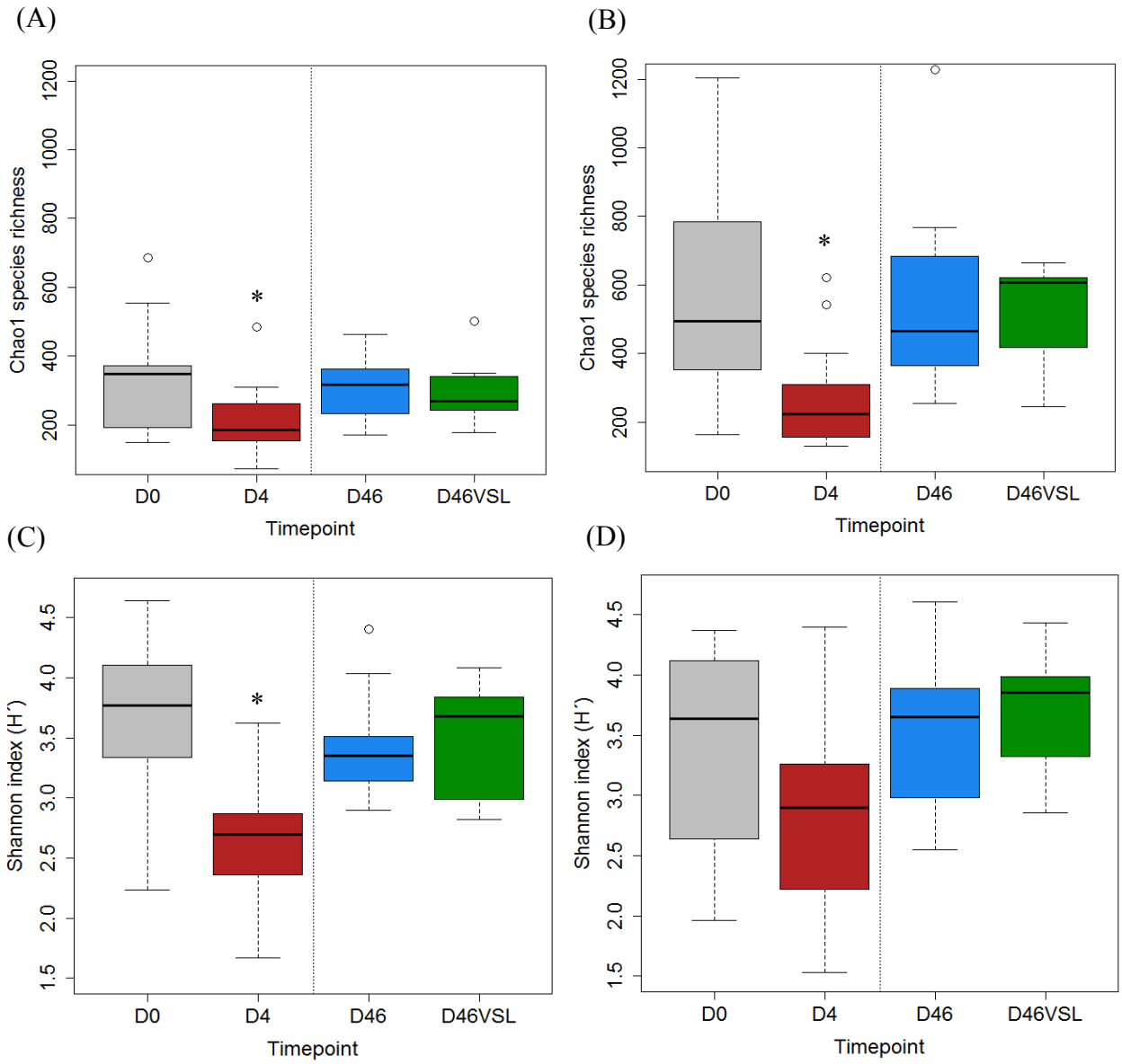

Figure 3-16: Boxplots of the Chao1 species richness for the present (A) and the active (B) and Shannon H´ for the present (C) and the active (D) mucosa-associated microbiota. Median, upper and lower quartile as well as upper and lower whisker are plotted. Grey (D0): Timepoint "Day 0" (n = 19), Red (D4): Timepoint "Day 4" after antibiotic treatment (n = 19), blue (D46): Timepoint "Day 46" after placebo therapy (n = 10), green (D46VSL): Timepoint "Day 46" after probiotic therapy (n = 9). * statistically significant compared to timepoint "Day 0" at a level of 0.05 after Bonferroni-Holm correction (n = 3).

When combining richness and evenness, diversity can be measured. In this case there was a significant decrease in the present microbiota (Figure 3-16: (C); p_{corr} = 2.8e-04 due to the antibiotic treatment, but not within the active microbiota (Figure 3-16: (D); p_{corr} = 0.0874). The effect of the probiotic compared to the placebo was not significant in both cases (p_{corr} = 0.3384 for the present bacteria; p_{corr} = 0.9744 for the active bacteria). The difference between the timepoints "Day 0" and "Day 46" was not significant within the present (p_{corr} = 0.2927) as well as in the active mucosa-associated microbiota (p_{corr} > 1).

In summary, the antibiotic treatment resulted in a more or less significant decrease in richness and diversity within the active and the present mucosa-associated microbiota. The regeneration of the microbiota was probiotic-independent. Further, richness as well as diversity seemed to recover to a high amount, nearly similar to the initial state, as there were no differences between the timepoints "Day 0" and "Day 46".

3.2.2.2 Beta-diversity

To investigate diversity between the samples, the unweighted and the weighted Bray-Curtis indices were calculated with the R package vegan. The indices were then converted into data points by a PCoA and plotted into a biplot.

Unweighted Bray-Curtis indices

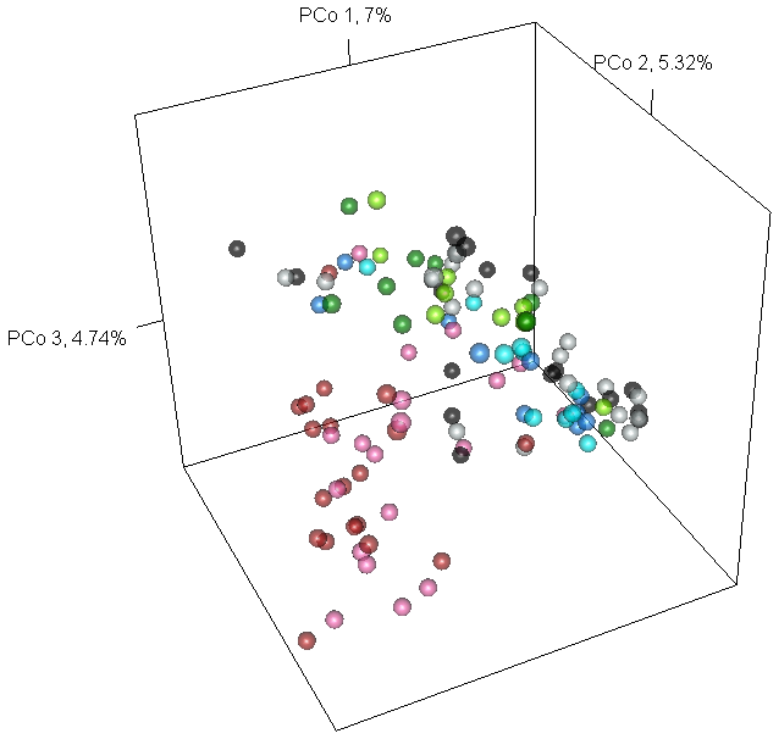

Figure 3-17: Biplot of the unweighted Bray-Curtis indices of the present and active mucosa-associated microbiota. "Day 0" (n = 19), present (●) and active (●); "Day 4" (after antibiotic treatment; n = 19), present (●) and active (●); "Day 46" (placebo group; n = 10), present (●) and active (●); "Day 46" (probiotic group; n = 9), present (●) and active (●).

Unweighted beta-diversity takes into account the absence and the presence of an OTU. Figure 3-17 shows the biplot of the unweighted Bray-Curtis indices of the present and the active mucosa-associated microbiota. The principal coordinate 1 represents 7% of the variation between the clusters, followed by 5.3% represented by the principal coordinate 2. The third axis explains 4.74%. It seems that if the red and pink circles, which indicate the timepoint "Day 4" after the antibiotic treatment, are separated compared to the remaining circles. To test for separated clusters formed by the treatments, an AMOVA was performed. The AMOVA showed that the clusters of the present compared to the active bacteria were not significant in either of the timepoints ($p_{corr} > 1$). There were no gender-dependant effects

within the active as well as in the present microbiota. Further there was no significant difference between the later probiotic and the later placebo group at either timepoint "Day 0" or "Day 4", indicating an appropriate randomization. Two more AMOVAs were performed to test between the treatments within the active and the present microbiota, respectively. The AMOVA of the present bacteria (Table 3-9 (A)) showed significant differences between the antibiotically treated (timepoints "Day 4", red circles) and the initial microbial composition at "Day 0" (black circles) as well as to both treatment groups (placebo and probiotic) at timepoint "Day 46" (dark green and dark blue circles). Further the probiotic group seemed still significantly altered at the end of the study (dark green circles) compared to the initial composition (black circles). However, there was no significant difference between the placebo and the probiotic treatment at timepoint "Day 46".

Table 3-9: Results of the AMOVA for unweighted Bray-Curtis indices of the (A) present and the (B) active mucosa-associated microbiota. 10^4 permutations were performed. Cells highlighted in grey show statistical significant results after Bonferroni-Holm correction for multiple testing (n = 6).

(A)

Timepoint			Day 4	Day 46	
	Treatment	Day 0	Antibiotic	Placebo	VSL#3
	Day 0		6e-05	0.3255	0.0399
Day 4	Antibiotic			6e-05	6e-05
Day 46	Placebo				0.3255
	VSL#3				

(B)

Timepoint			Day 4	Day 46	
	Treatment	Day 0	Antibiotic	Placebo	VSL#3
	Day 0		6e-05	0.0616	0.0616
Day 4	Antibiotic			0.0039	0.0002
Day 46	Placebo				0.1092
	VSL#3				

The results of the AMOVA for the active mucosa-associated microbiota revealed the results presented in Table 3-9 (B). There was a significant difference of the clusters formed by timepoint "Day 4" (pink circles) and "Day 0" (grey circles) as well as between "Day 4" and the placebo as well as the probiotic group of "Day 46" (light blue and light green circles). Again there was no difference between the placebo and the probiotic group.

To get an idea which OTUs were present in a specific cluster and therefore absent in another one, a Spearman correlation was conducted, correlating the OTUs to the axes of the biplot. Based on a minimum contribution of the OTUs of 0.5% to the overall similarity within a

SIMPER analysis, OTUs that fulfilled the a false-discovery rate of 0.05 are shown in Table 3-10.

Table 3-10: Statistical significant results of the Spearman correlation of OTUs to unweighted Bray-Curtis indices of the present and the active mucosa-associated microbiota. OTUs with a minimum contribution of 0.5% to the overall similarity. Fdr of 0.05. Cells highlighted in grey: OTUs that are plotted into the biplot in Figure 3-18 fulfilling the fdr of 1e-07.

OTU number/BLAST hit	PCo 1	PCo 2	PCo 3	length	p.min	q.val
26 Faecalibacterium	0.5340	0.0988	0.2470	0.5966	2.83e-09	2.21e-08
27 uncl. Lachnospiraceae	0.2327	-0.0323	-0.0965	0.2540	3.81e-02	4.95e-02
30 Bacteroides	0.0699	0.5704	-0.0932	0.5822	1.04e-10	1.62e-09
32 Parabacteroides	0.3121	-0.1654	0.0876	0.3639	2.17e-03	3.68e-03
34 Faecalibacterium	0.4869	0.3530	0.1369	0.6167	1.19e-07	5.15e-07
38 Faecalibacterium	0.5028	0.0101	0.1664	0.5297	3.57e-08	1.99e-07
40 Subdoligranulum	0.6037	0.2333	-0.1210	0.6584	3.49e-12	8.63e-11
46 Coprobacillus	0.3891	0.3198	-0.0113	0.5038	5.64e-05	1.33e-04
47 Blautia	0.6281	0.0255	0.2513	0.6770	2.22e-13	8.65e-12
48 uncl. Peptostreptococcaceae	0.3609	0.1524	0.2142	0.4465	2.39e-04	4.79e-04
51 uncl. Peptostreptococcaceae	0.4449	0.1193	0.0065	0.4607	2.12e-06	6.88e-06
56 Sutterella	0.3985	0.2170	0.1180	0.4688	3.39e-05	8.26e-05
65 Blautia	0.6595	0.0050	0.2155	0.6938	4.43e-15	3.45e-13
76 uncl. Lachnospiraceae	0.5363	0.0669	0.1936	0.5741	2.33e-09	2.02e-08
81 uncl. Lachnospiraceae	0.4547	0.1817	-0.2835	0.5658	1.12e-06	3.96e-06
91 uncl. Lachnospiraceae	0.5448	0.02300	-0.0290	0.5461	1.11e-09	1.23e-08
101 Ralstonia	-0.2653	0.4513	-0.0804	0.5296	1.40e-06	4.76e-06
119 Bacteroides	0.35155	0.1184	-0.0833	0.3802	3.76e-04	7.16e-04
154 uncl. Lachnospiraceae	0.38711	0.0171	-0.2282	0.4497	6.28e-05	1.44e-04
166 Holdemania	-0.0457	0.0415	-0.2453	0.2530	2.56e-02	3.50e-02
196 Roseburia	0.0436	0.0726	0.3832	0.3924	7.74e-02	1.68e-04
197 Sphingobium	-0.1968	0.4688	0.0320	0.5095	4.31e-07	1.77e-06
198 uncl. Lachnospiraceae	-0.1351	-0.1245	0.6015	0.6289	4.42e-12	8.63e-11
220 Collinsella	0.24541	0.2166	-0.4914	0.5904	8.50e-08	4.15e-07
231 Eubacterium	-0.4192	-0.1371	0.1216	0.4575	1.03e-05	2.88e-05
246 Streptococcus	-0.1279	0.1992	0.2411	0.3379	2.93e-02	3.94e-02
267 Finegoldia	0.0899	0.5263	0.3929	0.6629	5.45e-09	3.87e-08
268 Escherichia/Shigella	-0.0332	0.4568	0.3210	0.5593	9.73e-07	3.61e-06
279 Roseburia	0.0364	0.0034	0.5010	0.5023	4.12e-08	2.14e-07
291 Oscillibacter	0.3113	-0.0798	0.3230	0.4556	1.37e-03	2.43e-03
293 Coprobacillus	0.1480	0.2700	0.0879	0.3202	1.10e-02	1.68e-02
294 Streptococcus	0.0292	0.4347	0.4611	0.6343	7.31e-07	2.85e-06
320 uncl. Erysipelotrichaceae	-0.1169	-0.3089	0.1375	0.3578	2.48e-03	4.11e-03
349 Eubacterium	0.1106	0.2519	-0.2431	0.3671	2.06e-02	2.97e-02
362 uncl. Lachnospiraceae	0.5200	0.0059	0.1818	0.5509	9.12e-09	5.93e-08
363 Bacteroide	0.1590	0.0498	-0.2361	0.2890	3.43e-02	4.54e-02
364 Subdoligranulum	0.4314	0.3157	-0.2437	0.5874	4.97e-06	1.49e-05
365 Roseburia	0.5409	0.1268	0.0731	0.5604	1.56e-09	1.52e-08

OTU number/BLAST hit	PCo 1	PCo 2	PCo 3	length	p.min	q.val
384 Faecalibacterium	0.4123	0.1200	0.1253	0.4473	1.55e-05	4.16e-05
386 Faecalibacterium	0.5086	0.1717	-0.0701	0.5413	2.28e-08	1.37e-07
392 Coprococcus	0.1351	0.0570	-0.4043	0.4301	2.45e-05	6.16e-05
394 Bacteroides	-0.0051	-0.0669	-0.3252	0.3320	1.25e-03	2.26e-03
624 Holdemania	-0.2415	-0.0669	-0.4056	0.4768	2.27e-05	5.90e-05
631 Prevotella	0.1432	0.3468	0.0245	0.3760	4.71e-04	8.75e-04
661 Enterococcus	-0.2793	-0.0437	-0.0652	0.2902	7.84e-03	1.22e-02
668 Brevundimonas	0.1772	0.3691	0.1042	0.4225	1.60e-04	3.27e-04
699 uncl. Erysipelotrichaceae	-0.0248	-0.2548	0.1788	0.3122	1.87e-02	2.75e-02
763 Methylobacterium	0.08159	0.4358	-0.0312	0.4445	3.77e-06	1.18e-05
771 uncl. Incertae Sedis_XI	0.2092	0.4875	0.1448	0.5499	1.13e-07	5.15e-07
776 Roseburia	0.0111	-0.2883	0.4289	0.5170	5.77e-06	1.67e-05
821 Blautia	-0.0918	-0.1707	0.3065	0.3626	2.73e-03	4.44e-03
1071 Stenotrophomonas	-0.0627	0.2593	-0.0083	0.2669	1.60e-02	2.40e-02
1252 Coprobacillus	-0.0081	-0.1323	0.5549	0.5705	4.49e-10	5.83e-09
1291 Holdemania	-0.2565	0.0944	-0.3564	0.4491	2.99e-04	5.83e-04
1398 Pseudomonas	-0.0726	0.3786	-0.0320	0.3868	9.83e-05	2.07e-04
1426 Faecalibacterium	-0.0749	-0.1949	0.2870	0.3549	5.88e-03	9.36e-03
1453 Lactobacillus	0.0699	0.0184	0.3196	0.3276	1.59e-03	2.75e-03
1498 uncl. Prevotellaceae	0.0943	0.2505	-0.0248	0.2688	2.15e-02	3.00e-02
1517 Sutterella	0.3863	0.1008	-0.0207	0.3998	6.54e-05	1.46e-04
1786 Blautia	-0.0812	-0.0740	0.2507	0.2737	2.14e-02	3.00e-02

To depict in a biplot in which direction the OTUs point, the fdr was increased to 1e-07 resulting in 12 OTUs (highlighted in grey in Table 3-10). Figure 3-18 shows the resulting biplot with the correlated OTUs. OTUs with a positive PCo 1 point into the direction of the initial composition at timepoint "Day 0" and therefore into the opposite direction of the antibiotic treatment of "Day 4". Many of those OTUs have a homology to the genera *Blautia*, *Faecalibacterium* and the family *Lachnospiraceae*. Those genera were therefore present within the normal microbiota at the initial timepoint "Day 0", but absent within the antibiotically treated microbiota. OTUs with a negative first principal coordinate and a positive second principal coordinate might show into the direction of the probiotic group of the present microbiota (dark green circles), which clustered significantly separate as shown by the AMOVA.

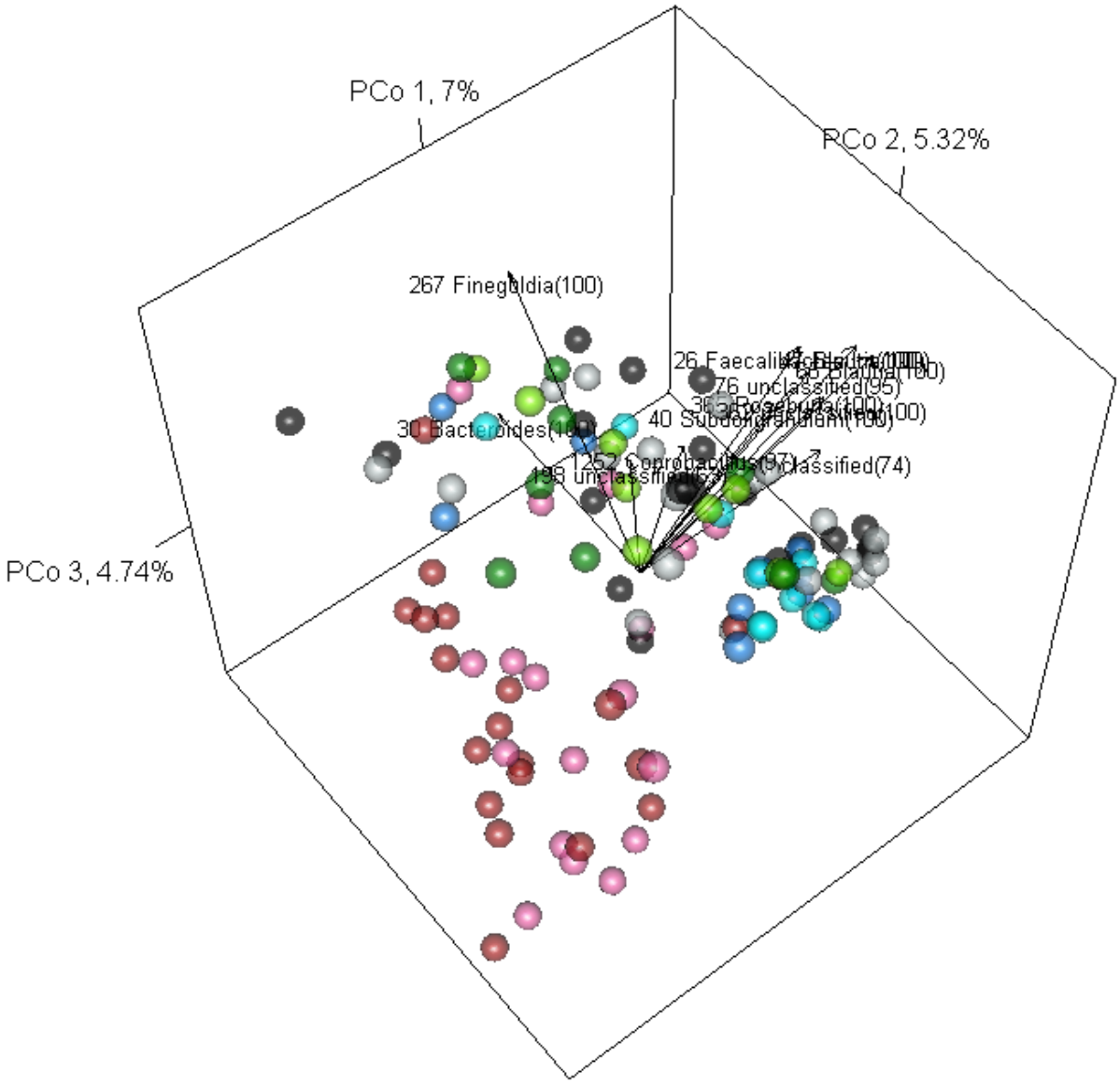

Figure 3-18: Biplot of unweighted Bray-Curtis indices of the present and active mucosa-associated microbiota and OTUs correlated to the axes. Correlated OTUs contribute at least 0.5% to the overall similarity and fulfilled the fdr of 1e-07. "Day 0" (n = 19), present (●) and active (●); "Day 4" (after antibiotic treatment, n = 19), present (●) and active (●); "Day 46" placebo group (n = 10), present (●) and active (●); "Day 46" probiotic group (n = 9), present (●) and active (●).

Weighted Bray-Curtis indices

As for the unweighted Bray-Curtis, a biplot was designed for the weighted Bray-Curtis indices, taking into account the abundances of the different OTUs. Figure 3-19 shows the result of the PCoA of weighted Bray-Curtis indices of the present and active mucosa-associated microbiota at the several treatments/timepoints. The highest variation of 7.74% is explained by the principal coordinate 1. The second PCo represents nearly 7% of the variation and the third PCo 5.22%. In general the lighter circles, representing the active bacteria, do not seem to separate very much from the darker circles, representing the present bacteria, in either of the treatment groups. The antibiotically treated microbiota, which is represented by the red and pink colored circles, seems to form a separate cluster apart from the other circles. A separation between the placebo (blueish) and the probiotic (greenish) treated active as well as present microbiota is not clearly visible.

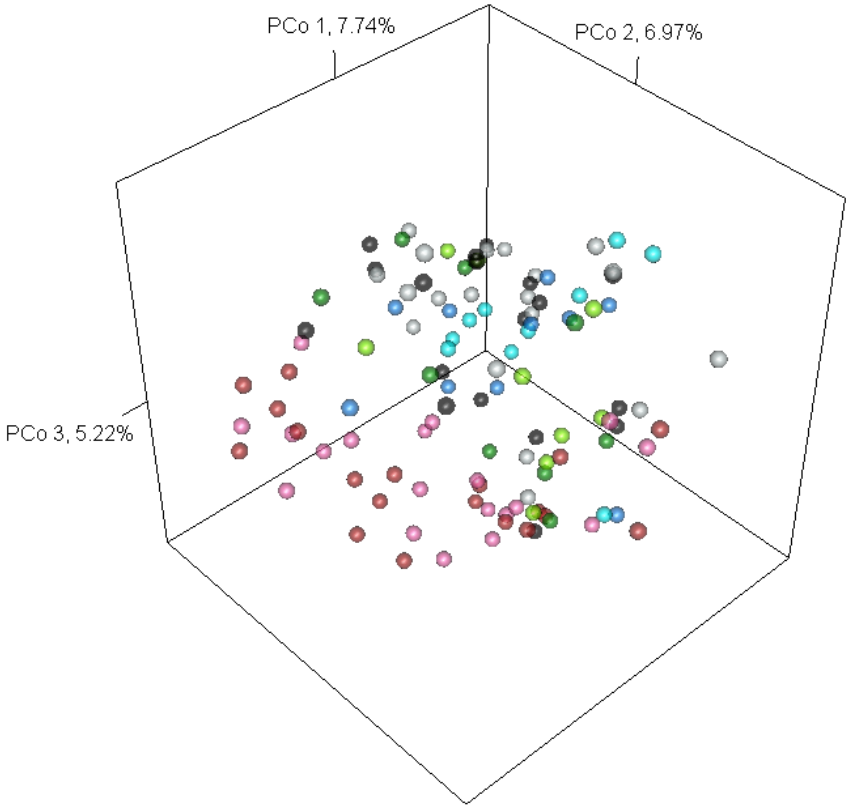

Figure 3-19: Biplot of weighted Bray-Curtis indices of the present and active mucosa-associated microbiota. "Day 0" (n = 19), present (●) and active (●); "Day 4" (after antibiotic treatment; n = 19), present (●) and active (●); "Day 46" placebo group (n = 10), present (●) and active (●); "Day 46" probiotic group (n = 9), present (●) and active (●).

For a detailed analysis of the differences between the clusters representing the different treatments/timepoints an AMOVA was performed as described for unweighted Bray-Curtis indices. No significant differences between the present and the active microbiota at either of the timepoints/treatments ($p_{corr} > 1$ for each comparison) could be detected. Furthermore, there were no gender-dependent effects within the active and the present mucosa-associated microbiota at the several timepoints, respectively.

Table 3-11: Results of the AMOVA for weighted Bray-Curtis indices of the (A) present and the (B) active mucosa-associated microbiota. 10^4 permutations were performed. Cells highlighted in grey show statistical significant results after Bonferroni-Holm correction for multiple testing (n = 6).

(A)

Timepoint			Day 4	Day 46	
	Treatment	Day 0	Antibiotic	Placebo	VSL#3
	Day 0				
Day 4	Antibiotic	6e-05			
Day 46	Placebo	1	0.0016		
	VSL#3	0.8691	0.0144	1	

(B)

Timepoint			Day 4	Day 46	
	Treatment	Day 0	Antibiotic	Placebo	VSL#3
	Day 0				
Day 4	Antibiotic	6e-05			
Day 46	Placebo	0.5734	6e-05		
	VSL#3	0.5486	0.0091	0.5486	

Table 3-11 (A) shows the result of the AMOVA for the present mucosa-associated microbiota. There is a significant difference between the timepoint ”Day 4” (red and pink circles), which is after the antibiotic treatment, and all other three timepoints/treatments. However, there are no differences between the initial composition of “Day 0” and the end of the study at “Day 46”, regardless of the treatment. Furthermore, there is no difference in the comparison of the placebo and the probiotic treatment. The results of the active mucosa-associated microbiota as depicted in Table 3-11 (B) are the same as within the present microbiota.

Due to some differences between the timepoints a Spearman correlation, a metastats approach as well as the search for indicator species were performed. This enables the identification of OTUs that are responsible for a separation of the different timepoints and treatments. The analyses were performed as described before. Only OTUs with a minimum contribution of 0.5% to the overall similarity as revealed in an upstream SIMPER analysis were taken into account.

Table 3-12: Results of the Spearman correlation of OTUs to weighted Bray-Curtis indices of the present and active mucosa-associated microbiota. OTUs with a minimum contribution of 0.5% to the overall similarity. Fdr of 0.05. Cells highlighted in grey: OTUs that fulfilled the fdr of 1.0 e-05 and are plotted into the biplot in Figure 3-20.

OTU number/BLAST hit	PCo 1	PCo 2	PCo 3	length	p.min	q.val
26 Faecalibacterium	0.6401	0.3251	0.5059	0.8783	5.23e-14	1.02e-12
30 Bacteroides	0.1698	-0.3950	-0.1280	0.4486	4.10e-05	1.85e-04
32 Parabacteroides	0.0843	0.2940	0.2036	0.3675	4.49e-03	1.17e-02
33 Bacteroides	-0.5925	0.5831	0.2632	0.8719	1.15e-11	1.28e-10
34 Faecalibacterium	0.3942	0.1577	0.1074	0.4380	4.27e-05	1.85e-04
38 Faecalibacterium	0.4853	0.2355	0.4637	0.7113	1.34e-07	1.04e-06
40 Subdoligranulum	0.3518	0.4341	0.0985	0.5674	4.19e-06	2.33e-05
46 Coprobacillus	0.3055	0.0983	-0.0817	0.3312	2.85e-03	7.93e-03
47 Blautia	0.7146	0.4581	0.2698	0.8907	1.30e-18	1.02e-16
48 uncl. Peptostreptococcaceae	0.4467	0.1981	-0.0622	0.4926	1.90e-06	1.14e-05
51 uncl. Peptostreptococcaceae	0.3923	0.3091	0.0492	0.5019	4.74e-05	1.95e-04
56 Sutterella	0.2501	0.1078	0.1756	0.3240	2.18e-03	4.37e-02
65 Blautia	0.7055	0.4085	0.2773	0.8611	5.69e-18	2.22e-16
76 uncl. Lachnospiraceae	0.6144	0.3952	0.1492	0.7455	1.08e-12	1.40e-11
81 uncl. Lachnospiraceae	0.3440	0.4725	-0.1679	0.6081	3.32e-07	2.36e-06
91 uncl. Lachnospiraceae	0.4581	0.3789	0.2592	0.6485	8.90e-07	5.79e-06
101 Ralstonia	-0.2354	-0.2138	-0.3634	0.4829	2.12e-04	8.27e-04
119 Bacteroides	0.3109	0.2734	0.1330	0.4348	2.28e-03	6.60e-03
154 uncl. Lachnospiraceae	0.2522	0.1414	-0.1679	0.3344	2.04e-02	4.18e-02
158 uncl. Firmicutes	-0.4051	-0.2311	-0.0385	0.4680	2.33e-05	1.14e-04
197 Sphingobium	-0.1468	-0.1824	-0.2532	0.3449	1.97e-02	4.15e-02
220 Collinsella	0.1245	0.2853	0.0206	0.3120	6.27e-03	1.58e-02
231 Eubacterium	-0.4178	-0.3720	-0.0760	0.5646	1.12e-05	5.83e-05
268 Escherichia/Shigella	0.0552	-0.6504	0.3540	0.7425	1.45e-14	3.78e-13
291 Oscillibacter	0.1478	-0.0023	0.2593	0.2985	1.60e-02	3.47e-02
294 Streptococcus	0.1616	-0.3041	-0.0808	0.3538	3.01e-03	8.09e-03
362 uncl. Lachnospiraceae	0.6273	0.2335	0.1391	0.6836	2.44e-13	3.81e-12
363 Bacteroides	0.0017	0.3233	-0.0269	0.3244	1.35e-03	4.39e-03
364 Subdoligranulum	0.2653	0.1997	0.0163	0.3325	1.30e-02	2.98e-02
365 Roseburia	0.5566	0.3410	-0.0629	0.6558	3.83e-10	3.73e-09
384 Faecalibacterium	0.4861	0.1386	0.1289	0.5216	1.26e-07	1.04e-06
386 Faecalibacterium	0.2932	0.3472	0.0846	0.4623	4.61e-04	1.71e-03
612 Prevotella	-0.0987	0.1334	-0.3180	0.3587	1.69e-03	5.28e-03
661 Enterococcus	-0.1670	0.0214	-0.3332	0.3733	8.77e-04	2.97e-03
771 uncl. Incertae Sedis_XI	0.2742	-0.0692	-0.1539	0.3219	9.48e-03	2.31e-02
904 Prevotella	-0.1147	0.1888	-0.2730	0.3512	9.89e-03	2.34e-02
1252 Coprobacillu	0.1225	-0.2601	0.2062	0.3538	1.56e-02	3.47e-02
1398 Pseudomonas	-0.1545	-0.1034	-0.3336	0.3818	8.61e-04	2.97e-03
2459 Parasutterella	-0.0884	-0.3126	0.0795	0.3345	2.12e-03	6.37e-03

To visualize which OTUs are responsible for the clustering of the treatment groups, the significantly correlated OTUs were plotted into the biplot. To reduce the number of OTUs only OTUs that survived the fdr of 1.0 e-05 are depicted in Figure 3-20.

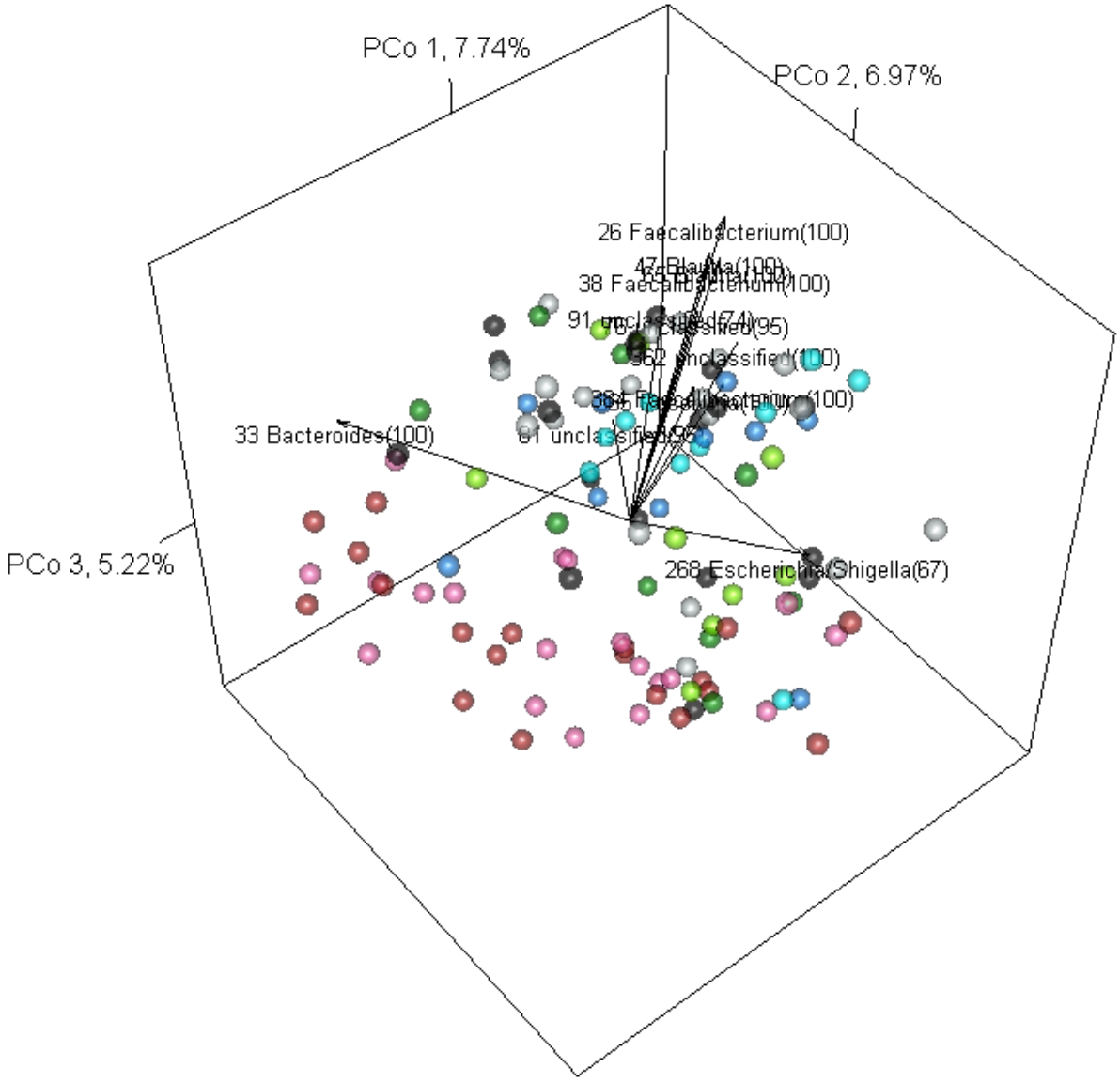

Figure 3-20: Biplot of weighted Bray-Curtis indices for the present and the active mucosa-associated microbiota and OTUs correlated to the axes. Correlated OTUs contribute at least 0.5% to the overall similarity and fulfilled the fdr of 1e-05. "Day 0" (n = 19), present (●) and active (●); "Day 4" (after antibiotic treatment, n = 19), present (●) and active (●); "Day 46" placebo group (n = 10), present (●) and active (●); "Day 46" probiotic group (n = 9), present (●) and active (●).

OTUs listed in Table 3-12 that have a negative value for the PCo 1 tend to be more abundant within the antibiotically treated microbiota. A classification revealed that those OTUs belong to genera like *Bacteroides*, *Prevotella*, *Pseudomonas* and *Ralstonia*. OTUs that have positive values for all of their three PCos point into the direction opposite of the samples representing the antibiotic treatment, these are OTUs having homology to *Faecalibacterium*, *Blautia* and

Subdoligranulum or *Lachnospiraceae.* Therefore they are more abundant in the normal as well as the placebo or probiotically treated microbiota and are rare after antibiotic treatment.

In addition to the correlation the metastats approach was used. The SIMPER analysis identified OTUs with a minimum contribution of 0.5% and was thereby reducing the dataset. The results for the comparison between the placebo and the probiotic-treated group at timepoint "Day 46" for the active as well as the present mucosa-associated microbiota is shown in Table 3-13.

Table 3-13: Statistical significant results of the metastats analysis comparing the probiotic and the placebo treated groups at "Day 46" within the active and the present microbiota. Ratio is relative to placebo. 1000 permutations were performed. p values after Bonferroni-Holm correction for multiple testing. Appears= present in probiotic, but absent in placebo group, Disappears= absent in probiotic group, but present in placebo. n = 10 within the placebo group, n = 9 within the probiotic group

	Present Bacteria	**Active Bacteria**
OTU number/BLAST hit	**ratio (log_{10})**	**ratio (log_{10})**
349 Eubacterium		0.020 (-1.706)
904 Prevotella		disappears
1498 uncl. Prevotellaceae	appears	appears
1693 Bacteroides	disappears	

The AMOVA shown before already revealed that there were no significant differences between the placebo and the probiotic group at timepoint "Day 46" within the present as well as in the active mucosa-associated microbiota. Therefore it is also expected to find less OTUs that are significantly represented differently between the treatment groups (table 3-15).

OTUs that are represented different between "Day 0" and "Day 4" (antibiotic) as well as between "Day 0" and "Day 46" (placebo or probiotic) are listed in Table 3-14.

Table 3-14: Statistical significant results of the metastats analysis comparing timepoint "Day 0" and "Day 46" within the present mucosa-associated microbiota. Ratio is relative to "Day 0". 1000 permutations were performed. p values after Bonferroni-Holm correction for multiple testing. Disappears = absent at "Day 46", but present at "Day 0". Appears = present at "Day 46", but absent at "Day 0". n = 19 ("Day 0"); n = 10 ("Day 46" Placebo); n = 9 ("Day 46" Probiotic). Cells highlighted in grey: Indicator species at 97% level.

	Day 4	**Day 46 Placebo**	**Day 46 Probiotic**
OTU number/BLAST hit	**ratio (log_{10})**	**ratio (log_{10})**	**ratio (log_{10})**
26 Faecalibacterium	0.018(-1.754)		
34 Faecalibacterium	0.098 (-1.009)		
38 Faecalibacterium	0.012 (-1.936)		
46 Coprobacillus	0.030 (-1.527)		
47 Blautia	0.029 (-1.536)		

OTU number/BLAST hit	Day 4 ratio (log_{10})	Day 46 Placebo ratio (log_{10})	Day 46 Probiotic ratio (log_{10})
56 Sutterella	disappears		
65 Blautia	0.016 (-1.799)		
91 uncl. Lachnospiraceae	0.004 (-2.423)		
158 uncl. Firmicutes	47.882 (1.680)		
231 Eubacterium	3.782 (0.578)		
362 uncl. Lachnospiraceae	0.092 (-1.035)		
364 Subdoligranulum	0.028(-1.546)		
384 Faecalibacterium		0.157 (-0.803)	
1071 Stenotrophomonas			disappears
1398 Pseudomonas	appears		

The AMOVA already showed no significant differences between the composition of the microbiota at "Day 0" compared to the placebo as well as the probiotic group at "Day 46". Therefore it is not unexpected that not many differently represented OTUs were found. The significant difference between the initial and the antibiotic-treated microbiota shows OTUs mainly having identity with the genera *Faecalibacterium*, *Blautia* and the family *Lachnospiraceae*. Those OTUs are highly abundant within the untreated microbiota and are highly reduced due to the antibiotic treatment.

This effect could be validated within the indicator species approach. At species level (97% identity) the OTUs 26, 34, 38, 47, 65 and 362 were identified as indicator species characterizing the difference between the timepoints "Day 0" and "Day 4" and therefore the influence of the antibiotic treatment. As shown before, the classification of these OTUs were found to have homology with *Blautia* and *Faecalibacterium* as well as with *Lachnospiraceae*. For the comparison of the other timepoints/treatments no indicator species could be found. This shows that there are no specific OTUs characterizing the probiotic group compared to the placebo. Furthermore, these results indicate a good recovery of the microbiota as there are no OTUs characterizing the placebo or the probiotically treated microbiota at "Day 46" in comparison to "Day 0". The search for indicator species on the genus level (95% identity) revealed the same results.

For the active bacteria the same analyses were performed (Table 3-15). The metastats analysis identified OTUs differently represented between the timepoints "Day 0" and "Day 4". Comparing the results to the present microbiota (table 3-14) the active microbiota showed more different OTUs as there was only one OTU found for the *Faecalibacterium* and *Blautia*, respectively. On the one hand OTUs that did not appear within the analysis of the present microbiota were found. However, those two OTUs (OTU 26 and 65) were also decreased

within the active mucosa-associated microbiota due to antibiotic treatment. On the other hand OTUs having identity to *Bacteroides*, *Enterococcus* and *Pseudomonas* as well as an OTU characterized by *Lachnospiraceae* seemed to be highly abundant within the antibiotic-treated microbiota. The comparison between "Day 0" and "Day 46" did not detect noteworthy differences.

Table 3-15: Statistical significant results of the metastats analysis comparing timepoint "Day 0" and "Day 46" within the active mucosa-associated microbiota. Ratio is relative to "Day 0". 1000 permutations were performed. p values after Bonferroni-Holm correction for multiple testing. Disappears = absent at "Day 46", but present at "Day 0". Appears = present at "Day 46", but absent at "Day 0". n = 19 ("Day 0"); n = 10 ("Day 46" Placebo); n = 9 ("Day 46" Probiotic). Cells highlighted in grey: Indicator species at 97% level.

	Day 4	Day 46 Placebo	Day 46 Probiotic
OTU number/BLAST hit	**ratio (log_{10})**	**ratio (log_{10})**	**ratio (log_{10})**
26 Faecalibacterium	0.033 (-1.488)		
56 Sutterella	0.020 (-1.696)		
65 Blautia	0.051 (-1.294)		
158 uncl. Firmicutes	50.273 (1.701)		
197 Sphingobium	disappears		
198 uncl. Lachnospiraceae	42.686 (1.630)		
231 Eubacterium	5.146 (0.711)		
293 Coprobacillus	0.009 (-2.055)		
365 Roseburia	0.078 (-1.109)		
394 Bacteroides	6.913 (0.084)		
631 Prevotella	disappears		
661 Enterococcus	431.868 (2.635)		
668 Brevundimonas	disappears	disappears	
763 Methylobacterium	0.013 (-1.891)		
1071 Stenotrophomonas	0.002 (-2.694)		
1291 Holdemania	appears		
1398 Pseudomonas	51.467 (1.712)		

The indicator species approach for the active mucosa-associated microbiota revealed the OTU 26 to be representative for the difference between the initial healthy and the antibiotically treated microbiota. OTU 26, which has identity to *Faecalibacterium*, was also shown to be an indicator species within the present mucosa-associated microbiota. In addition, an OTU having identity with *Blautia* was detected as indicator species on the genus level (95% identity). This OTU is highly abundant in the initial healthy microbiota and decreased due to the antibiotic treatment. For the comparison between the placebo and the probiotic therapy at "Day 46" as well as between the timepoints "Day 0" and "Day 46" no indicator species could be found.

As described for the luminal samples a Spearman correlation correlating the whole taxa (genus) to the axes was performed.

Table 3-16: Statistical significant results of the Spearman correlation of the taxa on genus level and weighted Bray-Curtis indices of the present and the active mucosa-associated microbiota. Taxa with a minimum contribution of 0.5% to the overall similarity. Fdr of 0.05. Cells highlighted in grey: Taxa that are plotted into the biplot in Figure 3-21 fulfilling the fdr of 0.001.

Taxon	PCo 1	PCo 2	PCo 3	length	p.min	q.val
Acinetobacter	-0.0563	-0.0983	-0.2718	0.2944	1.03e-02	1.59e-02
Bacteroides	-0.3760	0.1021	0.1180	0.4062	1.18e-04	3.00e-04
Blautia	0.5797	0.4794	0.0989	0.7588	4.18e-11	5.99e-10
uncl. Clostridiales	0.4316	0.2863	0.0874	0.5252	4.91e-06	3.01e-05
Collinsella	0.18764	0.2506	0.1004	0.3287	2.15e-02	2.80e-02
Coprobacillus	0.2678	-0.1104	0.4042	0.4973	2.46e-05	1.06e-04
Coprococcus	0.2557	0.3708	-0.0894	0.4592	1.46e-04	3.31e-04
uncl. Cyanobacteria	-0.0446	-0.1323	-0.3289	0.3573	1.06e-03	2.07e-03
Dorea	0.3568	0.3961	-0.0270	0.5338	3.86e-05	1.51e-04
Enterobacter	-0.0867	-0.4265	0.1310	0.4545	6.68e-06	3.19e-05
uncl. Enterobacteriaceae	-0.0931	-0.3914	0.3475	0.5316	4.99e-05	1.79e-04
Enterococcus	-0.1851	-0.0498	-0.3253	0.3776	1.24e-03	2.32e-03
Escherichia/Shigella	0.0516	-0.6273	0.3592	0.7247	2.45e-13	1.05e-11
Eubacterium	-0.2400	-0.0889	-0.1749	0.3100	3.03e-02	3.83e-02
Faecalibacterium	0.6117	0.3421	0.4079	0.8109	1.45e-12	3.12e-11
Finegoldia	0.1437	-0.2345	-0.10738	0.2952	3.61e-02	4.43e-02
uncl. Firmicutes	-0.3895	-0.2254	0.0186	0.4504	5.52e-05	1.83e-04
Holdemania	-0.3109	0.0278	-0.0287	0.3135	2.28e-03	3.93e-03
uncl. Incertae_Sedis_XI	0.1222	-0.3188	-0.2321	0.4129	1.64e-03	2.94e-03
uncl. Lachnospiraceae	0.42900	0.2723	0.1327	0.5251	5.74e-06	3.08e-05
Methylobacterium	-0.0403	-0.1173	-0.2515	0.2805	2.08e-02	2.80e-02
Oscillibacter	0.2435	0.1169	0.3077	0.4094	2.61e-03	4.32e-03
Parasutterella	-0.0766	-0.2670	-0.0323	0.2796	1.23e-02	1.77e-02
Peptoniphilus	0.0634	-0.3652	-0.1619	0.4044	1.94e-04	4.18e-04
uncl. Peptostreptococcaceae	0.3867	0.2554	-0.0901	0.4721	6.41e-05	1.97e-04
Prevotella	0.0640	0.0009	-0.3828	0.3881	7.90e-05	2.12e-04
Pseudomonas	-0.0869	-0.1168	-0.3850	0.4116	7.02e-05	2.01e-04
Ralstonia	-0.2477	-0.2248	-0.3728	0.5009	1.32e-04	3.16e-04
Roseburia	0.5007	0.2074	0.1675	0.5672	4.22e-08	3.63e-07
uncl. Ruminococcaceae	0.0414	0.2818	-0.0114	0.2850	7.16e-03	1.14e-02
Ruminococcus	0.5625	0.3963	0.1340	0.7010	2.21e-10	2.38e-09
Sphingobium	-0.1146	-0.1938	-0.2669	0.3491	1.23e-02	1.77e-02
Stenotrophomonas	-0.0529	-0.1749	-0.2641	0.3211	1.36e-02	1.88e-02
Subdoligranulum	0.4367	0.4150	0.0997	0.6106	3.56e-06	2.55e-05
Sutterella	0.3439	0.1370	0.2551	0.4496	5.38e-04	1.10e-03

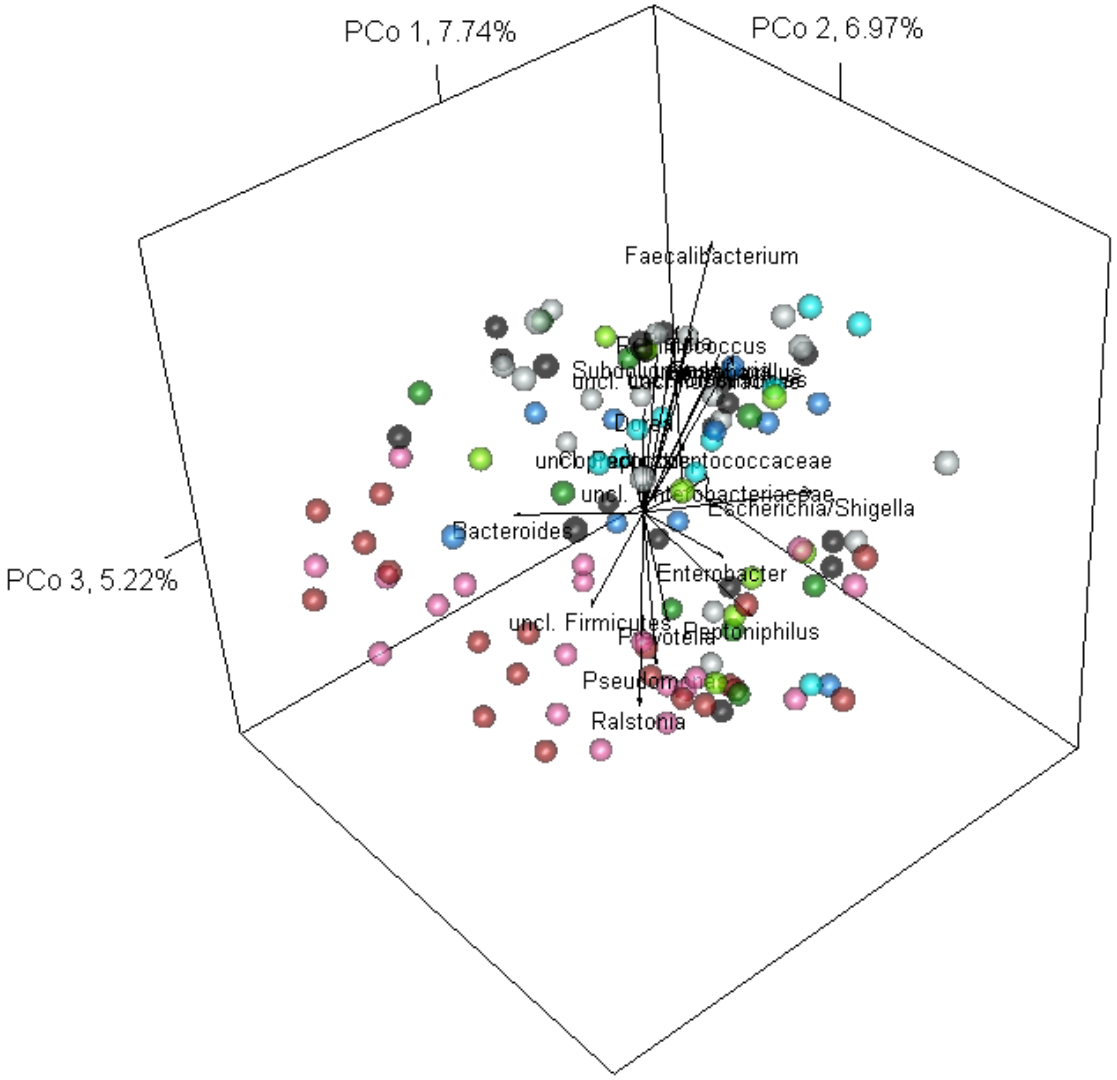

Figure 3-21: Biplot of weighted Bray-Curtis indices for the present and the active mucosa-associated microbiota and taxa correlated to the axes. Correlated OTUs contribute at least 0.5% to the overall similarity and fulfilled the fdr of 0.001. "Day 0" (n = 19), present (●) and active (●); "Day 4" (after antibiotic treatment, n = 19), present (●) and active (●); "Day 46" placebo group (n = 10), present (●) and active (●); "Day 46" probiotic group (n = 9), present (●) and active (●).

The correlation of the taxa to the axes shows that the genera *Faecalibacterium* and *Blautia*, which were also detected within the indicator approach, were highly correlated, showing into the direction of the healthy microbiota opposite of the antibiotically treated microbiota. The antibiotically treated microbiota seemed to be characterized by *Bacteroides*, *Pseudomonas* and *Ralstonia*. Due to the missing difference between the probiotic and the placebo as well as the initial group, a taxon on genus level characterising the probiotic one could not be identified.

3.3 Real-time PCR approach

3.3.1 Quantitative results of the luminal microbiota

The aim of the real-time PCR was to receive an impression of the quantity of the luminal and mucosa-associated microbiota. All bacteria and in addition the two phyla *Firmicutes* and *Bacteroidetes* were measured. The data were normalised to beta actin. With regard to the present luminal microbiota (Figure 3-22), they represented a relative amount of 2.9e+06 in median. Due to the antibiotic treatment there was a significant decrease (p_{corr} = 0.0137) up to 4e+05. The placebo and the probiotic treatment resulted in a higher relative amount within the probiotically treated group at all three timepoints, but the differences did not reach any significance (p_{corr} = 0.945 for timepoint "Day 46" and p_{corr} = 0.2102 for timepoints "Day 14" and "Day 28", respectively). Since the placebo was not significantly different from the probiotically treated in either of the timepoints, the placebo and the probiotic group were combined and compared to timepoint "Day 0". Neither between "Day 0" and "Day 14" (p_{corr} = 0.3525) nor between "Day 0" and "Day 28" (p_{corr} = 0.2087) and "Day 0" and "Day 46" (p_{corr} = 0.2087) there were found any significant differences. For luminal *Firmicutes* (median of 1.6e+06) no significant differences between the placebo and the probiotic treatment at either of the timepoints could be detected. The antibiotic treatment resulted in a significant decrease (p_{corr} = 0.0137) down to a relative amount of 1.3e+5.

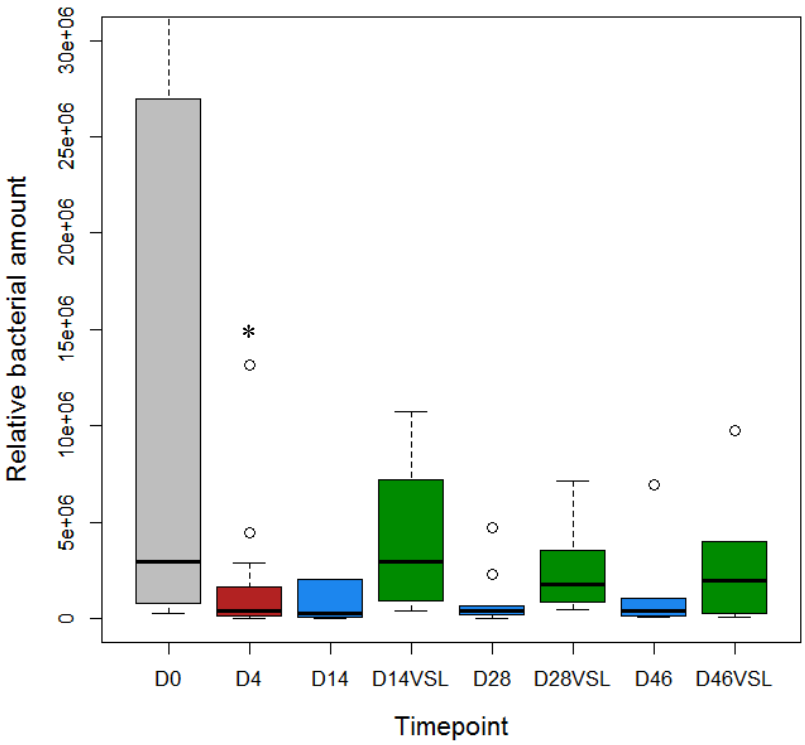

Figure 3-22: Changes in relative bacterial amount of the present luminal microbiota due to antibiotic treatment and subsequent placebo or probiotic therapy. All values are normalised to beta actin. Median, upper and lower quartile as well as upper and lower whisker are plotted. Grey (D0): Timepoint "Day 0" (n = 20), Red (D4): Timepoint "Day 4" after antibiotic treatment (n = 20), blue (D14, D28, D46): placebo therapy (n = 10), green (D14VSL, D28VSL, D46VSL): probiotic therapy (n = 10). * indicates significant difference compared to timepoint "D0" after Bonferroni-Holm correction.

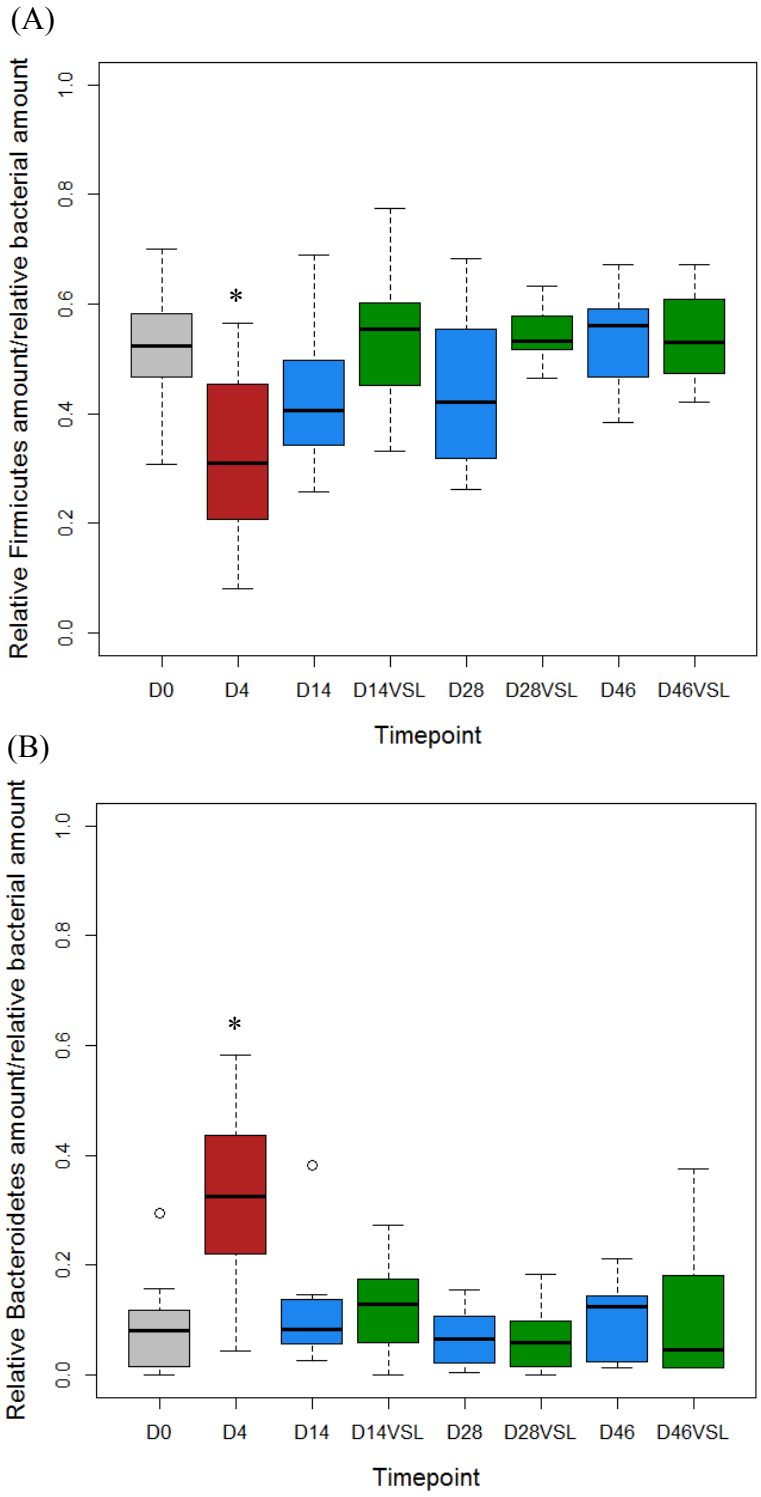

When comparing the relative amount of *Firmicutes* to total bacteria (Figure 3-23 (A)) the decrease due to the antibiotic persisted (p_{corr} = 2.7e-5). The differences between the placebo and the probiotic therapy were not significant at any timepoint, but they seemed to converge over time. The differences between the timepoints and "Day 0" were not significant (p_{corr} > 1). *Bacteroidetes* represented a relative amount of 1.4e+05 in median, but there were no significant differences between the placebo and the probiotic treatment at either of the three timepoints (p_{corr} = 0.2666 for "Day 14" and "Day 28" and p_{corr} = 0.945 for "Day 46", respectively), nor due to the antibiotic treatment (p_{corr} = 0.7983). The antibiotic just decreased the relative amount of *Bacteroidetes* to 1.3e+05 (p_{corr} = 0.7983). However, when

Figure 3-23: Changes in the relative bacterial amount of present luminal (A) Firmicutes and (B) Bacteroidetes due to antibiotic treatment and subsequent placebo or probiotic therapy. Normalised to relative bacterial amount. Relative amount of bacteria, Firmicutes and Bacteroidetes are normalised to beta actin. Median, upper and lower quartile as well as upper and lower whisker are plotted. Grey (D0): Timepoint "Day 0" (n = 20), Red (D4): Timepoint "Day 4" after antibiotic treatment (n = 20), blue (D14, D28, D46): placebo therapy (n = 10), green (D14VSL, D28VSL, D46VSL): probiotic therapy (n = 10). * indicates significant difference compared to timepoint "D0" after Bonferroni-Holm correction.

considering *Bacteroidetes* relative to total bacteria (Figure 3-23 (B)) the ratio increases significantly due to the antibiotic treatment (p_{corr} = 7.6e-06), indicating an overgrow of *Bacteroidetes*. Further there were no significant differences between the timepoint "Day 0" and the timepoints "Day 14" (p_{corr} = 0.2865), "Day 28" (p_{corr} = 0.996) and "Day 46" (p_{corr} = 0.996), respectively.

3.3.1 Quantitative results of the mucosa-associated microbiota

Whereas the amount of relative total bacteria (normalised to beta-actin) within the lumen at timepoint "Day 0" accounted for 2.9e+06, the active mucosa-associated microbiota showed an amount of 2176 and the present mucosa-associated microbiota resulted in 27 bacteria relative to beta actin. Concerning the mucosa-associated microbiota there were no significant differences due to the treatments (antibiotics vs. placebo vs. probiotics) or timepoints in the total active bacteria. *Firmicutes* (normalised to beta actin) as well as the relative amount of *Firmicutes* to total bacteria did not show any significant differences due to the treatments or timepoints. *Bacteroidetes* only showed a significant increase (p_{corr} = 0.003388) relative to total bacteria due to the antibiotic treatment. Total active mucosa-associated *Bacteroidetes* were not influenced in any way. The present mucosa-associated microbiota with regard to total bacteria, *Firmicutes* and *Bacteroidetes* as well as *Firmicutes* and *Bacteroidetes* relative to total bacteria was not altered in any way due to an influence of the antibiotic, the placebo or the probiotic at any of the timepoints.

4 Discussion

The aim of the present study was the investigation of the resilience phenomenon of the human intestinal microbiota under placebo and probiotic therapy after an antibiotic perturbation. The hypothesis was that the administration of a probiotic could result in different microbial profiles and an accelerated or more complete recovery. For this aim the intestinal microbiota of twenty healthy individuals was perturbed by a three day intake of the antibiotic paromomycin (Humatin®). A subsequent probiotic or placebo therapy for 43 days was administered to investigate the recovery and possible differences between the two treatment groups. This investigation was done by characterizing the microbial profiles of the luminal and the mucosa-associated microbiota at several timepoints. The microbial profiles were generated by amplifying the 16S rRNA and its corresponding gene and subsequent Sanger or 454 pyrosequencing. Further a relative quantification of the bacterial amount was done via real-time PCR.

To discuss the results that were obtained within this study, first the changes within the microbial profiles due to the antibiotic treatment will be set into the context of the existing literature. Afterwards resilience in general and especially the influence of administered probiotic VSL#3 will be discussed. Further the impact of VSL#3 on other factors than microbial profiles will be elucidated. Finally I will elaborate on the advantages and disadvantages of the two sequencing methods, Sanger- and pyrosequencing.

Most of the published studies used fecal samples to investigate the microbiota of the human gastrointestinal tract due to convenience of sampling (Davis et al. 2011; Duncan et al. 2008; Shen et al. 2006). Within the present study is was possible to generate microbial profiles of the luminal as well as of the mucosa-associated microbiota. This is a big advantage since it has not been clarified, whether fecal samples reflect the composition of the mucosal microbiota in an adequate way. It is discussed that the mucosa-associated microorganisms might be of greater importance to the host due to their interaction with the gut-associated lymphoid tissue (GALT) (Eckburg et al. 2005, Zoetendal et al. 2002). The present study is therefore the first one to investigate antibiotic-induced changes and the subsequent resilience phenomenon of luminal as well as mucosa-associated microbial profiles of the human colon and therein comparing placebo to probiotic therapy.

4.1 Effect of the antibiotic treatment

In general the results obtained within this study depend on the site of the colon (luminal microbiota or mucosa-associated microbiota). The antibiotic treatment resulted in a significant decrease in richness and diversity of the present microbiota at both sites. This was accompanied by a decreased abundance of OTUs with homology to the family *Lachnospiraceae* and the genera *Faecalibacterium* and *Blautia*. These OTUs were also identified as indicator species, therefore characterising the differences between the initial and the antibiotically treated microbiota at the luminal as well as the mucosa-associated site. The antibiotic treatment of the active mucosa-associated microbiota revealed only a single OTU as indicator species, suggesting that the influence of the antibiotic treatment onto the active mucosa-associated microbiota is smaller compared to the influence onto the present mucosa-associated as well as the luminal microbiota. However, also this single OTU was homologous to *Faecalibacterium*.

The decrease of richness, diversity and abundance of OTUs with homology to *Faecalibacterium, Blautia* and *Lachnospiraceae* as a result of antibiotic treatment is in agreement with other studies. A five day ciprofloxacin treatment resulted in a rapid decrease of richness and diversity as well as a reduced abundance of OTUs with homology to the luminal *Faecelibacterium* (Dethlefsen et al. 2008). A four day amoxicillin-clavulanic acid treatment decreased the luminal representation of members of *Clostridium* cluster IV (to which *Faecalibacterium* belongs) and *Clostridium* cluster XIVa (to which *Blautia* as well as *Lachnospiraceae* belong) (Young and Schmidt 2004). Reduced richness as well as a decrease of *Lachnospiraceae* was also discovered after a ten day vancomycin treatment within the luminal as well as the mucosa-associated microbiota in mice (Robinson and Young 2010).

Furthermore, Young and Schmidt (2004) observed an increase within *Enterobacteriaceae* and *Bacteroides*. An increase in *Bacteroides* could also be detected in the human fecal flora within a gnotobiotic mouse model after an amoxicillin-clavulanic acid treatment (Barc et al. 2004). Within the present study no increase of *Enterobacteriaceae* was found. An increased abundance of OTUs with homology to *Bacteroides* could be detected within the luminal and within the active mucosa-associated microbiota, but these OTUs were not characterised as indicator species. However, *Bacteroides* is the most abundant genus within the phylum *Bacteroidetes*. The quantitative amount of *Bacteroidetes* is not altered due to antibiotics as measured via qRT-PCR, but increases relative to total bacteria. This assumes a relative

overgrowth of *Bacteroidetes* within the present study. Besides these dominant OTUs the antibiotic treatment resulted in additional changes within the mucosa-associated bacteria within the present study. A significant increased abundance of OTUs with homology to *Eubacterium* and unclassified *Firmicutes* as well as a significant decreased abundance of OTUs homologous to *Sutterella* and *Coprobacillus* within the active and the present mucosa-associated microbiota was found. Furthermore, the active mucosa-associated bacteria showed an increased abundance of OTUs homologous to *Enterococcus* and *Pseudomonas*. Given the fact that these OTUs were not identified as indicator species and that each OTU consists of few sequences, makes them seem negligible on the one hand. On the other hand the sum of these OTUs contributes to the significant difference between the initial and the antibiotically treated microbial composition found within the AMOVA.

In conclusion the antibiotic treatment rather caused a decreased abundance of OTUs with homology to *Faecalibacterium*, *Blautia* and *Lachnospiraceae* than an increase of OTUs homologous to *Bacteroides* or other harmful bacteria. These changes within the abundance are not paromomycin-specific, but are the results of antibiotics in general. The mucosa-associated microbiota is less influenced by the antibiotic paromomycin than the luminal microbiota, which can be attributed to the fact that the applied paromomycin is only poorly absorbed (1-3%).

4.2 Resilience of the intestinal microbiota

In the present study the mucosa-associated microbiota showed a resilient behaviour of richness and diversity. No differences were detected when comparing “Day 0” and “Day 46”. Further no OTU was found that was different between the two timepoints. This accounts for the present as well as for the active mucosa-associated microbiota. The luminal microbiota was resilient according to richness, but not to diversity. Concerning the literature resilience depends on duration of the treatment and the antibiotic agent. It is important to note that different techniques applied to investigate resilience phenomena may significantly bias the outcome of the respective study. Several studies interrogating resilience of human intestinal microbiota after antibiotic treatment have been reported all which used different technical approaches. On the basis of T-RFLP a seven day clindamycin treatment resulted in an overall normalization of the fecal microbiota of otherwise healthy individuals within three months. Apart from this some perturbations persisted for two years as specific populations of the *Bacteroides* community did not return (Jernberg et al. 2007). Via culturing it could be shown

that richness and number of *Bacteroides* species returned to pretreatment conditions within 21 days, but that the species composition (diversity) was still significantly altered after 18 months (Löfmark et al. 2006). However, one has to consider that culture techniques are not be very reliable since they can detect only a small percentage of the dominant anaerobic bacteria (Eckburg et al. 2005). Sullivan et al. (2001) described a normalisation of the microbial composition a few weeks after the withdrawal of a clindamycin treatment. Measured via TTGE the initial luminal composition of healthy individuals that was disturbed by a five day course of amoxicillin could be reestablished within 60 days (De La Cochetiere et al. 2005). The study by Young and Schmidt (2004) used clone libraries from an acute sinusitis case and showed that major bacterial groups were partially restored within 14 days after a single course of amoxicillin-clavulanic acid. Although investigated in mice, the generation of clone libraries showed nearly baseline values in richness and diversity in the fecal as well as caecal mucosa-associated microbiota within three weeks cessation of a ten day course of vancomycin (Robinson and Young 2010). A clarithromycin and metronidazole treatment administered to patients with either gastric or duodenal ulcers immediately decreased the Shannon index of the luminal microbiota due to the antibiotic treatment as observed in a 454 pyrosequencing approach. Four weeks after cessation of the antibiotic treatment it returned to initial levels (Jakobsson et al. 2010). Dethlefsen et al. (2008) also used the 454 pyrosequencing approach and described a resilient taxonomic composition within four weeks after a five day course of ciprofloxacin in fecal samples of healthy individuals. But it was also reported that several taxa failed to recover within six months.

With regard to specific bacteria Young and Schmidt (2004) showed that two weeks after cessation of amoxicillin-clavulanic acid *Clostridium* cluster XIVa and *Clostridium* cluster IV reappeared, whereas *Clostridium* cluster XIV showed an accelerated resilience. The present study obtained the same results. The OTU with homology to *Blautia* recovered within 11 days after the cessation of the paromomycin treatment as there were no significant differences when comparing “Day 14” and “Day 0”. In contrast, the OTU with homology to *Faecalibacterium* was still significantly decreased at “Day 28”, but was finally able to recover until “Day 46”. Therefore also the present study identified an accelerated recovery of *Blautia*, which is a member of the *Clostridium* cluster XIV. The level of OTUs homologous to *Bacteroides* normalised within 11 days after cessation of the antibiotic treatment. A normalisation of *Bacteroides* within a few days had been shown in other studies before (Löfmark et al. 2006; Barc et al. 2004; Young and Schmidt 2004). The fact that

Faecalibacterium displays a delayed resilience is crucial since *Faecalibacterium prausnitzii* was described as an anti-inflammatory commensal which was also found to be reduced in patients with Crohn´s disease as measured by qRT-PCR (Sokol 2008). Lower concentrations of *Faecalibacterium prausnitzii* have been asssociated with a reduced protection of the gut mucosa (Jia 2010; Sokol 2009). It has been shown that the antiinflammatory properties resulted in decrease of C-reactive protein and significant lower amounts of IL-12 and IFN-γ, but in a higher secretion of IL-10 in PBMCs (peripheral blood mononuclear cells). On the cellular level as well as in TNBS (trinitrobenzene sulfonic acid) colitis models *Faecalibacterium* fulfilled antiinflammatory properties by secreting metabolites that are able to block NF-kB activation and IL-8 production.

Since one antibiotic course has pervasive effects onto the microbiota it is assumed that a repeated antibiotic treatment results in a more severe perturbation. Dethlefsen et al. (2011) investigated the effect of two five day courses of ciprofloxacin separated by six months onto the luminal microbiota. The microbiota recovered after the first, but was distinct although stabilised after the second antibiotic course. The consequences of the altered composition are unclear. With regard to disease it has been shown that the risk for Crohn´s disease increased with the number of antibiotic courses during childhood (Hviid et al. 2010). Another side effect of an antibiotic treatment is the increase of resistance genes that can be monitored for up to four years after the cessation of an antibiotic (Jakobsson et al. 2010; Ubeda et al. 2010; Sjölund et al. 2005; Sjölund et al. 2003). In addition, there is a high level of transfer of resistance genes within the intestine (Lester et al. 2006; Salyers et al. 2006; Scott et al. 2002; Shoemaker et al. 2001).

The present study shows that the pervasive effect of an antibiotic treatment is reversible with regard to microbial profiles since at least major groups that account for the microbial profiles were able recover in a relatively short time. This is in agreement with several other studies. However, resilience depends on the antibiotic agent itself as well as on dose and duration, but also on the body site. The present study is one of the few examples where simultaneously fecal as well as mucosa-associated microbial profiles were investigated. It has been shown that paromomycin treatment resulted in a complete recovery of the mucosa-associated microbiota, whereas the luminal microbiota did not show complete resilience with regard to diversity.

4.3 Effect of the probiotic treatment onto resilience

It may be assumed that application of probiotics may restore an imbalance within the luminal and/or mucosa-associated microbiota caused by antibiotics in an accelerated way. VSL#3 was chosen because it is a multistrain probiotic (four *Lactobacillus* strains, three *Bifidobacterium* strains and one strain of *Streptococcus thermophilus*) and therefore might be more potent than a single strain probiotic (Chapman et al. 2011). Several studies have demonstrated beneficial effects of VSL#3 in maintenance of remission in chronic inflammatory bowel disease, especially pouchitis and ulcerative colitis (Miele et al. 2009; Kühbacher et al. 2006). In the murine model VSL#3 was able to decrease TNBS-induced colitis (Uronis et al. 2010). The exact mechanism is unclear, but it seems that gut health is promoted through stimulation instead of suppression of the innate immune system. In the murine model local stimulation of epithelial innate immune responses by VSL#3 such as an increased production of epithelial-derived TNF-α and restoration of epithelial barrier function prevented the onset of intestinal inflammation (Pagnini et al. 2010).

Within the present study the SIMPER-reduced dataset of the luminal microbiota comprised three OTUs with homology to *Streptococcus* and three OTUs with homology to *Lactobacillus*, but none with homology to *Bifidobacterium*. A BLAST (basic local alignment search tool) against the 16S ribosomal RNA sequences database of the NCBI (National Center for Biotechnology Information) revealed that all three OTUs homologous to *Streptococcus* were indeed homologous to *Streptococcus thermophilus*, which is a constituent of VSL#3. The BLAST against sequences of the *Lactobacillus* OTUs revealed that only one of the three OTUs was a constituent of the applied probiotic, *Lactobacillus acidophilus* (OTU 1008). The other two were identified as *Lactobacillus mucosae* and *Lactobacillus johnsonii*. This makes *Streptococcus thermophilus* the highest concentrated strain among the VSL#3 constituents within the present study and explains the result that significant differences between the placebo and the probiotically treated group as well as between the probiotically treated microbiota and the initial composition were only detetctable in abundance of *Streptococcus*, but not of *Lactobacillus* or *Bifidobacterium*. The superiority of *Streptococcus* compared to the other seven constituents of VSL#3 was observed before (Pagnini et al. 2010). However, Brigidi et al. (2003) observed a significant increase of *Lactobacilli*, *Bifidobacteria* and *Streptococcus thermophilus* in the human feces when administered to VSL#3 measured via culture and PCR technique. Within the present study no further differences within the luminal microbial profiles due to VSL#3 were detected, which is in agreement with several other

studies. Brigidi et al. (2003) were not able to detect any significant changes in *Enterococci*, *Coliforms*, *Bacteroides* and *Clostridium perfringens* (Brigidi et al. 2003). In patients with irritable bowel syndrome and predominant diarrhea, where VSL#3 is known to sustain remission (Huynh et al. 2009; Karimi et al. 2005; Bibiloni et al. 2005), no effect of VSL#3 onto the luminal microbiota could be shown (Michail and Kenche 2011; Brigidi et al. 2003). A study by McNulty et al. (2011) used *Bifidobacterium animalis*, *Lactobacillus delbruekii*, *Lactococcus lactis* and *Streptococcus thermophilus* and therefore two strains that are constituents of VSL#3. No significant changes in bacterial species composition were found within luminal microbial profiles of human female twin pairs. Even the administered probiotic bacteria could not be found. Profiles of gnotobiotic mice harboring a 15-species model human gut microbiota, only showed a significant decrease of an *Actinobacteria* strain and an increase of administered *B. animalis* as well as *L. lactis* (McNulty et al. 2011).

Concerning the mucosa-associated microbiota the dataset of the present study contained OTUs with homology to *Streptococcus thermophilus* and *Lactobacillus acidophilus,* but VSL#3 treatment did not result in significant changes of the administered or other bacteria. OTUs with homology to *Bifidobacterium* were not detected at all. Bibiloni et al. (2005) investigated the mucosa-associated microbiota of individuals in remission of ulcerative colitis that were administered to VSL#3. *Streptococcus thermophilus* and *Bifidobacterium infantis* could only be detected in three of eleven individuals via DGGE (Bibiloni et al. 2005).

In general the present study shows that VSL#3 constituents were able to survive the passage through the gastrointestinal tract and reach the large bowel, but were not able to colonize the mucosa. No influence of VSL#3 was observed on microbial profiles, apart from a significant increase of luminal *Streptococcus thermophilus*, as well as on microbial richness or diversity. The luminal colonisation is only temporal as shortly after cessation of the probiotic therapy the VSL#3 constituents will be excreted within a few days. This results in the assumption that probiotics have to be taken lifelong (Brigidi et al. 2003; Tannock et al. 2000; Venturi et al. 1999; Chapman et al. 2006). However, also a long term consumption of a probiotic merely altered the *Lactobacillus* population, but did not affect the populations of obligate anaerobic bacteria, which are numerically dominant within the fecal microbiota (Tannock et al. 2000).

The present as well as previously published studies show no influence of VSL#3 on microbial profiles. Furthermore, the present study observed that resilience is independent of probiotic therapy, or at least independent of VSL#3, when administered subsequently to antibiotic

treatment. Another possibility is the concomitant administration of anti- and probiotics. In a study by Jernberg et al. (2005) fecal samples from eight healthy volunteers allocated to a seven day course of clindamycin and a concomitant 14 day course with probiotic (containing *L. acidophilus*, *L. paracasei* and *B. lactis*) or normal yoghurt were investigated via cultivation experiments. 14 days after cessation of antibiotics (and 7 day after cessation of probiotics) the fecal microbiota of the placebo group was still repressed, whereas the probiotically treated microbiota had mainly recovered to pretreatment levels. Another study showed that the numbers of *Lactobacillus* as well as *Bifidobacterium* were not significantly altered after a concomitant 7 day treatment with clindamycin and a probiotic (one *Bifidobacterium* and two *Lactobacillus* strains) treatment, but significantly decreased within the fecal microbiota of the placebo group (Sullivan et al. 2003). A seven day course with amoxicillin/clavulanate concomitant to a three week administration of probiotic *Bifidobacteria* and *Lactobacilli* resulted in a less disturbed microbiota according to T-RFLP and culture data and a more similar composition to baseline than the placebo treated group (Engelbrektson et al. 2009). In contrast a seven day course of amoxicillin concomitant to a 14 day course of a multistrain probiotic (that further contained inulin enriched oligofructose and therefore not only the bacteria, but also nutrients for the bacteria) only resulted in an increase in *Enterococci* and a less frequent bowel movement within the probiotically treated group of otherwise healthy volunteers. At the end of the study no differences compared to day 0 within the probiotic as well as in the placebo group were discovered (Koning et al. 2008). The mechanisms why the concomitant application of antibiotics and probiotics should be more beneficial than the subsequent use are speculative. It is assumed that the beneficial effect of probiotics is due to the metabolism of supplemented bacteria. Probiotic bacteria can metabolise luminal components and thereby generate substrates that may act as nutrients for other bacteria. Due to metabolism, the physical environment changes to a preferential one with lower pH (Engelbrektson et al. 2009). However, these mechansims are generally described for the benefit of probiotic bacteria and do not explain the possible advantage of a concomitant antibiotic/probiotic therapy to a subsequent one.

4.4 Alternative effects of probiotic therapy

VSL#3, but also *Lactobacillus* and *Bifidobacterium infantis* alone, have been described to exhibit beneficial effects on bloating and result in a reduced flatulence as well as a slower transit time in patients suffering from irritable bowel syndrome with bloating (Ringel-Kulka et al.; Kim et al. 2005; Kim et al. 2003). Furthermore, VSL#3 normalised the bowel habits

and stool consistency in patients with irritable bowel syndrome or functional diarrhea (Brigidi et al. 2001). Within the present study no questionnaire was compiled asking for bowel functions and gastrointestinal symptoms. However, none of the study participants reported indisposition or even diarrhea. The absence of any reported gastrointestinal symptoms could therefore indicate that the gut microbiota is functionally unaffected by antibiotics as well as probiotics (Dethlefsen et al. 2011).

The functional component can be linked to beneficial metabolites of supplemented bacteria. As mentioned previously, probiotics metabolise luminal components thereby generating substrates or a physical environment which is preferred by other bacteria central to the broader stability of the microbiota. Especially the concentration as well as the distribution of organic compounds like carbohydrates, short chain fatty acids (SCFA) and bile acids can be significantly altered due to changes of the gut microbiota (Macfarlane and Mcfarlane, 2011; Högenauer et al. 1998). As shown in the murine model a probiotic treatment did not result in significant changes within bacterial composition, but within expression of microbiome-encoded enzymes, which were prominently involved in the carbohydrate metabolism (McNulty et al. 2011). The colonic bacteria, but mainly anaerobes, ferment unabsorbed carbohydrates as an energy source and produce lactic acid as well as the SCFAs butyrate, propionate and acetate (Floch 2010; Cummings et al. 1987). The SCFAs are absorbed and can be directly used by colonic mucosal epithelial cells with butyrate being the most important and preferred source of colonocytes. Propionate and acetate are systemically used within the body (Cook et al. 1998; Roediger et al. 1980; McNeil et al 1978). The production of SCFAs is important as it has been shown that a reduction of SCFA as a result of reduced levels of colonic anaerobes could directly lead to functional disorders of the colonic mucosa (Toping et al. 2001). Butyrate and propionate were described to have aniinflammatory capacities and also seemed to be beneficial by inhibiting NF-κB (Tedelind et al. 2007; Segain et al. 2000). The SCFAs can reduce the pH in the colon and thereby inhibit the growth of pathogenic bacteria as well as increase the calcium uptake by increasing the solubility of the calcium (Wong and Jenkins 2007; Van den Heuvel et al. 1999). *Streptococcus thermophilus* was identified to increase the values of propionate and butyrate (Rizkalla et al. 2000). Acetate and lactate can be produced by *Streptococcus* as well as by *Lactobacillus* and by *Bifidobacteria*, which can then be converted into butyrate and propionate through cross-feeding by other bacteria (e.g. *Eubacterium halii*, *Faecalibacterium prausnitzii*) (Belenguer et al. 2006; Morrison et al. 2006; Duncan et al. 2004). These studies lead to the conclusion that the effects

of probiotics target on metabolic functions rather than microbial composition. It would therefore be interesting to measure metabolites like SCFA and to investigate the influence of a subsequent antibiotic and VSL#3 treatment on these.

4.5 General discussion of sequencing methods

The two sequencing methods used in the present study were the chain termination sequencing according to the method of Sanger and the 454 pyrosequencing approach. Both have in common that DNA or RNA is extracted from a sample. PCR primer then bind to conserved regions of the 16S rRNA gene amplifying the intermediate variable regions. Therefore both methods can be effected by biased PCR amplification of microbial populations in the sample. In addition, the Sanger method requires a cloning step that is missing in the pyrosequencing approach, making the latter less error-prone. A further advantage of pyrosequencing is the immense output of averaged 200.000 reads obtained per single run on a GS-FLX. Within the present study, sample pooling allowed for the simultaneous sequencing of 30 to 40 samples, thereby generating 5000 reads per sample within a single run. On the capillary Sanger sequencer one run generated 96 sequences and therefore half a sample. A further disadvantage is that the Sanger method limits the ability of discovering less-abundant members of a microbial community due to the fact that only 192 clones have been picked. The incomplete profile was also visible in low coverage and for some samples quite steep rarefaction curves. On the other hand it can be stated that longer 16S rRNA gene sequences enable the highest possible degree of taxonomic resolution. Nevertheless, the sequencing according to the method of Sanger was shown as a technique that is able to reveal significant shifts within the community structure. The pyrosequencing approach generates a much larger amount of sequences at lower costs and therefore gives a more complete picture, but there is less phylogenetic information generated from a single read due to the short length (Margulies et al. 2005). However, it has been shown that reads spanning variable regions of the 16S rRNA gene are highly informative and that it is even better to generate more short sequences than less longer sequences (Liu et al. 2007). Several papers have already demonstrated the power of pyrosequencing (Sogin et al. 2006; McKenna et al. 2008). In the present study the V1 to V4 and the V1 to V2 regions were used for the Sanger and the pyrosequencing approach, respectively. The V1 to V4 region was chosen as it has been shown that segments around the V2 and V4 region have the lowest error rate (Wang 2007). For pyrosequencing the V1 to V2 region was amplified as the V2 is the longest among all nine variable regions. Furthermore,

V1 and V2 are closer to each other than V3 and V4, which enabled sequencing of two consecutive regions (Baker et al. 2003).

A critical point within analysis is the fact that different amounts of reads per sample were generated within the pyrosequencing approach. It is common to normalise the reads to the lowest number found in all samples. Normalisation per se has to be performed since it has been observed that the number of false OTUs is correlated with the number of sequences. It enables all sequences to be wrong with same probability, whereas most of the false OTUs seemed to be chimera that could not be detected before. Normalisation itself is a random selection, which is not an ideal solution (Schloss et al. 2009). However, it has little influence on efficiency of 16S rRNA gene discovery when working with thousands of reads (Hale et al. 2009; Harris et al. 2010). Further it has been shown that 1000 sequences per sample are adequate for analysis (Momozawa et al. 2011). Within the present study it was possible to generate 1506 denoised sequences per sample, which allowed for a reliable analysis.

4.6 Outlook

The present study is the first to investigate resilience of the luminal as well as the mucosa-associated microbiota of the human colon after a subsequent antibiotic and probiotic therapy with newest technology. It was shown that microbial richness as well as diversity within the present and active mucosa-associated microbiota was resilient after cessation of a three day course of paromomycin. In contrast, the luminal microbiota was resilient in richness, but not in diversity as it was not able to recover to pretreatment values within 43 days. OTUs that were significantly altered due to antibiotic treatment were able to restore until the end of the study within both body sites. Resilience was probiotic-independet. Except for a significant increase of VSL#3 constituent *Streptococcus thermophilus* within the luminal microbiota, no significant differences in microbial profiles were found as a result of probiotc therapy within the luminal as well as the mucosa-associated microbiota.

However, several studies reported benefits for diseased people when administered VSL#3. VSL#3 was described as a good alternative within sustainment of remission in IBD and prevention of onset or relapses in pouchitis (Mimura et al. 2004; Bibiloni et al. 2005; Sood et al. 2009; Holubar et al. 2010). Patients had a higher quality of life (Guandalini et al. 2010; Bowen et al. 2007; Delia et al. 2007; D´Souza et al. 2002) due to VSL#3-dependent reduction of bleeding, bloating and flatulence (Tursi et al. 2010; Gionchetti et al. 2007; Kim et al. 2005). Since the microbial composition is not or only to a very small extend altered by

probiotics, the beneficial effects have to be caused by other factors. Studies have shown effects of probiotic treatment on bacterial metabolites and expression of microbiome-encoded enzymes (McNulty et al. 2011; Okombo et al. 2010; Belenguer et al. 2006). The metabolites themselves were discussed to have an influence on molecular level (Tedelind et al. 2007; Segain et al. 2000). A direct effect of probiotics on molecular level was also observed and resulted in a protected epithelial barrier, stimulation of innate immunity and less proinflammatory cytokines (Dai et al. 2012; Pagnini et al. 2010; Ng et al. 2010; O´Mahoney et al. 2005; McCarthy et al. 2003). Although the molecular mechanisms of probiotic-induced beneficial effects remain poorly understood they somehow contributed to human health.

In conclusion it seems promising to look for functional rather than compositional changes of the human gut microbiota when studying resilience and the influence of probiotics. Future studies should address questions related to alterations of metabolies like SCFA and metabolism-dependent enzymes as well as further elucidate molecular mechansims. Also basic knowledge of probiotics like optimal dose, duration of treatment and composition of administered probiotic is completely lacking as research is just at the very beginning. The understanding of how probiotics contribute to human health will eventually result in a more adequate treatment of individuals suffering from harm- and painful diseases and will therefore enable a higher quality of life.

5 Summary

Each human being harbors an individual and quite stable community of microorganisms within the gastrointestinal tract, whereas the highest density can be found in the large intestine. The ability of the microbiota to recover after an external perturbation is referred to as the resilience phenomenon.

The aim of this study was the investigation of resilience of the colonic microbiota after a three day course of antibiotic perturbation with paromomycin and a subsequent therapy with probiotic VSL#3 or placebo over a period of 43 days. For this observation 16S rRNA gene libraries of the luminal as well as 16S rRNA and 16S rRNA gene amplicon libraries of the mucosa-associated microbiota were generated and sequenced via sequencing techniques according to the method of Sanger and pyrosequencing, respectively. This enabled the establishment of microbial profiles at different timepoints throughout the whole study. A quantitative real-time PCR was performed additionally.

Antibiotic treatment resulted in decrease of richness and diversity within the luminal as well as the present and active mucosa-associated microbiota. This was underlined by a decrease in abundance of Operational Taxonomic Units (OTUs) homologous to *Lachnospiraceae*, *Faecalibacterium* and *Blautia*, which were identified as indicator species. Subsequent resilience was characterised by a complete recovery of richness and diversity of the mucosa-associated microbiota. Diversity of the luminal microbiota was not restored to pretreatment levels until the end of the study. Abundances of OTUs altered due to antibiotc treatment recovered in the course of the study in the luminal as well as the mucosa-associated microbiota. Probiotc VSL#3 had no influence on resilience of diversity and richness. Apart from a significant increase of luminal VSL#3 constituent *Streptococcus thermophilus* no further changes of microbial profiles were observed in either the luminal or the mucosa-associated microbiota due to probiotic therapy.

Probiotic VSL#3 did not result in accelerated resilience of microbial composition after antibiotic perturbation. It must be emphasized that VSL#3 was shown to improve bowel function and symptoms in diseased individuals as well as result in an increase of short chain fatty acids and beneficial effects on molecular level within other studies. VSL#3 is therefore assumed to influence function rather than composition of the colonic microbiota. Future studies should address functional-related questions, thereby elucidating possible mechanisms by which probiotics confer a health benefit to the human host.

6 Zusammenfassung

Jeder Mensch besitzt eine individuelle und relativ stabile Gemeinschaft von Mikroorganismen innerhalb des Gastrointestinaltraktes, wobei die höchste Dichte innerhalb des Dickdarmes zu finden ist. Die Fähigkeit der Mikrobiota nach einer Schädigung zu regenerieren wird als Resilienz-Phänomen bezeichnet.

Ziel dieser Studie war die Untersuchung der Resilienz der humanen Dickdarmmikrobiota nach einer drei-tägigen Perturbation mit dem Antibiotikum Paromomycin und anschließender 43-tägiger Probiotika- oder Plazebobehandlung. Dafür wurden 16S rRNA-Genbibliotheken der luminalen sowie 16S rRNA und 16S rRNA-Gen Amplikonbibliotheken der mukosa-assoziierten Mikrobiota generiert und mittels Sanger- bzw. Pyrosequenzierung analysiert. Dies ermöglichte die Erstellung von mikrobiellen Profilen zu unterschiedlichen Zeitpunkten der Studie. Zusätzlich wurde eine quantitative real-time PCR durchgeführt.

Die Antibiotikabehandlung resultierte in einer Abnahme des Artenreichtums und der -diversität der luminalen sowie der mukosa-assoziierten Mikrobiota. Dies wurde durch eine Abnahme in der Abundanz von Operational Taxonomic Units (OTUs) mit Homologie zu *Lachnospiraceae*, *Faecalibacterium* und *Blautia*, die auch als Indikator Spezies identifiziert wurden, unterstrichen. Die nachfolgende Resilienz war durch eine vollständige Regeneration von Artenreichtum und -diversität der mukosa-assoziierten Mikrobiota gekennzeichnet. Die Diversität der luminalen Mikrobiota konnte bis zum Ende der Studie das anfänglichen Niveau nicht erreichen. Die durch die Antibiotikagabe veränderten Abundanzen der OTUs der luminalen wie auch der mukosa-assoziierten Mikrobiota erholten sich im Laufe der Studie. Das Probiotikum VSL#3 hatte keinen Einfluss auf die Resilienz von Artenreichtum und -diversität. Außer einem signifikanten Anstieg des im VSL#3 enthaltenen *Streptococcus thermophilus* im Lumen, konnten keine weiteren Veränderungen in den mikrobiellen Profilen durch die Probiotikagabe beobachtet werden.

Das Probiotikum VSL#3 hatte keinen Einfluss auf die Resilienz der mikrobiellen Zusammensetzung nach Antibiotikagabe. Allerdings wurde gezeigt, dass VSL#3 Gabe eine Verbesserung von Darmfunktion und Symptomen bei erkrankten Individuen sowie einen Anstieg von kurzkettigen Fettsäuren und günstige Einflüsse auf molekularer Ebene zur Folge hatte. Daher wird angenommen, dass VSL#3 eher die Funktionen als die Zusammensetzung der Mikrobiota beeinflusst. Zukünftige Studien sollten funktionell bedingte Fragestellungen beantworten, die es ermöglichen die Mechanismen, durch die Probiotika ihre vorteilhafte Wirkung hervorrufen, aufzuklären.

7 Appendix

7.1 Characteristics of study participants

Table 7-1: Characteristics of study participants.

Individual	Age	Gender	Height meters (m)	Weight kilogramme (kg)	BMI m^2/kg
1	26	Female	1.66	63	22.9
2	27	Female	1.75	63	20.6
3	26	Female	1.72	69	23.3
4	28	Male	1.74	68	22.5
5	25	Male	1.79	70	21.8
6	30	Male	1.80	85	26.2
7	26	Female	1.75	80	26.1
8	27	Female	1.82	71	21.4
9	30	Female	1.78	67	21.1
10	26	Female	1.70	60	20.8
11	28	Female	1.78	74	23.4
12	24	Female	1.73	59	19.7
13	30	Male	1.87	75	21.4
14	29	Female	1.70	66	22.8
15	23	Male	1.85	85	24.8
16	25	Female	1.81	65	19.8
17	23	Female	1.57	59	23.9
18	24	Female	1.60	62	24.2
19	25	Female	1.77	98	31.3
20	26	Female	1.77	80	25.5

7.2 Individual values for alpha-diversity of the luminal microbiota

Table 7-2: Individuals values for alpha diversity of the luminal microbiota.

Individual	Timepoint	Number of sequences	Goods coverage	Observed OTUs	Chao1 richness	Shannon diversity
1	0	165	0.5515	98	323	4.23
	4	165	0.6485	77	242	3.74
	14	168	0.6607	79	224	3.77
	28	161	0.6584	78	192	3.83
	46	169	0.6036	91	261	4.00
2	0	169	0.5325	107	327	4.45
	4	156	0.8269	38	155	2.71
	14	162	0.7037	71	212	3.71
	28	156	0.3910	109	556	4.22
	46	155	0.2000	131	1656	4.66

Individual	Timepoint	Number of sequences	Goods coverage	Observed OTUs	Chao1 richness	Shannon diversity
3	0	178	0.5674	106	431	4.41
	4	159	0.6981	61	222	2.99
	14	161	0.4969	102	507	4.36
	28	160	0.6000	83	335	3.94
	46	168	0.5298	101	443	4.27
4	0	160	0.5750	90	280	4.06
	4	144	0.5764	71	437	3.44
	14	149	0.4497	92	566	3.79
	28	128	0.4922	81	341	4.10
	46	151	0.5033	97	405	4.34
5	0	149	0.1275	139	1071	4.91
	4	155	0.3935	108	594	4.27
	14	171	0.4035	121	550	4.51
	28	173	0.7283	76	159	3.94
	46	170	0.6647	86	175	4.03
6	0	156	0.3141	122	689	4.63
	4	146	0.5616	85	287	4.12
	14	153	0.3725	110	1250	4.43
	28	156	0.5321	88	351	3.73
	46	160	0.1938	138	1170	4.78
7	0	149	0.2685	122	858	4.67
	4	147	0.6667	68	215	3.62
	14	152	0.6447	74	253	3.84
	28	159	0.3899	113	695	4.46
	46	148	0.3716	105	961	4.37
8	0	162	0.4691	110	354	4.48
	4	152	0.4013	103	1127	4.23
	14	161	0.4721	100	457	4.04
	28	170	0.4706	101	769	3.83
	46	152	0.4605	91	755	3.79
9	0	160	0.3938	120	453	4.66
	4	149	0.7450	55	143	3.14
	14	148	0.6284	77	226	3.89
	28	136	0.4926	87	322	4.17
	46	167	0.5808	90	358	4.02
10	0	125	0.5120	80	233	4.13
	4	170	0.3471	127	999	4.64
	14	163	0.4479	104	605	4.03
	28	173	0.7110	68	204	3.09
	46	141	0.7234	52	176	2.87

Individual	Timepoint	Number of sequences	Goods coverage	Observed OTUs	Chao1 richness	Shannon diversity
11	0	148	0.5338	92	248	4.24
	4	161	0.6957	61	208	2.56
	14	147	0.5034	90	353	4.06
	28	166	0.4578	108	609	4.37
	46	135	0.2815	110	627	4.57
12	0	161	0.2795	132	738	4.77
	4	179	0.8156	47	135	2.66
	14	161	0.5839	87	529	4.06
	28	171	0.4620	113	462	4.42
	46	133	0.3383	107	380	4.59
13	0	147	0.1905	130	1008	4.80
	4	164	0.2988	127	1220	4.57
	14	153	0.4118	108	472	4.40
	28	141	0.2128	121	1139	4.70
	46	152	0.2105	134	683	4.84
14	0	167	0.1257	153	2799	4.97
	4	169	0.3254	131	936	4.72
	14	169	0.4970	103	460	4.07
	28	174	0.6839	76	211	3.48
	46	178	0.6685	74	264	3.13
15	0	171	0.6082	101	202	4.36
	4	173	0.8844	27	217	1.75
	14	161	0.4907	99	763	4.20
	28	137	0.2774	116	463	4.69
	46	168	0.4167	112	706	4.24
16	0	167	0.0419	163	4403	5.08
	4	142	0.0423	139	2434	4.93
	14	150	0.0733	144	2062	4.95
	28	170	0.1824	153	891	4.99
	46	173	0.2023	153	941	4.98
17	0	152	0.1118	143	1274	4.94
	4	152	0.6184	72	279	3.47
	14	159	0.2453	132	925	4.71
	28	150	0.2067	130	910	4.76
	46	150	0.2667	117	1616	4.38
18	0	164	0.4268	112	509	4.34
	4	173	0.7225	73	154	3.61
	14	164	0.7927	52	132	3.19
	28	163	0.6626	74	260	3.67
	46	161	0.4783	101	599	4.24

Individual	Timepoint	Number of sequences	Goods coverage	Observed OTUs	Chao1 richness	Shannon diversity
19	0	162	0.5988	89	297	4.14
	4	185	0.9459	20	28	1.74
	14	168	0.7798	60	127	3.44
	28	176	0.8750	48	69	3.17
	46	151	0.7152	63	153	3.50
20	0	174	0.5402	102	453	4.29
	4	153	0.4118	107	608	4.40
	14	179	0.7486	58	256	3.04
	28	172	0.7384	57	387	2.88
	46	155	0.7097	52	1042	2.52

7.3 Individual values for alpha-diversity of the mucosa-associated microbiota

Table 7-3: Individual values for alpha diversity of the mucosa-associated microbiota.

		Present microbiota					Active microbiota				
Individual	**Timepoint**	**Number of sequences**	**Goods coverage**	**Observed OTUs**	**Chao1 richness**	**Shannon diversity**	**Number of sequences**	**Goods coverage**	**Observed OTUs**	**Chao1 richness**	**Shannon diversity**
1	0	1506	0.9216	277	424	4.64	1506	0.9197	219	421	3.64
	4	1506	0.9641	152	197	3.63	1506	0.9097	256	543	4.40
	46	1506	0.9429	185	344	4.03	1506	0.8997	229	768	3.89
2	0	1506	0.9449	181	343	3.98	1506	0.9177	201	494	3.70
	4	1506	0.9708	60	297	1.82	1506	0.9529	137	223	2.90
	46	1506	0.9695	133	176	3.55	1506	0.9031	228	620	3.85
3	0	1506	0.9143	237	555	4.23	1506	0.8805	275	946	4.31
	4	1506	0.9588	120	309	3.28	1506	0.9728	87	146	2.38
	46	1506	0.9442	162	291	3.51	1506	0.9309	170	413	2.98
4	0	1506	0.9369	207	347	4.27	1506	0.9363	170	368	2.70
	4	1506	0.9661	135	184	3.44	1506	0.9396	193	307	3.89
	46	1506	0.9216	201	501	3.68	1506	0.8938	254	664	3.98
5	0	1506	0.9389	186	360	4.07	1506	0.8858	256	956	4.20
	4	1506	0.9675	84	252	2.75	1506	0.9489	155	301	3.63
	46	1506	0.9542	130	343	3.38	1506	0.9017	211	684	3.66
6	0	1506	0.9343	201	374	3.90	1506	0.8811	278	776	4.14
	4	1506	0.9748	87	165	2.79	1506	0.9548	119	372	3.15
	46	1506	0.9403	184	351	3.94	1506	0.9044	230	611	3.95
7	0	1506	0.9402	213	347	3.77	1506	0.9396	164	368	2.67
	4	1506	0.9655	103	163	2.42	1506	0.9489	148	265	3.13
	46	1506	0.9582	158	214	3.33	1506	0.9309	197	364	3.64

		Present microbiota					Active microbiota				
Individual	**Timepoint**	**Number of sequences**	**Goods coverage**	**Observed OTUs**	**Chao1 richness**	**Shannon diversity**	**Number of sequences**	**Goods coverage**	**Observed OTUs**	**Chao1 richness**	**Shannon diversity**
8	0	1506	0.9701	95	153	2.59	1506	0.9462	122	338	2.47
	4	1506	0.9641	99	278	2.92	1506	0.9714	88	201	3.12
	46	1506	0.9535	147	268	2.99	1506	0.9296	182	646	3.71
9	0	1506	0.9416	194	347	3.60	1506	0.9064	233	752	3.60
	4	1506	0.9562	127	229	2.77	1506	0.9774	56	168	1.53
	46	1506	0.9509	146	275	3.51	1506	0.9449	141	303	2.55
11	0	1506	0.9343	177	371	3.62	1506	0.9044	219	791	3.82
	4	1506	0.9442	162	271	3.16	1506	0.9402	150	400	2.89
	46	1506	0.9548	174	241	3.84	1506	0.9548	135	243	3.05
12	0	1506	0.9150	246	478	4.22	1506	0.8758	279	806	3.92
	4	1506	0.9794	50	116	1.67	1506	0.9794	53	146	1.94
	46	1506	0.9416	158	413	3.26	1506	0.9177	199	453	3.36
13	0	1506	0.9515	189	286	4.09	1506	0.8964	263	680	4.21
	4	1506	0.9675	93	177	2.70	1506	0.9661	92	172	1.93
	46	1506	0.9336	238	362	4.40	1506	0.9124	264	475	4.60
14	0	1506	0.9668	112	206	3.30	1506	0.9343	172	403	3.42
	4	1506	0.9708	76	171	2.45	1506	0.9595	92	295	2.68
	46	1506	0.9708	108	187	2.98	1506	0.9323	160	418	3.32
15	0	1506	0.9456	168	343	3.37	1506	0.8924	267	675	4.09
	4	1506	0.9515	137	231	2.60	1506	0.9356	202	313	3.33
	46	1506	0.9336	171	462	3.14	1506	0.8639	277	1227	4.02
16	0	1506	0.9708	108	164	2.29	1506	0.9568	104	226	2.11
	4	1506	0.9270	169	485	2.82	1506	0.9104	210	621	3.37
	46	1506	0.9575	195	248	4.08	1506	0.9064	255	608	4.43

		Present microbiota					Active microbiota				
Individual	**Timepoint**	**Number of sequences**	**Goods coverage**	**Observed OTUs**	**Chao1 richness**	**Shannon diversity**	**Number of sequences**	**Goods coverage**	**Observed OTUs**	**Chao1 richness**	**Shannon diversity**
17	0	1506	0.9708	115	149	2.83	1506	0.9628	91	201	1.96
	4	1506	0.9774	75	122	2.60	1506	0.9728	98	149,25	3.19
	46	1506	0.9455	144	339	2.82	1506	0.9316	159	378	2.86
18	0	1506	0.9655	105	179	2.23	1506	0.9641	101	163	2.12
	4	1506	0.9867	46	84	2.10	1506	0.9748	68	156	2.43
	46	1506	0.9615	114	232	3.04	1506	0.9256	185	551	3.69
19	0	1506	0.9681	125	176	3.43	1506	0.9661	96	255	2.61
	4	1506	0.9861	46	72	2.06	1506	0.9807	47	128	1.80
	46	1506	0.9661	100	171	2.89	1506	0.9562	111	254	2.69
20	0	1506	0.9178	210	687	4.11	1506	0.8692	285	1204	4.37
	4	1506	0.9801	55	142	2.30	1506	0.9807	53	155	2.06
	46	1506	0.9588	120	309	3.70	1506	0.9190	209	530	4.14

8 References

Antonopoulos DA, Huse SM, Morrison HG, Schmidt TM et al. Reproducible community dynamics of the gastrointestinal microbiota following antibiotic perturbation. *Infect Immun.* 2009; 77(6):2367–2375

Avadhani A, Miley H. Probiotics for prevention of antibiotic-associated diarrhea and Clostridium difficile-associated disease in hospitalized adults--a meta-analysis. *J Am Acad Nurse Pract.* 2011; 23(6):269-74

Bäckhed F, Ley RE, Sonnenburg JL, Peterson DA et al. Host-bacterial mutualism in the human intestine. *Science.* 2005; 307:1915-1919

Baker GC, Smith JJ, Cowan DA. Review and re-analysis of domain-specific 16S primers. *J Microbiol Methods.* 2003; 55(3):541-55

Barc MC, Bourlioux F, Rigottier-Gois L, Charrin-Sarnel C et al. Effect of amoxicillin-clavulanic acid on human fecal flora in a gnotobiotic mouse model assessed with fluorescence hybridization using group-specific 16S rRNA probes in combination with flow cytometry. *Antimicrob Agents Chemother*. 2004 Apr;48(4):1365-8

Belenguer A, Duncan SH, Calder AG, Holtrop G et al. Two routes of metabolic cross-feeding between Bifidobacterium adolescentis and butyrate-producing anaerobes from the human gut. *Appl Environ Microbiol* 2006; 72:3593-9

Benjamini Y, Hochberg Y. Controlling the false discovery rate: A practical and powerful approach to multiple testing. *J R Stat Soc*. 1995; 57(1):289-300

Bibiloni R, Fedorak RN, Tannock GW, Madsen KL et al. VSL#3 probiotic-mixture induces remission in patients with active ulcerative colitis. *Am Journal Gastroenterol.* 2005; 100:1539-1546

Bonifait L, Chandad F, Grenier D. Probiotics for oral helath: Myth or reality? *JCDA.* 2009; 75(8):585-590

Borchers AT, Selmi C, Meyers FJ, Kleen CL et al. Probiotics and immunity. *J Gastroenterol.* 2009; 44:26-46

Bowen JM, Stringer AM, Gibson RJ, Yeoh AS et al. VSL#3 probiotic treatment reduces chemotherapy-induced diarrhea and weight loss. *Cancer Biol Ther.* 2007; 6(9):1449-54

Bray RJ and Curtis JT. An ordination of the upland forest communities of southern Wisconsin. *Ecol. Monogr.* 1957.; 27:325-349

Brigidi P, Swennen E, Vitali B, Rossi M, Matteuzzi D. PCR detection of Bifidobacterium strains and Streptococcus thermophilus in feces of human subjects after oral bacteriotherapy and yogurt consumption. *Int J Food Microbiol*. 2003; 81(3):203-9

Brigidi P, Vitali B, Swennen E, Bazzocchi G, Matteuzzi D. Effects of probiotic administration upon the composition and enzymatic activity of human fecal microbiota in patients with irritable bowel syndrome or functional diarrhea. *Res Microbiol.* 2001; 152(8):735-41

Clarke KR. Non-parametric multivariate analysis of changes in community structure. *Australian Journal of Ecology.* 1993; 18:117-143

Chao A. Non-parametric estimation of the number of classes in a population. *Scand J Statist.* 1984; 11:265-270

Chao A and Lee SM. Estimating the number of classes via sample coverage. *J Am Stat Assoc.* 1992; 87:210-217

Chapman CMC, Gibson GR, Rowland I. Health benefits of probiotics: are mixtures more effective than single strains? *Eur J Nutr*. 2011; 50:1-17

Chapman TM, Plosker GL, Figgitt DP. VSL#3 probiotic mixture. A review of its use in chronic inflammatory bowel disease. *Drugs*. 2006; 66(10):1371-1387

Claesson M, Cusack S, O´Sullivan O, Greene-Diniz R et al. Composition, variability, and temporal stability of the intestinal microbiota of the elderly. *PNAS.* 2011; 109(1):4586-4591

Cole JR, Wang Q, Cardenas E, Fish Jet al. The Ribosomal Database Project: improved alignments and new tools for rRNA analysis. *Nucleic Acids Res.* 2008; 37 (Database issue):D141-145

Cook SI, Sellin JH. Review article: short chain fatty acids in health and disease. *Aliment Pharmacol Ther.* 1998; 12(6):499-507

Costello EK, Lauber CL, Hamady M, Fierer N et al. Bacterial community variation in human body habitats across space and time. *Science.* 2009; 326:1694-1697

Cotter PD, Hill C, Ross RP. Bacteriocins: Developing innate immunity for food*. Nat Rev Microbiol.* 2005; 3(10): 777-788

Cummings JH, Pomare EW, Branch WJ, Naylor CP, Macfarlane GT. Short chain fatty acids in human large intestine, portal, hepatic and venous blood. *Gut*. 1987; 28(10):1221-7

Dai C, Zhao DH, Jiang M. VSL#3 probiotics regulate the intestinal epithelial barrier in vivo and in vitro via the p38 and ERK signaling pathways. *Int J Mol Med.* 2012; 29(2):202-8

Davidson RN, den Boer M, Ritmejer K. Paromomycin. *Trans R soc Trop Med Hyg.* 2009; 103(7):653-660

Davis LM, Martínez I, Walter J, Goin C, Hutkins RW. Barcoded pyrosequencing reveals that consumption of galactooligosaccharides results in a highly specific bifidogenic response in humans. *PLoS One.* 2011;6(9):e25200

De La Cochetière MF, Durand T, Lepage P, Bourreille Aet al. Resilience of the dominant human fecal microbiota upon short-course antibiotic challenge. *J Clin Microbiol.* 2005; 43(11):5588-92

Delia P, Sansotta G, Donato V, Frosina P et al. Use of probiotics for prevention of radiation-induced diarrhea. *Tumori.* 2007; 93(2):suppl 1-6.

Dethlefsen L, Relman DA. Incomplete recovery and individualized responses of the human distal gut microbiota to repeated antibiotic perturbation. *Proc Natl Acad Sci U S A*. 2011; 108 Suppl 1:4554-61

Dethlefsen L, Huse S, Sogin ML, Relman DA. The pervasive effects of an antibiotic on the human gut microbiota, as revealed by deep 16S rRNA sequencing. *PLoS Biol.* 2008; 6(11):e280

Drakes M, Blanchard T, Czinn S. Bacterial probiotic modulation of dendritic cells. *Infect Immun*. 2004; 72(6):3299-309

D'Souza AL, Rajkumar C, Cooke J, Bulpitt CJ. Probiotics in prevention of antibiotic associated diarrhoea: meta-analysis. *BMJ*. 2002; 324(7350):1361

Dufrêne M and Legendre P. 1997. Species assemblages and indicator species: the need for a flexible asymmetrical approach. *Ecological Monographs.* 1997; 67:345-366

Duncan SH, Lobley GE, Holtrop G, Ince J et al. Human colonic microbiota associated with diet, obesity and weight loss. *Int J Obes (Lond).* 2008; 32(11):1720-4

Duncan SH, Holtrop G, Lobley GE, Calder AG et al. Contribution of acetate to butyrate formation by human faecal bacteria. *Br J Nutr.* 2004; 91(6):915-23

Eckburg PB, Bik EM, Bernstein CN, Purdom Eet al. Diversity of the human intestinal microbial flora. *Science*. 2005; 308(5728):1635-1638

Engelbrektson A, Korzenik JR, Pittler A, Sanders ME, Klaenhammer TR et al. Probiotics to minimize the disruption of faecal microbiota in healthy subjects undergoing antibiotic therapy. J *Med Microbiol*. 2009; 58(Pt 5):663-70

Floch MH. The effect of probiotics on host metabolism. The microbiota and fermentation. *J Clin Gastroenterol*. 2010; 44:S19-21

Fooks LJ, Gibson GR. Probiotics as modulators of the gut flora. *Br J Nutr*. 2002; 88 Suppl 1:S39-49

Franks AH, Harmsen HJ, Raangs GC, Jansen GJet al. Variations of bacterial populations in human feces measured by fluorescent in situ hybridization with group-specific 16S rRNA-targeted oligonucleotide probes. *Appl Environ Microbiol*. 1998; 64(9):3336-45

Gillevet P, Sikaroodi M, Keshavarzian A, Mutlu EA. Quantitative assessment of the human gut microbiome using multitag pyrosequencing. *Chem Biodivers.* 2010; 7(5):1065-75

Gionchetti P, Rizzello F, Morselli C, Poggioli G et al. High-dose probiotics for the treatment of active pouchitis. *Dis Colon Rectum.* 2007; 50(12):2075-82; discussion 2082-4

Gionchetti P, Rizzello F, Venturi A, Brigidi Pet al. Oral bacteriotherapy as maintenance treatment in patients with chronic pouchitis: a double-blind, placebo-controlled trial. *Gastroenterology*. 2000; 119(2):305-9

Giongo A, Crabb DB, Davis-Richardson AG, Chauliac D et al. PANGEA: pipeline for analysis of next generation amplicons. *ISME J.* 2010; 4(7):852-61

Gómez-Llorente C, Muñoz S, Gil A. Role of Toll-like receptors in the development of immunotolerance mediated by probiotics. *Proc Nutr Soc.* 2010; 69(3):381-9

Good IJ. The population frequencies of species and the estimation of population parameters. *Biometrika* 1953; 40: 237-264

Guandalini S, Magazzù G, Chiaro A, La Balestra Vet al. VSL#3 improves symptoms in children with irritable bowel syndrome: a multicenter, randomized, placebo-controlled, double-blind, crossover study. *J Pediatr Gastroenterol Nutr*. 2010; 51(1):24-30

Hale MC, McCormick CR, Jackson JR, Dewoody JA. Next-generation pyrosequencing of gonad transcriptomes in the polyploid lake sturgeon (Acipenser fulvescens): the relative merits of normalization and rarefaction in gene discovery. *BMC Genomics*. 2009; 10:203

Hammer Ø, Harper DAT and Ryan PD. PAST: Paleontological Statistics Software Package for Education and Data Analysis. Palaeontologia Electronica. 2001; 4(1):9pp

Harris JK, Sahl JW, Castoe TA, Wagner BD et al. Comparison of normalization methods for construction of large, multiplex amplicon pools for next-generation sequencing. *Appl Environ Microbiol*. 2010; 76(12):3863-8

Hart AL, Lammers K, Brigidi P, Vitali Bet al. Modulation of human dendritic cell phenotype and function by probiotic bacteria. *Gut*. 2004; 53(11):1602-9

Högenauer C, Hammer HF, Krejs GJ, Reisinger EC. Mechanisms and management of antibiotic-associated diarrhea. *Clin Infect Dis*. 1998; 27(4):702-10

Holm S. A simple sequentially rejective multiple test procedure. *Scand J Statist*. 1979; 6:65.70

Holubar SD, Cima RR, Sandborn WJ, Pardi DS. Treatment and prevention of pouchitis after ileal pouch-anal anastomosis for chronic ulcerative colitis. *Cochrane Database Syst Rev.* 2010; (6):CD001176

Hooper LV, Gordon JI. Commensal host-bacterial relationships in the gut. *Science*. 2001; 292(5519):1115-8

Huynh HQ, deBruyn J, Guan L, Diaz H, Li M et al. Probiotic preparation VSL#3 induces remission in children with mild to moderate acute ulcerative colitis: a pilot study. *Inflamm Bowel Dis*. 2009; 15(5):760-8

Hviid A, Svanström H, Frisch M.: Antibiotic use and inflammatory bowel diseases in childhood. *Gut.* 2011; 60(1):49-54

Isaacs K, Herfarth H. Role of probiotic therapy in IBD. *Inflamm Bowel Dis*. 2008; 14(11):1597-605

Jakobsson HE, Jernberg C, Andersson AF, Sjölund-Karlsson Met al. Short-term antibiotic treatment has differing long-term impacts on the human throat and gut microbiome. *PLoS One*. 2010; 5(3):e9836

Jernberg C, Löfmark S, Edlund C, Jansson JK. Long-term impacts of antibiotic exposure on the human intestinal microbiota. Microbiology. 2010; 156(Pt 11):3216-23

Jernberg C, Löfmark S, Edlund C, Jansson JK. Long-term ecological impacts of antibiotic administration on the human intestinal microbiota. *ISME J*. 2007; 1(1):56-66

Jernberg C, Sullivan A, Edlund C, Jansson JK. Monitoring of antibiotic-induced alterations in the human intestinal microflora and detection of probiotic strains by use of terminal restriction fragment length polymorphism. *Appl Environ Microbiol.* 2005; 71(1):501-6

Jia W, Whitehead RN, Griffiths L, Dawson C et al. Is the abundance of Faecalibacterium prausnitzii relevant to Crohn's disease? FEMS Microbiol Lett. 2010; 310(2):138-44

Jijon H, Backer J, Diaz H, Yeung Het al. DNA from probiotic bacteria modulates murine and human epithelial and immune function. *Gastroenterology*. 2004; 126(5):1358-73

Karimi O, Peña AS, van Bodegraven AA. Probiotics (VSL#3) in arthralgia in patients with ulcerative colitis and Crohn's disease: a pilot study. *Drugs Today (Barc)*. 2005; 41(7):453-9

Kim HJ, Vazquez Roque MI, Camilleri M, Stephens D, et al. A randomized controlled trial of a probiotic combination VSL# 3 and placebo in irritable bowel syndrome with bloating. *Neurogastroenterol Motil.* 2005; 17(5):687-96

Kim HJ, Camilleri M, McKinzie S, Lempke MBet al. A randomized controlled trial of a probiotic, VSL#3, on gut transit and symptoms in diarrhoea-predominant irritable bowel syndrome. *Aliment Pharmacol Ther*. 2003; 17(7):895-904

Koning CJ, Jonkers DM, Stobberingh EE, Mulder L et al. The effect of a multispecies probiotic on the intestinal microbiota and bowel movements in healthy volunteers taking the antibiotic amoxycillin. *Am J Gastroenterol.* 2008; 103(1):178-89.

Kühbacher T, Ott SJ, Helwig U, Mimura Tet al. Bacterial and fungal microbiota in relation to probiotic therapy (VSL#3) in pouchitis. *Gut*. 2006; 55(6):833-41

Legendre P, Legendre L. Numerical ecology. *Elsevier science*, Amsterdam. 1998

Lester CH, Frimodt-Møller N, Sørensen TL, Monnet DL, Hammerum AM. In vivo transfer of the vanA resistance gene from an Enterococcus faecium isolate of animal origin to an E. faecium isolate of human origin in the intestines of human volunteers. *Antimicrob Agents Chemother*. 2006; 50(2):596-9

Ley RE, Bäckhed F, Turnbaugh P, Lozupone CA et al. Obesity alters gut microbial ecology. *Proc Natl Acad Sci U S A*. 2005; 102(31):11070-5

Liu Z, Lozupone C, Hamady M, Bushman FD, Knight R. Short pyrosequencing reads suffice for accurate microbial community analysis. Nucleic Acids Research. 2007;365(18):e120

Löfmark S, Jernberg C, Jansson JK, Edlund C. Clindamycin-induced enrichment and long-term persistence of resistant Bacteroides spp. and resistance genes. *J Antimicrob Chemother*. 2006; 58(6):1160-7

MacPhee RA, Hummelen R, Bisanz JE, Miller WL, Reid G. Probiotic strategies for the treatment and prevention of bacterial vaginosis. *Expert Opin Pharmacother*. 2010; 11(18):2985-95

Madsen K. The use of probiotics in gastrointestinal disease. *Can J Gastroenterol* 2001; 15(12):817-822

Magurran, AE. Ecological diversity and its measurement. 1988; Princeton University Press, Princeton

Macfarlane GT, Macfarlane S. Fermentation in the human large intestine: its physiologic consequences and the potential contribution of prebiotics. *J Clin Gastroenterol*. 2011; 45 Suppl:S120-7

Mann HB, Whitney DR. On a test of whether one of two random variables is stochastically larger than the other. *Ann Math Stat*. 1947: 18(1):50-60

Margulies M, Egholm M, Altman WE, Attiya S. et al. Genome sequencing in open microfabricated high density picoliter reactors. *Nature*. 2005; 437(7057):376-380

McCarthy J, O'Mahony L, O'Callaghan L, Sheil B et al. Double blind, placebo controlled trial of two probiotic strains in interleukin 10 knockout mice and mechanistic link with cytokine balance. Gut. 2003; 52(7):975-80

McFarland LV. Evidence-based review of probiotics for antibiotic-associated diarrhea and Clostridium difficile infections. *Anaerobe*. 2009; 15(6):274-80

McKenna P, Hoffmann C, Minkah N, Aye PP et al. The macaque gut microbiome in health, lentiviral infection, and chronic enterocolitis. *PLoS Pathog*. 2008; 4(2):e20

McNeil NI, Cummings JH, James WP. Short chain fatty acid absorption by the human large intestine. *Gut*. 1978; 19(9):819-22

McNulty NP, Yatsunenko T, Hsiao A, Faith JJ et al. The impact of a consortium of fermented milk strains on the gut microbiome of gnotobiotic mice and monozygotic twins. *Sci Transl Med.* 2011; 3(106):106ra106

Mai V, Morris JG Jr. Colonic bacterial flora: changing understandings in the molecular age. *J Nutr.* 2004; 134(2):459-64

Mai V, Ukhanova M, Baer DJ. Understanding the extent and sources of variation in gut microbiota studies; a prerequisite for esablishing associations with disease. *Diversity* 2010; 2:1085-1096

Margulies M, Egholm M, Altman WE, Attiya S et al. Genome sequencing in microfabricated high-density picolitre reactors. *Nature*. 2005; 437(7057):376-80

Michail S, Kenche H. Gut microbiota is not modified by Randomized, Double-blind, Placebo-controlled Trial of VSL#3 in Diarrhea-predominant Irritable Bowel Syndrome. *Probiotics Antimicrob Proteins*. 2011; 3(1):1-7

Miele E, Pascarella F, Giannetti E, Quaglietta Let al. Effect of a probiotic preparation (VSL#3) on induction and maintenance of remission in children with ulcerative colitis. *Am J Gastroenterol*. 2009; 104(2):437-43

Mimura T, Rizzello F, Helwig U, Poggioli G et al. Once daily high dose probiotic therapy (VSL#3) for maintaining remission in recurrent or refractory pouchitis. Gut. 2004; 53(1):108-14

Momozawa Y, Deffontaine V, Louis E, Medrano JF. Characterization of bacteria in biopsies of colon and stools by high throughput sequencing of the V2 region of bacterial 16S rRNA gene in human. *PLoS One*. 2011; 6(2):e16952

Morrison DJ, Mackay WG, Edwards CA, Preston T et al. Butyrate production from oligofructose fermentation by human fecal flora: what is the contribution of extracellular acetate and lactate? *Br J Nutr*. 2006; 96:570-7

Neish AS. Microbes in gastrointestinal health and disease. *Gastroenterology.* 2009; 136(1):65-80

Ng SC, Plamondon S, Kamm MA, Hart AL et al. Immunosuppressive effects via human intestinal dendritic cells of probiotic bacteria and steroids in the treatment of acute ulcerative colitis. *Inflamm Bowel Dis.* 2010; 16(8):1286-98

Okombo J and Liebman M. Probiotic-induced reduction of gastrointestinal oxalate absorption in healthy subjects. *Urol Res.* 2010; 38(3):169-78

O'Mahony L, McCarthy J, Kelly P, Hurley G et al. Lactobacillus and bifidobacterium in irritable bowel syndrome: symptom responses and relationship to cytokine profiles. *Gastroenterology.* 2005 Mar;128(3):541-51

Ott SJ, Musfeldt M, Wenderoth DF, Hampe Jet al. Reduction in diversity of the colonic mucosa associated bacterial microflora in patients with active inflammatory bowel disease. *Gut*. 2004; 53(5):685-93

Otte JM, Podolsky DK. Functional modulation of enterocytes by gram-positive and gram-negative microorganisms. *Am J Physiol Gastrointest Liver Physiol*. 2004; 286(4):G613-26

Pagnini C, Saeed R, Bamias G, Arseneau KO et al. Probiotics promote gut health through stimulation of epithelial innate immunity. *Proc Natl Acad Sci U S A*. 2010; 107(1):454-9

Petnicki-Ocwieja T, Hrncir T, Liu YJ, Biswas A et al. Nod2 is required for the regulation of commensal microbiota in the intestine. *Proc Natl Acad Sci U S A*. 2009; 106(37):15813-8

Qin J, Li R, Raes J, Arumugam M et al. A human gut microbial gene catalogue established by metagenomic sequencing. *Nature*. 2010; 464(7285):59-65

Rausch P, Rehman A, Künzel S, Häsler R et al. Colonic mucosa-associated microbiota is influenced by an interaction of Crohn disease and FUT2 (Secretor) genotype. *Proc Natl Acad Sci U S A*. 2011; 108(47):19030-5

Rehman A, Lepage P, Nolte A, Hellmig Set al. Transcriptional activity of the dominant gut mucosal microbiota in chronic inflammatory bowel disease patients. *J Med Microbiol*. 2010; 59(Pt 9):1114-22

Rehman A, Sina C, Gavrilova O, Häsler R et al. Nod2 is essential for temporal development of intestinal microbial communities. Gut. 2011; 60(10):1354-62

Reid G, Younes JA, Van der Mei HC, Gloor GBet al. Microbiota restoration: natural and supplemented recovery of human microbial communities. *Nat Rev Microbiol*. 2011; 9(1):27-38

Ringel-Kulka T, Palsson OS, Maier D, Carroll I et al. Probiotic bacteria Lactobacillus acidophilus NCFM and Bifidobacterium lactis Bi-07 versus placebo for the symptoms of bloating in patients with functional bowel disorders. A double-blind study. *J Clin Gastroenterol*. 2011; 45:518-525

Rizkalla SW, Luo J, Kabir M, Chevalier A et al. Chronic consumption of fresh but not heated yogurt improves breath-hydrogen status and short-chain fatty acid profiles: a controlled study in healthy men with or without lactose maldigestion. *Am J Clin Nutr*. 2000; 72(6):1474-9

Robinson CJ, Young VB. Antibiotic administration alters the community structure of the gastrointestinal micobiota. *Gut Microbes*. 2010; 1(4):279-284

Roediger WE. Role of anaerobic bacteria in the metabolic welfare of the colonic mucosa in man. *Gut.* 1980; 21(9):793-8

Salyers A, Shoemaker NB. Reservoirs of antibiotic resistance genes. *Anim Biotechnol.* 2006;17(2):137-46

Sanger F, Nicklen S, Coulson AR. DANN sequencing with chain-terminating inhibitors. *Proc Natl Acad Sci USA*. 1977; 74(12):5463-5467

Schlee M, Harder J, Köten B, Stange EFet al. Probiotic lactobacilli and VSL#3 induce enterocyte beta-defensin 2. *Clin Exp Immunol*. 2008; 151(3):528-35

Schloss PD, Westcott SL, Ryabin T, Hall JRet al. Introducing mothur: open-source, platform-independent, community-supported software for describing and comparing microbial communities. *Appl Environ Microbiol*. 2009; 75(23):7537-41

Scott KP. The role of conjugative transposons in spreading antibiotic resistance between bacteria that inhabit the gastrointestinal tract. *Cell Mol Life Sci*. 2002; 59(12):2071-82

Segain JP, Raingeard de la Blétière D, Bourreille A, Leray V et al. Butyrate inhibits inflammatory responses through NFkappaB inhibition: implications for Crohn's disease. *Gut*. 2000; 47(3):397-403

Shannon CE. A mathematical theory of communications. *Bell System Technical Journal.* 1948; 27: 379-423

Shen J, Zhang B, Wei G, Pang X et al. Molecular profiling of the Clostridium leptum subgroup in human fecal microflora by PCR-denaturing gradient gel electrophoresis and clone library analysis. *Appl Environ Microbiol.* 2006; 72(8):5232-8.

Shoemaker NB, Vlamakis H, Hayes K, Salyers AA. Evidence for extensive resistance gene transfer among Bacteroides spp. and among Bacteroides and other genera in the human colon. *Appl Environ Microbiol*. 2001; 67(2):561-8

Sjölund M, Tano E, Blaser MJ, Andersson DI, Engstrand L. Persistence of resistant Staphylococcus epidermidis after single course of clarithromycin. *Emerg Infect Dis*. 2005; 11(9):1389-93

Sjölund M, Wreiber K, Andersson DI, Blaser MJ, Engstrand L. Long-term persistence of resistant Enterococcus species after antibiotics to eradicate Helicobacter pylori. *Ann Intern Med*. 2003; 139(6):483-7

Sogin ML, Morrison HG, Huber JA, Mark Welch D. Microbial diversity in the deep sea and the underexplored "rare biosphere". *Proc Natl Acad Sci U S A*. 2006; 103(32):12115-20

Sokol H, Seksik P, Furet JP, Firmesse O et al. Low counts of Faecalibacterium prausnitzii in colitis microbiota. *Inflamm Bowel Dis*. 2009; 15(8):1183-9

Sokol H, Pigneur B, Watterlot L, Lakhdari O et al. Faecalibacterium prausnitzii is an anti-inflammatory commensal bacterium identified by gut microbiota analysis of Crohn disease patients. *Proc Natl Acad Sci U S A*. 2008; 105(43):16731-6

Sood A, Midha V, Makharia GK, Ahuja V et al. The probiotic preparation, VSL#3 induces remission in patients with mild-to-moderately active ulcerative colitis. *Clin Gastroenterol Hepatol.* 2009; 7(11):1202-9, 1209.e1.

Sullivan A, Barkholt L, Nord CE. Lactobacillus acidophilus, Bifidobacterium lactis and Lactobacillus F19 prevent antibiotic-associated ecological disturbances of Bacteroides fragilis in the intestine. *J Antimicrob Chemother*. 2003; 52(2):308-11

Sullivan A, Edlund C, Nord CE. Effect of antimicrobial agents on the ecological balance of human microflora. *Lancet Infect Dis*. 2001; 1(2):101-14

Takeda K, Akira S. Toll-like receptors in innate immunity. *Int Immunol*. 2005; 17(1):1-14

Tang ML, Lahtinen SJ, Boyle RJ. Probiotics and prebiotics: clinical effects in allergic disease. *Curr Opin Pediatr*. 2010; 22(5):626-34

Tannock GW, Munro K, Harmsen HJ, Welling GW et al. Analysis of the fecal microflora of human subjects consuming a probiotic product containing Lactobacillus rhamnosus DR20. *Appl Environ Microbiol*. 2000; 66(6):2578-88

Tap J, Mondot S, Levenez F, Pelletier E et al. Towards the human intestinal microbiota phylogenetic core. *Environ Microbiol.* 2009; 11(10):2574-84

Tedelind S, Westberg F, Kjerrulf M, Vidal A. Anti-inflammatory properties of the short-chain fatty acids acetate and propionate: a study with relevance to inflammatory bowel disease. *World J Gastroenterol*. 2007; 13(20):2826-32

Short-chain fatty acids and human colonic function: roles of resistant starch and nonstarch polysaccharides.

Topping DL, Clifton PM. Short-chain fatty acids and human colonic function: roles of resistant starch and nonstarch polysaccharides. *Physiol Rev*. 2001; 81(3):1031-64

Turnbaugh PJ, Hamady M, Yatsunenko T, Cantarel BLet al. A core gut microbiome in obese and lean twins. *Nature*. 2009; 457(7228):480-4

Tursi A, Brandimarte G, Papa A, Giglio A. Treatment of relapsing mild-to-moderate ulcerative colitis with the probiotic VSL#3 as adjunctive to a standard pharmaceutical treatment: A double-blind, randomized, placebo-controlled study. *Am J Gastroenterol*. 2010; 105:2218-2227

Ubeda C, Taur Y, Jenq RR, Equinda MJ et al. Vancomycin-resistant Enterococcus domination of intestinal microbiota is enabled by antibiotic treatment in mice and precedes bloodstream invasion in humans. *J Clin Invest*. 2010; 120(12):4332-41

Ulisse S, Gionchetti P, D'Alò S, Russo FP et al. Expression of cytokines, inducible nitric oxide synthase, and matrix metalloproteinases in pouchitis: effects of probiotic treatment. *Am J Gastroenterol*. 2001; 96(9):2691-9

Uronis JM, Arthur JC, Keku T, Fodor A. Gut microbial diversity is reduced by the probiotic VSL#3 and correlates with decreased TNBS-induced colitis. *Inflamm bowel dis* 2011; 17(1):289-97

Vanderpool C, Yan F, Polk DB. Mechanisms of probiotic action: Implications for therapeutic applications in inflammatory bowel diseases. *Inflamm Bowel Dis.* 2008; 14(11):1585-96

Van den Heuvel EG, Muijs T, van Dokkum W, Schaafsma G. Lactulose stimulated calcium absorption in postmenopausal women. *J Bone Miner Res*. 1999;14(7):1211-6

Venturi A, Gionchetti P, Rizzello F, Johansson R et al. Impact on the composition of the faecal flora by a new probiotic preparation: preliminary data on maintenance treatment of patients with ulcerative colitis. *Aliment Pharmacol Ther.* 1999; 13(8):1103-8

Verna EC, Lucak S. Use of probiotics in gastrointestinal disorders: what to recommend? *Therap Adv Gastroenterol*. 2010; 3(5):307-19

Wang Q, Garrity GM, Tiedje JM, Cole JR. Naïve Bayesian Classifier for Rapid Assignment of rRNA Sequences into the New Bacterial Taxonomy. *Appl Environ Microbiol*. 2007; 73(16):5261-7

White JR, Nagarajan N, Pop M. Statistical methods for detecting differentially abundant features in clinical metagenomic samples. *PLoS Comput Biol.* 2009; 5(4):e1000352

Whitman WB, Coleman DC, Wiebe WJ. Prokaryotes: the unseen majority. *Proc Natl Acad Sci U S A*. 1998; 95(12):6578-83

Whittaker RH. Evolution and measurement of species diversity. *Taxon*. 1972; 21, 213-251

Wilcoxon F. Individual comparisons by ranking methods. *Biometrics* 1945;1(6):80-83

Wong JM, Jenkins DJ. Carbohydrate digestibility and metabolic effects. *J Nutr.* 2007; 137(11 Suppl):2539S-2546S

World Health Organization. Joint FAO/WHO expert consultation on evaluation of health and nutritional properties of probiotics in food including powder milk with live lactic acid bacteria. 2001.Food and Agriculture Organization of the United Nations, World Health Organization

Young VB, Schmidt TM. Antibiotic-associated diarrhea accompanied by large-scale alterations in the composition of the fecal microbiota. *J Clin Microbiol*. 2004; 42(3):1203-6

Zoetendal EG, Akkermans AD, De Vos WM. Temperature gradient gel electrophoresis analysis of 16S rRNA from human fecal samples reveals stable and host-specific communities of active bacteria. *Appl Environ Microbiol*. 1998; 64(10):3854-9

Zoetendal EG, Akkermans ADL, Akkermans-van Vliet WM, de Visser JAGM, de Vos M. The host genotype affects the bacterial community in the human gastrointestinal tract. *Microb ecol health dis*. 2001; 13:129-134

Zoetendal EG, von Wright A, Vilpponen-Salmela T, Ben-Amor Ket al. Mucosa-associated bacteria in the human gastrointestinal tract are uniformly distributed along the colon and differ from the community recovered from feces. *Appl Environ Microbiol*. 2002; 68(7):3401-7

9 Danksagung

An dieser Stelle möchte ich mich bei allen bedanken, die zum Gelingen dieser Arbeit beigetragen haben. Dabei möchte ich folgende Personen besonders hervorheben:

Herrn Prof. Dr. Stefan Schreiber möchte ich für die Möglichkeit danken über dieses interessante Thema promovieren und diese Arbeit mit modernsten Methoden durchführen zu können.

Herrn Prof. Dr. Frank Döring danke ich für die Übernahme meiner Betreuung und die freundliche Unterstützung.

Herrn Prof. Dr. Philip Rosenstiel möchte ich ebenfalls für die Betreuung und seine konstruktive Kritik danken.

Frau Dr. Anette Friedrichs danke ich für Hilfe jeglicher Art, Motivation und das Korrekturlesen. Weiterhin danke ich PD. Dr. Stephan Ott.

Ein großer Dank gilt Herrn Dr. Sven Neulinger für das Überlassen des R Skriptes zur Berechnung der Spearman Korrelationen und das Näherbringen von R allgemein. Henrik Knecht danke ich für das gemeinsame Ausprobieren neuer Computerprogramme sowie das Austüfteln der besten Analysestrategie.

Frau Dr. Amke Caliebe danke ich für die kompetente statistische Beratung.

Danke auch an Dr. Robert Häsler für die Beantwortung meiner Fragen rund um die qRT-PCR, sowie an Dorina Ölsner für die Durchführung derselbigen.

Anita Dietsch und Melanie Friskovec, Ina Baumgartner und Sandra Greve sowie Markus Schilhabel danke ich für die Durchführung der Pyro- bzw. Sangersequenzierung. Ohne Euch hätte ich keine Daten zum Auswerten bekommen.

Manuela Kramp, Sanaz Sedghpour Sabet, Birgit Pieper und Katja Cloppenborg-Schmidt danke ich für eine nette Arbeitsatmosphäre und die technische Hilfe ("Das Eppi sägen wir jetzt auf!").

Ein ganz großer Dank geht an Britt Petersen und Rabea Kleindorp. Ohne euch wäre das Arbeitsleben nur halb so lustig. Egal was alles schief lief, die Mittagspause mit euch hat für alles entschädigt. Britt, dir danke ich weiterhin für das Korrekturlesen in letzter Minute.

Meinen Kieler-Mädels Annegret, Marja, Julia, Bylle, Jana und Kristina danke ich für ihre Freundschaft, Ablenkung und aufmunternde Worte, wenn es mal nicht so lief.

Steffi, Steffi, Tanja, Lea und Kathrin danke ich für eine Freundschaft, die seit der Kindheit besteht. Es ist toll zu wissen Freunde wie euch zu haben.

Ein sehr herzlicher Dank geht an Johann. Es ist so schön dich gefunden zu haben.

Mein größter Dank aber gilt meinen Eltern. Ohne eure Hilfe, Liebe und Zuversicht in allen Lebenslagen wäre ich nie so weit gekommen!!!